Biotransformation of Sulfonamide Antibiotics in Activated Sludge: The Formation of Pterin Conjugates Leads to Sustained Risk

SUPPORTING INFORMATION

Stefan Achermann[1,2], Valeria Bianco[1,2], Cresten B. Mansfeldt[1], Bernadette Vogler[1], Boris A. Kolvenbach[3], Philippe F.X. Corvini[3,4], Kathrin Fenner[1,2,5,*]

[1]Eawag, Swiss Federal Institute of Aquatic Science and Technology, 8600 Dübendorf, Switzerland.

[2]Institute of Biogeochemistry and Pollutant Dynamics, ETH Zürich, 8092 Zürich, Switzerland.

[3]Institute for Ecopreneurship, School of Life Sciences, University of Applied Sciences and Arts Northwestern Switzerland, 4132 Muttenz, Switzerland. [4]State Key Laboratory for Pollution Control and Resource Reuse, School of the Environment, Nanjing University, Nanjing 210093, PR China.

[5]Department of Chemistry, University of Zürich, 8057 Zürich, Switzerland.

*Corresponding author (email: kathrin.fenner@eawag.ch)

This supporting information (SI) is organized in 16 sections (S1-S16, see table of content on the following page) and comprises 17 figures and 13 tables. Additionally, in section S7 chromatograms and measured mass spectra for 37 transformation products are provided.

Content

S1 Chemical Reference Compounds 3
S2 Batch Experiments 4
S3 Internal Standard Solution 8
S4 Radioactivity in Cell Pellet Washing Solution 9
S5 LC-HRMS/MS Measurements Batch Experiments 10
S6 Suspect Screening Parameters 13
S7 Transformation Product Structure Elucidation 16
S8 LC-HRMS/MS Measurements WWTP Samples 58
S9 Biotransformation of ^{14}C-SDZ 59
S10 Mineralization 61
S11 Sorption and Abiotic Controls 62
S12 Biotransformation of ^{14}C-SMX 63
S13 TP formation for SDZ, SMZ, SPY and STZ 64
S14 Biotransformation of N4-Acetyl-SAs 67
S15 Transformation Product Mass Balance Estimation 68
S16 Pterin-Conjugate Pathway Related TPs in WWTPs 73

References 74

S1 Chemical Reference Compounds

Chemical reference materials are listed in Table S1.1. Further information on the ^{14}C-labeled compounds was provided in previous studies ([1] (SMX) and [2] (SDZ)) in which experiments with solutions from the same reference materials were conducted.

Table S1.1: List of chemical reference compounds and suppliers.

Chemical	Supplier
2-Aminopyridine	Sigma-Aldrich
2-Aminothiazole	Sigma-Aldrich
3-amino-5-methylisoxazole	Sigma-Aldrich
N4-acetyl-sulfadiazine	Eawag AUA Synthesis
N4-acetyl-sulfamethazine	Sigma-Aldrich
N4-acetyl-sulfamethoxazole	Sigma-Aldrich
N4-acetyl-sulfamethoxazole-D5	TRC Canada
N4-acetyl-sulfapyridine	Sigma-Aldrich
N4-acetyl-sulfathiazole	Eawag AUA Synthesis
N4-acetyl-sulfathiazole-D4	TRC Canada
Pterin-Sulfathiazole	SynphaBase[a]
Sulfadiazine	Sigma-Aldrich
Sulfadiazine-D4	TRC Canada
Sulfamethazine	Sigma-Aldrich
Sulfamethazine-D4	TRC Canada
Sulfamethoxazole	Sigma-Aldrich
Sulfamethoxazole-D4	TRC Canada
Sulfamethoxazole-glucoronide	TRC Canada
Sulfapyrdine-D4	TRC Canada
Sulfapyridine	Riedel-de-Haën
Sulfathiazole	Sigma-Aldrich
Sulfathiazole-D4	TRC Canada

[a]Custom synthesis by SynphaBase (Switzerland) for a study conducted earlier.[3]

S2 Batch Experiments

Sampling of activated sludge: For each of the three series of experiments, activated sludge (denoted AS1, AS2 and AS3) was collected from the same aerated, nitrifying treatment basin from the WWTP Neugut in Dübendorf, Switzerland (less than three hours before the batch experiments were started). The WWTP Neugut treats wastewater from 105,000 people equivalent with an approximate industrial contribution of 50% in COD (chemical oxygen demand) load. The secondary treatment includes nitrification, denitrification and biological phosphorous removal and is operated at a solids retention time of 13 days and a hydraulic retention time of approximately 18 hours (without settling tank). Further details have recently been summarized by Bourgin *et al*.[4]

Transport of collected activated sludge: At the WWTP, the activated sludge was collected in 2.5 L glass flasks that were half filled. During transport to the laboratory, the bottles were opened and shaken regularly to avoid depletion of dissolved oxygen. In the laboratory, the activated sludge was immediately poured into an open glass beaker and stirred (using a magnetic stirrer).

Measurements of TSS and nitrogen species: After collection of activated sludge at the WWTP, TSS, chemical oxygen demand (COD) and nitrogen species (NH_4^+, NO_2^-, NO_3^-) were measured in the laboratory for the three series of experiments (AS1-AS3) (Table S2.1). Concentrations of ammonium and nitrite were below limits of detection. The measured nitrate may result both from non-complete denitrification at the WWTP and from oxidized ammonium released from the sludge microbes after sludge collection.

Table S2.1: TSS, nitrogen (NH_4^+, NO_2^-, NO_3^-) and COD measurements

activated sludge	sampling date	TSS[a] [g/L]	NH_4-N[b] [mg/L]	NO_2-N[c] [mg/L]	NO_3-N[d] [mg/L]	COD[e] [mg/L]
AS1	21.03.2017	3.70 ± 0.08	<0.2	<0.6	9.76	25.2
AS2	12.06.2017	3.45 ± 0.04	<0.2	<0.6	5.96	n/a
AS3	18.07.2017	2.80 ± 0.02	<0.2	<0.6	4.75	15.9

[a]For TSS measurements (mean and standard deviation from triplicate measurements), AS was sampled (10 mL) and processed as described elsewhere.[5] [b]NH_4-N was measured using Hach Lange test cuvettes (LCK 203) [c]NO_2-N was measured using Hach Lange test cuvettes (LCK 342) [d]NO_3-N was measured using Hach Lange test cuvettes (LCK 339) [e]COD (chemical oxygen demand) was measured using Hach Lange test cuvettes (LCK 314).

Biotransformation batch experiments: All batch experiments are listed in Table S2.2. As described in the methods section of the main text, all experiments were performed in glass bottles (100 mL) placed on a circulating shaker table. Using non-gasketed caps, this approach allows to maintain complete mixing and aerobic conditions over the time-course of the experiments as described elsewhere.[6, 7] Helbling *et al*. reported that the dissolved oxygen remained relatively constant in this experimental set-up at 7.9 ± 0.4 mg/L.[7]

During all three experimental campaigns, pH values were recorded. **Measurements of pH during biotransformation experiments with SMX and SDZ:** Daily pH measurements were performed in the non-spiked control reactors (all three replicates) resulting in values of 8.03 ± 0.09, 8.27 ± 0.08, 8.28 ± 0.09, 8.01 ± 0.04 (mean and standard deviation) for days 1, 2, 3 and 4, respectively. At the end of the experiment, similar pH values across added chemicals and replicates were confirmed by measuring the pH in all biotransformation reactors (^{14}C-SMX, SMX, ^{14}C-SDZ, SDZ, all replicates each), with an average value of 8.15 ± 0.12. **Measurements of pH during biotransformation experiments with SMZ, SPY and STZ:** Measurements were performed over time in separate batches (duplicate) spiked with SMZ, SPY, STZ and SMX: 8.16 ± 0.13 (day 1), 8.28 ± 0.07 (day 2), 8.14± 0.04 (day 3), 7.87 ± 0.24 (day 4). **Measurements of pH during biotransformation experiments with Pterin-STZ:** Measurements were conducted on day 2 after addition of pterin-STZ: 8.12 ± 0.08 (triplicate batch reactors).

Table S2.2: Listing of batch experiments conducted.

added compound	AS	replicates	V	initial conc[3]	activity[c]	sampling points	sample V	transfer V	ISTD
			mL	[ug/L]	[kBq]	[h]	[mL]	[µL]	[ug/L]
14C-SMX	AS1	3	40	405	61.2	0, 2, 4, 8, 10, 24, 48, 72	1.5 (2)[f]	750 (1500)[f]	-
14C-SDZ	AS1	3	40	115	40.8	0, 2, 4, 8, 10, 24, 48, 72	1.5 (2)[f]	750 (1500)[f]	-
14C-SMX control	AS1-AC[a]	3	40	278	42.0[d]	0, 2, 24, 48, 72	1.5	750	-
14C-SDZ control	AS1-AC[a]	3	40	116	41.2	0, 2, 24, 48, 72	1.5	750	-
non-spiked control	AS1	3	40	-	-	0, 2, 4, 8, 10, 24, 48, 72	1.5 (2)[f]	750 (1500)[f]	24
SMX	AS1	3	40	250	-	0, 2, 4, 8, 10, 24, 48, 72	1.5 (2)[f]	750 (1500)[f]	24
SDZ	AS1	3	40	250	-	0, 2, 4, 8, 10, 24, 48, 72	1.5 (2)[f]	750 (1500)[f]	24
SPY	AS2	2	50	50	-	0, 1, 2, 5, 10, 24, 48, 72[e]	1.5	750	4.8
SMZ	AS2	2	50	50	-	0, 1, 2, 5, 10, 24, 48, 72[e]	1.5	750	4.8
STZ	AS2	2	50	50	-	0, 1, 2, 5, 10, 24, 48, 72[e]	1.5	750	4.8
N4-acetyl-SMX	AS2	2	50	50	-	0, 1, 2, 5, 10, 24, 48, 72[e]	1.5	750	4.8
control (SMZ, SPY, STZ)	AS1-AC[a]	2	50	50	-	0, 72	1.5	750	4.8
control (SMZ, SPY, STZ)	AS2-ACF[b]	2	50	50	-	0, 72	1.5	750	4.8
non-spiked control	AS2	1	50	-	-	0, 1, 2, 5, 10, 24, 48, 72	1.5	750	4.8
pterin-STZ	AS3	3	50	50	-	0, 2, 4, 8, 24, 48	1.5	500	-
non-spiked control	AS3	3	50	-	-	0, 2, 4, 8, 24, 48	1.5	500	-

[a]AC indicates that the activated sludge was autoclaved prior to incubation. [b] ACF indicates that autoclaved activated sludge filtrate was used as abiotic control. [c] For experiments with 14C-labeled SAs, the chemical concentration of the spiking solution was only approximately known. Therefore, the radioactivity recovered in the medium at the first sampling point (and molar concentrations calculated thereof) are reported here. [d] The number represents the average of 2 replicates. In the third replicate an radioactivity of 94.4 kBq was spiked. [e] Because of limited availability of measurement time, only samples collected after 0, 10 and 48 h were measured for the second replicate. (All samples of replicate 1 were measured) [f] Larger volumes were sampled 24, 48 and 72 h after start of incubation.

Rate constants: As it has frequently been described for microbial communities (e.g.,[8-11]), first-order kinetics were observed for the biotransformation of the five parent sulfonamides. Applying linear regression analysis on the logarithmic concentration-time series (8 data points per time series), first-order rate constants were calculated (Table S.2.3). In similar batch experiments described by Gulde *et al.*,[12] with similar starting concentrations of spiked chemicals and organic solvents, no substantial change in TSS was observed over 4 days. Therefore, we converted the observed first-order rate constants into TSS-normalized second order rate constants (provided in the main text and in Table S2.3), supporting the comparability with other studies. Under aerobic conditions, biomass-normalized rate constants in the same order of magnitude have earlier been reported for SMX.[1, 13]

Table S2.3: Biotransformation rate constants

SA	observed k	TSS	TSS-normalized k[a]	r^2
	[d^{-1}]	[g/L]	[L/(gTSS×d)]	
SMX	0.31 ± 0.02	3.70 ± 0.08	0.083 ± 0.006	0.98
SDZ	0.36 ± 0.03	3.70 ± 0.08	0.093 ± 0.009	0.95
SMZ	0.40 ± 0.04	3.45 ± 0.04	0.11 ± 0.01	0.95
STZ	1.65 ± 0.03	3.45 ± 0.04	0.45 ± 0.01	>0.99
SPY	0.73 ± 0.03	3.45 ± 0.04	0.20 ± 0.01	0.99

[a]Estimates for the standard deviation of TSS-normalized rate constants were obtained by error propagation of the standard deviations of the observed rate constants and the triplicate TSS measurements using the software R (version 3.3.0) and the package ("propagate").

S3 Internal Standard Solution

Two internal standard solutions were prepared containing the chemicals listed in Table S3.1. For samples from the SMX and SDZ biotransformation experiments, a solution with a concentration of 625 µg/L for each analyte was prepared in ethanol. For quantification of SMZ, SPY and STZ, a solution with a concentration of 125 µg/L for each analyte in ethanol was used. The final internal standard concentrations in the samples are detailed in Table S2.2.

Table S3.1: Chemicals contained in the internal standard solutions.

Name
N4-acetyl-sulfamethazine-D4
N4-acetyl-sulfamethoxazole-D5
Sulfadiazine-D4
Sulfamethazine-D4
Sulfamethoxazole-D4
Sulfapyridine-D4
Sulfathiazole-D4

S4 Radioactivity in Cell Pellet Washing Solution

After centrifugation of the activated sludge samples, the supernatant could not be completely removed by pipetting. Therefore, the analyzed solids washing solution (1 mL, 1M NaOH) contained radioactivity both from the remaining aqueous phase and from ^{14}C material that was weakly adsorbed to the activated sludge solids. To estimate the fraction originating from the aqueous phase, the weight difference between empty sample tubes and sample tubes containing the cell pellet (after centrifugation and removal of the aqueous phase) was assessed. The difference in weight represents the sum of the biomass fraction and the remaining aqueous phase. Using the TSS measurements, the dry matter content per sample could be determined and, assuming 20% bacterial dry matter content in wet bacteria,[14] the estimated biomass weight was subtracted to obtain the weight of the remaining supernatant. Knowing the radioactivity in the aqueous phase at each time point, the fraction of the radioactivity in the washing solution that was most likely attributable to the remaining aqueous fraction was subtracted from the total measured radioactivity of the washing solution. The radioactivity in the washing solution before and after correction is presented as percentage of the total radioactivity in the aqueous fraction at the first measurement time point (Table S4.1). Since the radioactivity in the washing solution only constitute a minor fraction of the total radioactivity and, in particular, the estimated fraction that is attributable to adsorption is below 5%, the activities measured in the washing solution are not further considered in the mass balance. For SDZ, radioactivity measured in the washing solution was in a similar range (slightly lower), and the data analysis was conducted as for SMX.

Table S4.1: Radioactivity in the washing solution as percentage of the radioactivity in the supernatant of the sample collected after 0 h.

SMX: radioactivity washing solution	t0	t2	t4	t8	t10	t24	t48	t72
washing solution (aqueous phase + adsorbed fraction)	3.8	4.4	4.3	3.2	4.2	5.8	7.3	7.3
washing solution corrected (adsorbed fraction)	1.5	2.0	1.9	0.8	1.7	2.3	3.8	4.0

S5 LC-HRMS/MS Measurements Batch Experiments

For chromatographic separation, a gradient program was run using nanopure water (Barnstead Nanopure, Thermo Scientific) and methanol (HPLC grade, Fisher Scientific) as the mobile phase both augmented with 0.1% formic acid (98-100%, Merck) as follows: the initial solvent ratio 95:5 water/methanol was maintained for 1 min, increased to 5:95 water/methanol over 16 minutes, held for 8 minutes and then set to 95:5 again for reconditioning before the next run (5 minutes). Electrospray ionization was triggered at a capillary temperature of 320 °C and with a spray voltage of +4 kV and -3 kV in positive and negative ionization mode, respectively. Mass calibration and mass accuracy were checked (deviation <5 ppm) with an in-house amino acid solution prior to the measurements.

Samples from the SMX and SDZ experiments were measured in full-scan positive/negative switching mode with a resolution of 140000 at *m/z* 200. Additionally, data-dependent MS^2 spectra were recorded for samples of one replicate for each sulfonamide (positive and negative ionization mode in two separate analysis runs). Samples from SPY, SMZ, STZ and TP spike experiments were measured separately in positive and negative ionization mode with a resolution of 280000 at *m/z* 200 (full-scan) and data-dependent MS/MS acquisition. Data-dependent MS^2 spectra were recorded at a resolution of 17500 at *m/z* 200 (isolation window of 1 *m/z*) and using an inclusion list (list of suspected transformation products, section S15) to trigger the acquisition of fragmentation spectra whenever a signal corresponding to a listed mass was detected in the full-scan mass spectrum. Samples from the pterin-STZ biotransformation experiment were measured in full-scan positive/negative switching mode with a resolution of 140000 at *m/z* 200. An overview of measurement settings for all samples is provided in Table S5.1.

For quantification, internal standards were added to all samples and calibration samples as described in the main text. An isotope-labeled standard was available for each sulfonamide and for two metabolites (N4-acetyl-sulfamethoxazole and N4-acetyl-sulfamethazine). For other analytes, the best matching isotope-labeled standard in terms of structure and retention time was assigned (Table S5.2). Using the software Tracefinder EFS 3.2 (Thermo Scientific), the concentration for each analyte was determined by calculating the ratio of the analyte peak area over the corresponding isotope-labeled standard peak area in each sample and compared to the ratio obtained from the calibration curve samples. The calibration curves were obtained by a weighted (1/x) linear least square regression.

Table S5.1: Measured LC-HRMS/MS samples and analytical parameters.

Samples	matrix	replicates measured	sampling points	guard cartridge	injection volume	MS (QE, QE+)[a]	acquisition mode	resolution
			[h]		[µL]			
SMX	AS1	3/3	0, 2, 4, 8, 10, 24, 48, 72	no	100	QE	switch	140000
		1/3	0, 2, 4, 8, 10, 24, 48, 72	no	100	QE	DD[b]	140000
SDZ	AS1	3/3	0, 2, 4, 8, 10, 24, 48, 72	no	100	QE	switch	140000
		1/3	0, 2, 4, 8, 10, 24, 48, 72	no	100	QE	DD[b]	140000
non-spiked control	AS1	3/3	0, 2, 4, 8, 10, 24, 48, 72	no	100	QE	switch	140000
calibration samples[c]	water			no	100	QE	switch	140000
SPY	AS2	2/2	0, 1, 2, 5, 10, 24, 48, 72[d]	yes	100	QE+	DD[b]	280000
SMZ	AS2	2/2	0, 1, 2, 5, 10, 24, 48, 72[d]	yes	100	QE+	DD[b]	280000
STZ	AS2	2/2	0, 1, 2, 5, 10, 24, 48, 72[d]	yes	100	QE+	DD[b]	280000
N4-acetyl-SMX	AS2	2/2	0, 1, 2, 5, 10, 24, 48, 72[d]	yes	100	QE+	DD[b]	280000
control (SMZ, SPY, STZ)	AS2-AC[e]	2/2	0, 72	yes	100	QE+	switch	70000
control (SMZ, SPY, STZ)	AS2-ACF[f]	2/2	0, 72	yes	100	QE+	switch	70000
non-spiked control	AS2	1/1	0, 1, 2, 5, 10, 24, 48, 72	yes	100	QE+	DD[b]	280000
calibration samples[g]	water			yes	100	QE+	switch	70000
pterin-STZ	AS3	3/3	0, 2, 4, 8, 24, 48	yes	100	QE+	switch	140000
non-spiked control	AS3	3/3	0, 2, 4, 8, 24, 48	yes	100	QE+	switch	140000

[a]Measurements were conducted on a Q Exactive (QE) or Q Exactive Plus (QE+) mass spectrometer (Thermo Fisher Scientific). [b]DD indicates data-dependent MS2 acquisition. [c]Calibration levels: 200, 500, 1000, 2000, 5000, 10000, 20000, 50000, 100000, 200000, 300000 ng/L [d]For the second replicate, only time points 0, 10, 48 h were measured [e]AC indicates that the activated sludge was autoclaved prior to incubation. [f]ACF indicates that autoclaved activated sludge filtrate was used as abiotic control. [g]Calibration levels: 200, 350, 500, 1000, 2000, 3500, 5000, 10000, 20000, 35000, 50000, 75000 ng/L.

141 **Table S5.2: Assigned internal standards and limits of quantification**

Analyte	Internal standard	LOQ [ng/L]
Sulfamethoxazole	Sulfamethoxazole-D4	200
N4-acetyl-sulfamethoxazole	N4-acetyl-sulfamethoxazole-D5	200
3-amino-5-methyliosxazole	Sulfamethoxazole-D4	200
N1-glucoronide-sulfamethoxazole	Sulfamethoxazole-D4	500
Sulfadiazine	Sulfadiazine-D4	200
N4-acetyl-sulfadiazine	Sulfadiazine-D4	200
Sulfamethazine	Sulfamethazine-13C6	200
N4-acetyl-sulfamethazine	Sulfamethazine-13C6	200
Sulfathiazole	Sulfathiazole-D4	200
2-aminothiazole	Sulfathiazole-D4	200
N4-acetyl-sulfathiazole	N4-acetyl-sulfathiazole-D4	200
Pterin-sulfathiazole	Sulfathiazole-D4	1000
Sulfapyridine	Sulfapyridine-D4	200
2-aminopyridine	Sulfapyridine-D4	200
N4-acetyl-sulfapyridine	Sulfapyridine-D4	200

142

143

144

S6 Suspect Screening Parameters

Suspect screening lists were compiled by predicting TPs using the EAWAG pathway prediction system (EAWAG-PPS, http://eawag-bbd.ethz.ch/predict/) and considering previously reported TPs.[3, 15-21] Transformations reported in literature for a specific SA were used to calculate analogous TPs for the five sulfonamides investigated. Additionally, mass shifts of common biotransformation reactions were calculated and applied to all five investigated sulfonamides (including hydroxylation, dihydroxylation, demethylation, dehydrogenation, hydrogenation, decarboxylation, hydration and conjugation to glucuronide-SA, sulfate-SA, taurine-SA, glutathione-SA, cysteine-SA, glycine-SA, formyl-SA, acetyl-SA, succinyl-SA, propionyl-SA, malonyl-SA and fumaryl-SA). After completion of a first TP screening, further possible downstream TPs were predicted for the most intense TP peaks and a second TP screening was performed with the updated suspect list. The Compound Discoverer workflow design is shown in Figure S6.1 and the parameter settings are detailed in Table S6.1.

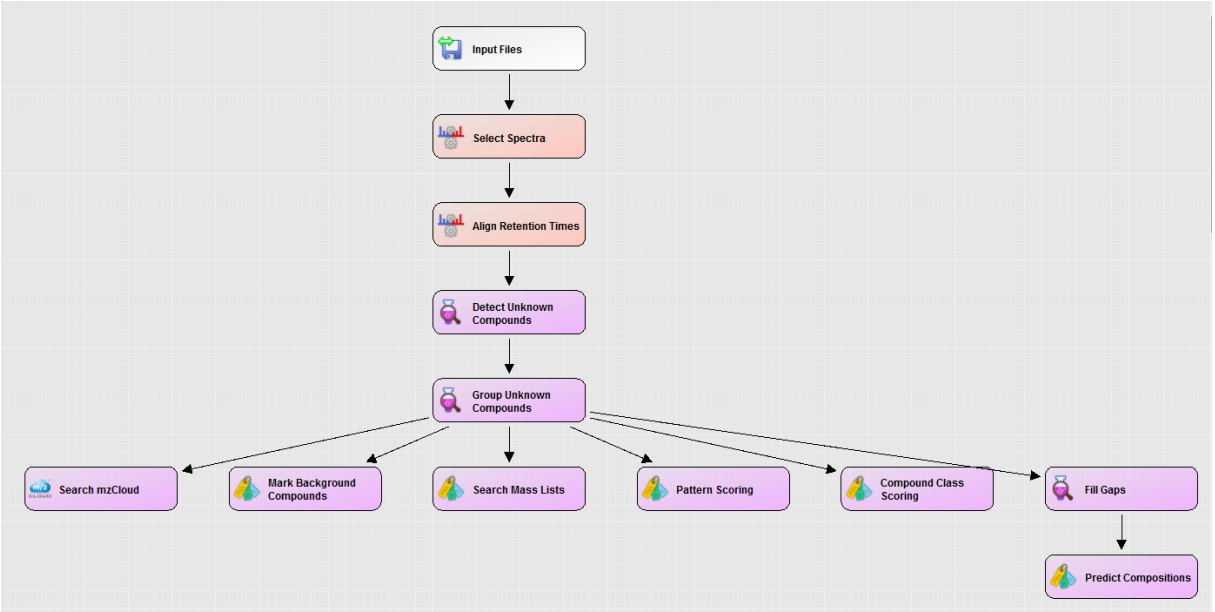

Figure S6.1: Workflow applied in Compound Discoverer 2.1

Table S6.1 Applied settings in Compound Discoverer 2.1

Processing Node	Applied Parameter Settings
Select Spectra	Presettings
Align Retention Times	Alignment Model: Adaptive curve Maximum Shift: 2 min Mass Tolerance: 5 ppm
Detect Unknown Compounds	Mass Tolerance: 5 ppm Intensity Tolerance: 30% S/N Threshold: 3 Min Peak Intensity: 10000 Ions: [M+FA-H]-1; [M+H]+1; [M+K]+1; [M+Na]+1; [M+NH4]+1; [M-H]-1; [M-H+TFA]-1; [M-H-H2O]-1 Min Element Counts: C H Max Element Counts: C90 H190 Br3 Cl4 F6 K2 N10 Na2 O18 P3 S5
Group Unknown Compounds	Mass Tolerance: 5 ppm RT Toerance: 0.2 min Preferred Ions: [M+H]+1; [M-H]-1
Search mzCloud	Compound Classes: All Match Ion Activation Type: True Match Ion Activation Energy: Match with Tolerance Ion Activation Energy Tolerance: 20 Apply Intensity Threshold: True Identity Search: HighChem HighRes Similarity Search: Similarity Reverse Match Factor Threshold: 50
Mark Background Compounds	Max. Sample/Blanks: 5 Max. Blank/Samples: 0 Hide Background: True
Search Mass Lists	Input files: \EFS HRAM Compound Database.csv Consider Retention Time: True RT tolerance: 0.05

	Mass Tolerance: 5 ppm
Pattern Scoring	Isotope Patterns: C6H5SO2; C6H7N2SO2
	Mass Tolerance: 5 ppm
	Intensity Tolerance: 30 %
	SN Threshold: 3
	Min. Spectral Fit: 0 %
Compound Class Scoring	S/N Threshold: 50
	High Acc. Mass Tolerance: 2.5 mmu
	Low Acc. Mass Tolerance: 0.5 Da
	Allow AIF Scoring: True
Fill Gaps	Mass Tolerance: 5 ppm
	S/N Threshold: 1.5
Predict Compositions	Mass Tolerance: 5 ppm
	Min. Element Counts: C H
	Max Element Counts: C90 H190 Br3 Cl4 N10 O18 P3 S5
	Min. RDBE: 0
	Max. RDBE: 40
	Min. H/C: 0.1
	Max H/C: 3.5
	Max. # Candidates: 10
	Intensity Tolerance: 30 %
	Intensity Threshold: 0.1 %
	S/N Threshold: 3
	Use Dynamic Recalibration: True
	Use Fragments Matching: True
	Mass Tolerance: 5 ppm
	S/N Threshold: 3

163

164

S7 Transformation Product Structure Elucidation

As stated in the main text, only TP candidate peaks were considered for which the signal was clearly higher in the biotransformation reactors compared to the non-spiked control reactors. Below, additional evidence leading to the proposed molecular structures and assigned confidence levels[22] is presented for TPs for which no reference standard was available. Recurring MS^2 fragments that were observed in analogous TPs from different SA parents, and which in parts have already been observed in previous studies, are summarized in Table S7.1. Chromatographic peaks, MS^1 spectra and, when available, MS^2 spectra are shown below. For the sake of readability, *m/z* values of fragments are abbreviated and presented as nominal masses. Measured exact *m/z* values are provided in Table S7.1 and in the mass spectra below.

Pterin-SA: For pterin-STZ, a reference standard was available which eluted at the same retention time as the emerging peak with identical mass in the biotransformation experiment (confidence level 1). For pterin-SMX, pterin-SMZ and pterin-SDZ a fragment at *m/z* 331 was found that had been observed elsewhere.[3] Additionally, a number of fragments reported and interpreted by Stravs *et al*. were detected (*m/z* 349, 331, 283, 267 and 176) and hence these pterin-TPs were assigned a 2b confidence level.[18] Retention times for all pterin-SAs were between 0.8−1.8 min higher than for the respective parent molecules, and comparable retention time shifts were observed previously by Richter *et al*.,[3] who also used a silica-based C18 column. For SPY, no MS^2 spectrum was measured, but the similarities in retention time shifts and formation patterns support the proposed structure (tentative structure, confidence level 3).

Dihydropterin-SA: Dihydropterin-SMX was the only detected dihydropterin-SA. Fragment *m/z* 333 was detected previously for dihydropterin-STZ (Richter *et al.*),[3] and the fragments *m/z* 351 and *m/z* 178 correspond to fragments *m/z* 349 and *m/z* 176 observed for pterin-SAs, respectively, with a mass shift of two mass units. Similarity in retention time compared to pterin-SMX (difference of 0.2 min) further supports the proposed molecular structure (confidence level 2b).

PtO-SA: In line with the fragmentation patterns observed for pterin-SAs and dihydropterin-SMX, we observed fragment *m/z* 332 for PtO-SMX, PtO-SDZ and PtO-SMZ. In this fragment, the pteridine

moiety is still connected to the aniline part but the variable moiety of the SAs (3A5MI in the case of SMX) is lost. The fragments detected at *m/z* 350, 332, 284, 268 and 177 have previously been observed for PtO-SMX, and a fragmentation pathway was proposed.[18] All PtO-SAs showed similar retention times to the corresponding pterin-SAs (within 0.3 min, the strongest difference was observed for SPY). The biochemical reaction transforming 2-amino-4-hydroxypteridine (pterin) to 2,4(1H,3H)-pteridinedione has previously been observed and is known to be catalyzed by the enzyme pterin-deaminase that is present in diverse species.[23, 24] More specifically, this reaction was observed in the biodegradation of folic acid, which has a similar molecular structure as the pterin-SAs.[25, 26] On a side note, pterin deaminases were found to act much slower on 7,8-dihydropterins, potentially explaining why the corresponding products of dihydropterin-SA hydrolysis were not observed in our study.[27] Altogether, although alternative molecular structures for this TP could not completely be excluded from the mass spectrometric evidence alone, combined evidence from literature and our controlled experimental settings support the proposed transformation pathway, and we consider the formation of the suggested molecular structure for the PtO-SAs highly likely (confidence level 2b). No MS^2 spectra were obtained for PtO-STZ and PtO-SPY, however the similarities in retention time shifts and formation patterns support the proposed molecular structures (tentative structure, confidence level 3).

Ac-OH-SA: Analysis of fragmentation spectra of Ac-OH-SMX confirmed strong similarities with the spectrum and interpretation of Ac-OH-SMX presented by Stravs *et al*.[18] (Table S7.1). Similar to the pterin-SAs, several fragments (e.g., *m/z* 214, 166, 150) suggest substitution at the aniline moiety (most likely at the aniline-nitrogen) of the sulfonamides. The fragments at *m/z* 166, 150, 108 were observed in MS^2 spectra of SMX, SDZ, SPY and SMZ. Whereas Majewsky *et al*.[20] discussed the structurally similar TP hydroxylated acetyl, in the study be Stravs *et al*., this structure could be excluded by comparing retention times to a reference standard. Here, we observed strong similarities in fragmentation spectra between Ac-OH-SMX and the corresponding TP reported by Stravs *et al*.[18] In particular, the fragment at *m/z* 106 was suggested to arise from decarboxylation of fragment *m/z* 150 which would not be expected for hydroxylated acetyl. Also, hydroxylated N4-acetyl-SAs would be expected to be formed out of N4-acetyl-SA; however, we confirmed the formation out of pterin-SA. As expected for molecules containing carboxylic acid moieties, the Ac-OH-SAs were also detected in

negative ionization mode (confidence level 3, tentative structure). All N4-Ac-OH-SAs showed similar retention time shifts compared to their parents (0.8−1.3 min). No MS^2 spectrum was recorded for Ac-OH-STZ.

N4-formyl: In comparison with Ac-OH-SAs, a series of fragments shifted by *m/z* 30 (CH2O) were observed for all five detected N4-formyl-SAs (*m/z* 184, 136 and 120), confirming the similarity in structure. Compared to the parent structures, retention times were positively shifted (0.1–1.1 min). Formation of N4-formyl-SAs and the MS^2 fragments at *m/z* 184, 136 and 120 have previously been described,[28, 29] therefore, we consider the proposed molecular structure N4-formyl-SA highly likely (confidence level 2b).

Table S7.1: MS^2 fragments of TPs related to the pterin biotransformation pathway.

TP	*m/z* (calc.)	proposed structure[a]	SMX	SDZ	SMZ	SPY	STZ	Reference
Pterin-SA						na[b]	standard[c]	
	349.0714	TP−*R+H2O*	349.0709	349.0708	349.0711			18
	331.0608	TP−*R*	331.0606	331.0596	331.0611			3, 18
	283.0938	TP−*R−SO2+H2O*	283.0926	283.0921	283.0930			18
	267.0989	TP−*R−SO2*	267.0985	267.0988	267.0994			18
	176.0567	pterin	176.0559	176.0570	176.0575			18
Dihydropterin-SA				nd[d]	nd[d]	nd[d]	nd[d]	
	351.0870	TP−*R+H2O*	351.0577					3
	333.0764	TP−*R*	333.0750					
	178.0723	dihydropterin	178.0720					
PtO-SA						na[b]	na[b]	
	350.0554	TP−*R+H2O*	350.0544	350.0543	350.0551			18
	332.0448	TP−*R*	332.0428	332.0416	332.0438			18
	284.0778	TP−*R-SO2+H2O*	284.0760	284.0766	284.0775			18
	268.0829	TP−*R-SO2*	268.0815	268.0811	268.0827			18
	177.0407	PtO	177.0418	177.0410	177.0404			18
Ac-OH-SA							na[b]	
	246.0873	TP−*SO2−H2*	246.0870					18
	214.0169	TP−*R*	214.0163	214.0175		214.0172		18
	189.0897	246−*C2HO2*	189.0891					18
	166.0499	108+*C2H2O2*	166.0496	166.0494	166.0497	166.0502		18
	151.0628	TP−*R−SO2*	151.0625			151.0630		18
	150.0550	TP−*R−SO2*	150.0551	150.0548	150.0550	150.0552		18
	108.0444	rearrangement	108.0444	108.0441	108.0445	108.0445		20
	106.0651	150−*CO2*	106.0650	106.0650	106.0650	106.0654		18
N4-formyl-SA								
	184.0063	TP−*SO2-H2*	184.0059	184.0061	184.0061	184.0062	184.0062	29
	136.0393	108+*CO*	136.0390	136.0390	136.0392	136.0393	136.0393	29
	120.0444	TP−*R−SO2*	120.0441	120.0442	120.0443	120.0443	120.0442	28

[a]*R* represents the variable moiety of the SAs (3A5MI in the case of SMX). [b]no MS^2 spectrum available. [c]structure confirmed by chemical reference standard. [d]TP not detected.

SA+O: TPs with the molecular formula SA+O were observed for SMX, SDZ, SMZ and SPY, supposedly corresponding to a hydroxylation or N-oxidation reaction. For SMX+O, detecting fragments *m/z* 172 and 124 (mass shift of 12 mass units compared to formyl) and the unaltered 3A5MI (*m/z* 99) suggests hydroxylation at the N4 position and formation of the hydroxylamine. The three fragments at *m/z* 99, 124 and 172 were also confirmed for N4-hydroxy-SMX by Majewsky *et al*.[20] (confidence level 3). In contrast, for SDZ, SMZ and SPY, the fragments at *m/z* 124 and172 were not observed and structures of the TPs remained unclear (confidence level 4).

Pterin-SA+H2O: TPs corresponding to masses of pterin-SA+H2O were detected for SMX and SDZ. We hypothesized that these TPs could represent an intermediate hydrolysis product of the pterin-moiety (Figure 5) or a possible intermediate in the biotransformation reaction from pterin to PtO. MS^2 spectra confirmed that the TPs originate from a pterin-structure (confidence level 3).

Pterin-SA + O: A TP with a mass shift corresponding to a monooxygenation of the pterin-SA was detected for SMX and SDZ. Fragment *m/z* 347 could indicate that oxidation occurred at the pterin-moiety, but present evidence did not allow further determining of the exact structure.

SA + C3H2O3: TPs with masses corresponding to SA+C3H2O3 were detected for SMX and SPY, possibly representing N4-malonyl-SAs as suggested in Figure 5 in the main text. No MS^2 spectra were obtained.

2A46DP (SMZ): Analysis of the MS^2 fragmentation spectrum confirms the hypothesized formation of the 2-amino-4,6-dimethyl-pyrimidine in analogy to 3A5MI formation from SMX.

Chromatograms and mass spectra: On the following pages, chromatographic peaks (from a LC-HRMS/MS system) and mass spectra are presented. Different colors of the chromatographic peaks (top left of each page) represent different samples in which the transformation product was detected. Measured *m/z* values and adducts ($[M+H]^+$ or $[M-H]^-$) are shown in the MS^1 full-scan spectra on the top right of each page. In the MS^2 spectra, the presented annotated fragment structures represent positive matches with fragments predicted for the suspected TP structure in Compound Discoverer. Retention time, ionization mode, extracted mass and the applied collision energy is shown in the header of each presented MS^2 spectrum. Atomic modification represents the change in molecular formula compared to the parent sulfonamide.

SMX: PtO-SMX

Chromatogram

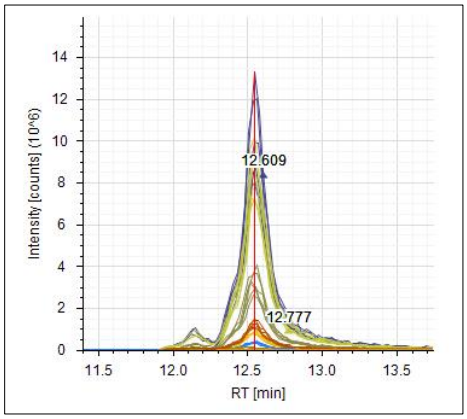

MS Spectrum

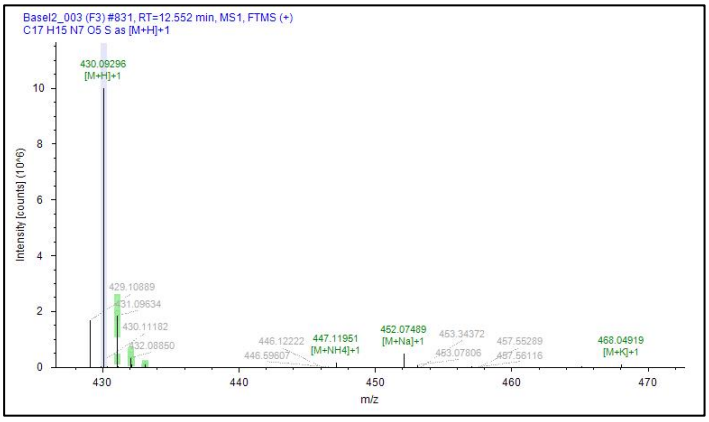

MS^2 Spectrum

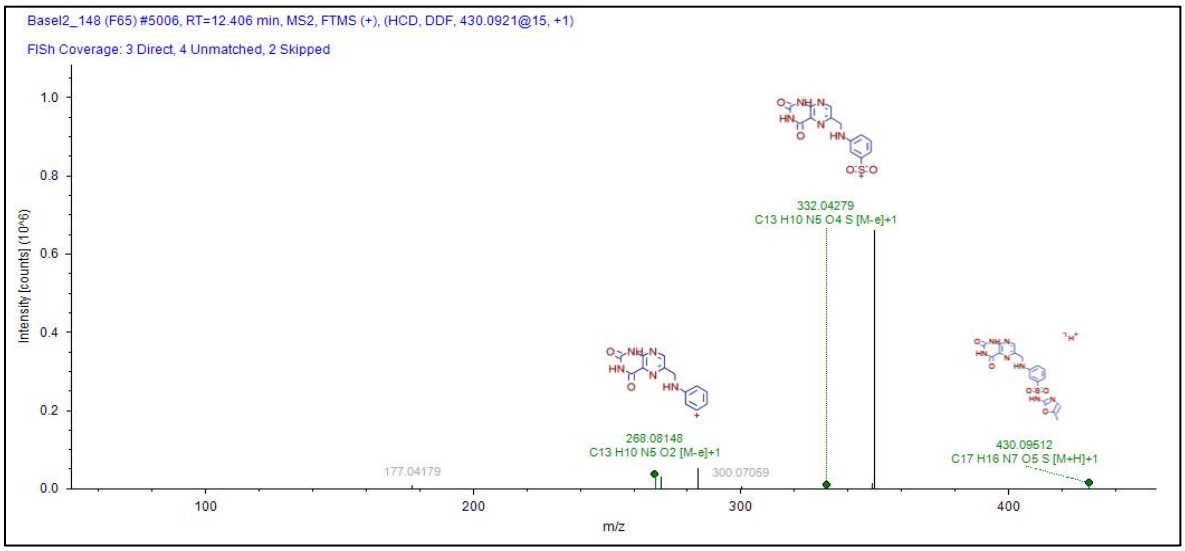

Formula:

C17 H15 N7 O5 S

Atomic Modification:

+ C7 H4 N4 O2

Proposed Structure:

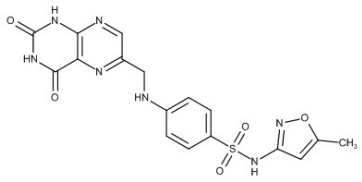

Confidence Level:

Level 2b

SMX: Pterin-SMX

Chromatogram

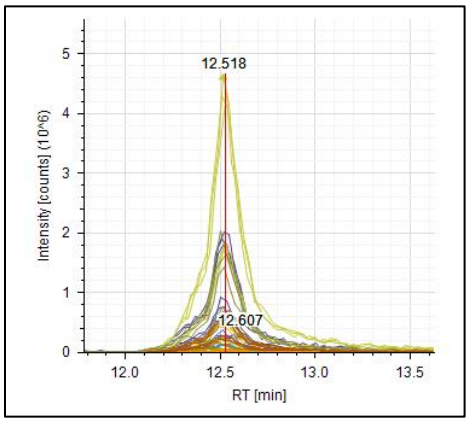

MS Spectrum

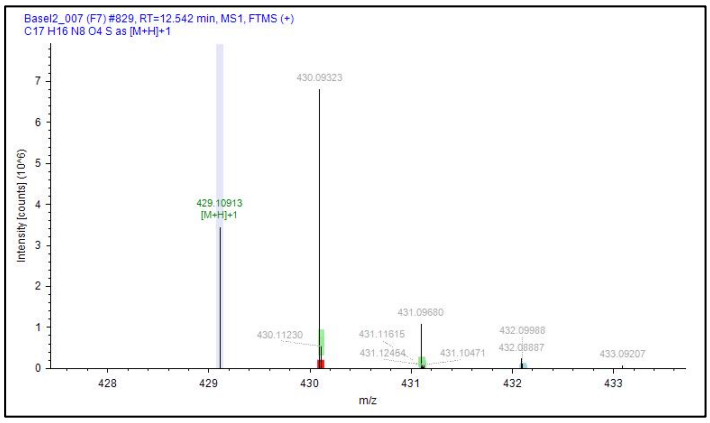

MS^2 Spectrum

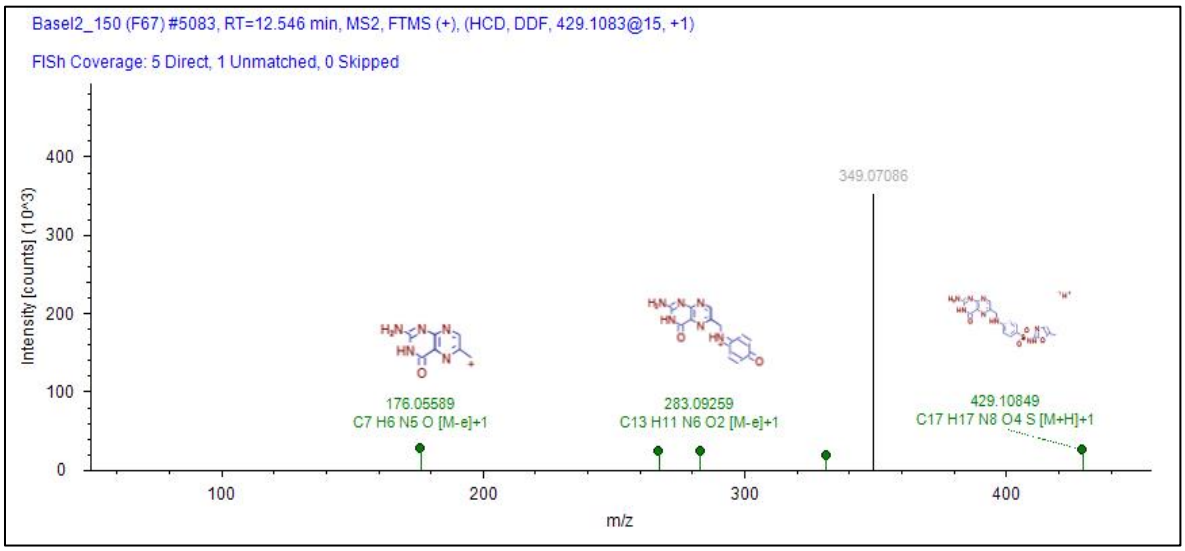

Formula:

C17 H16 N8 O4 S

Atomic Modification:

+ C7 H5 N5 O

Proposed Structure:

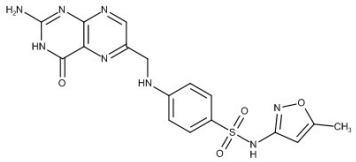

Confidence Level:

Level 2a

SMX: N4-formyl-SMX

Chromatogram

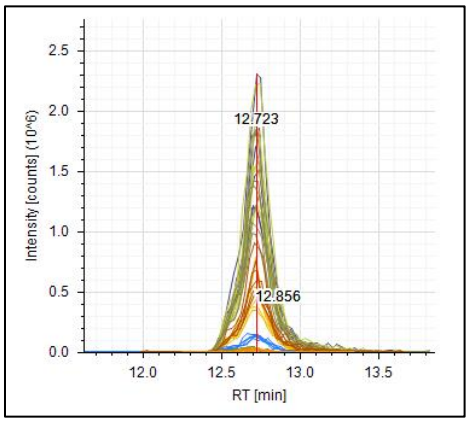

MS Spectrum

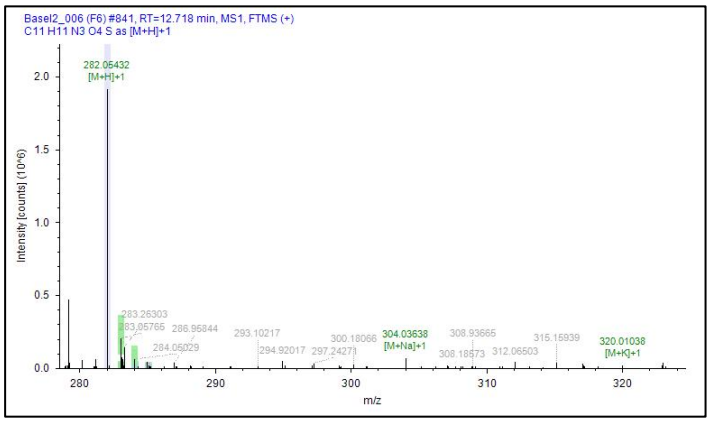

MS^2 Spectrum

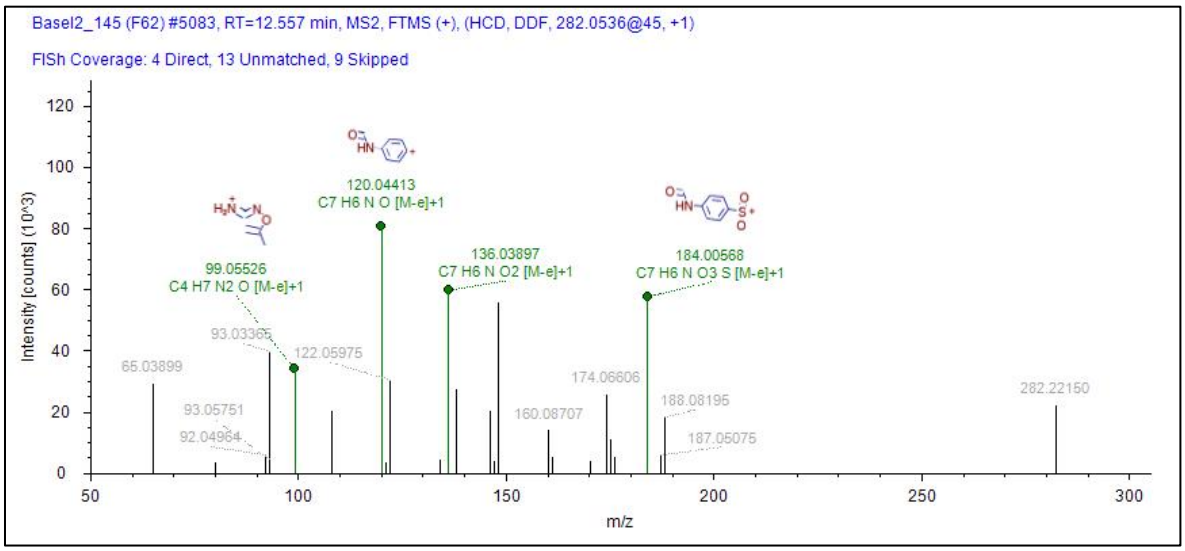

Formula:

C11 H11 N3 O4 S

Atomic Modification:

+ C O

Proposed Structure:

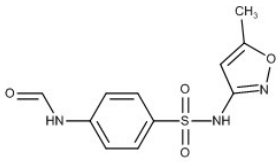

Confidence Level:

Level 2b

SMX: SMX + O

Chromatogram

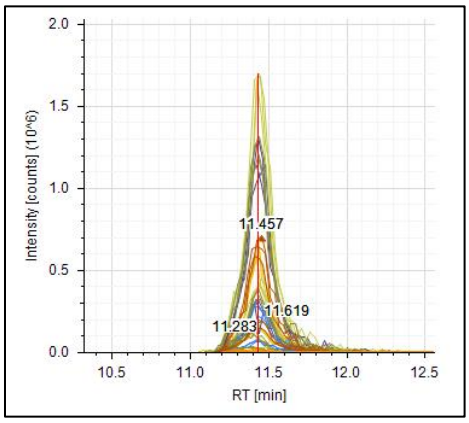

MS Spectrum

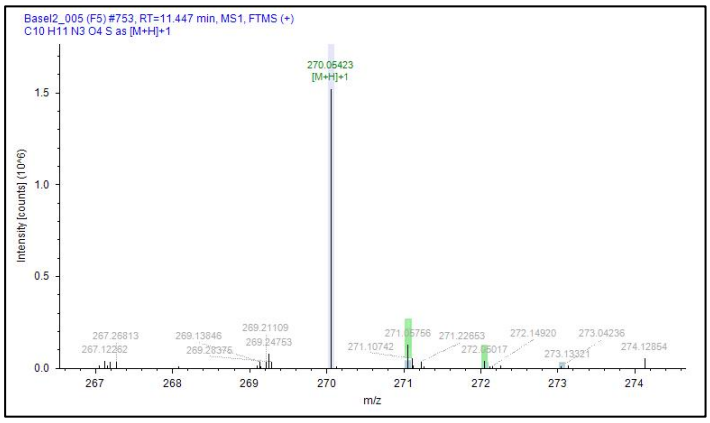

MS^2 Spectrum

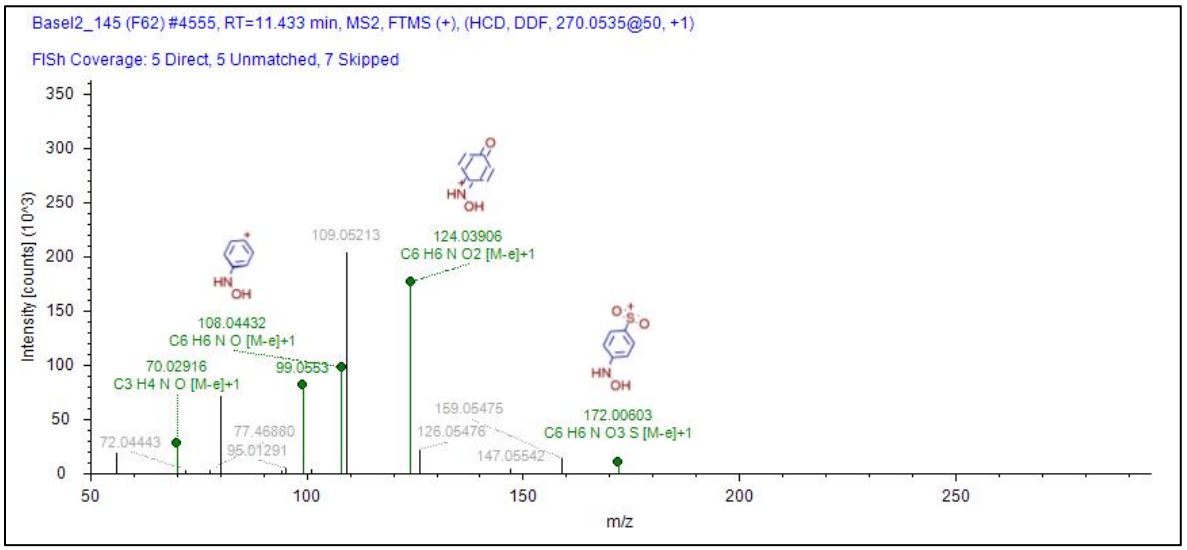

Formula:
C10 H11 N3 O4 S

Comment:
Alternative structures (e.g, hydroxylation at anilin-ring) might be possible.

Atomic Modification:
+ O

Proposed Structure:

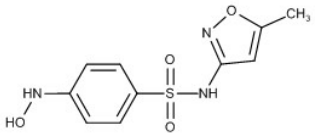

Confidence Level:
Level 3

SMX: 3-amino-5-methylisoxazole

Chromatogram

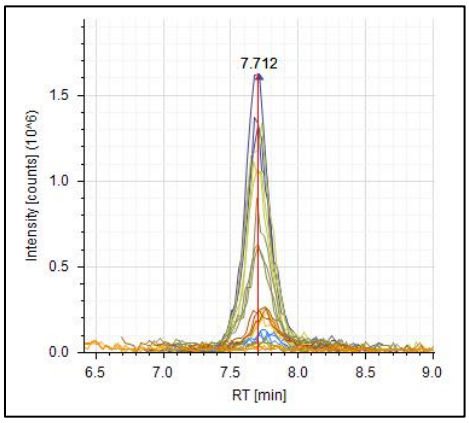

MS Spectrum

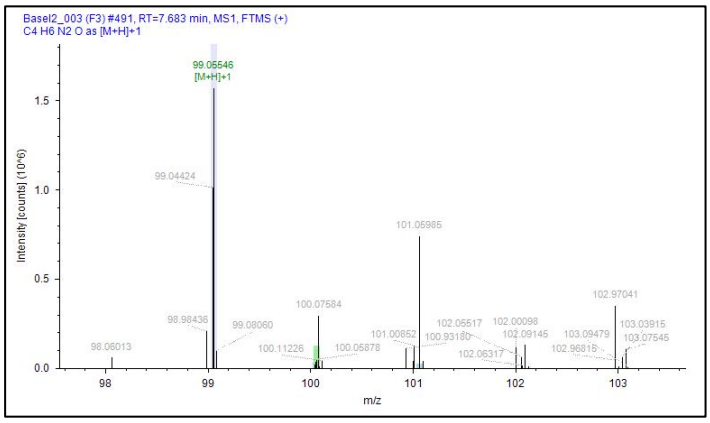

MS^2 Spectrum not available

Formula:

C4 H6 N2 O

Comment:

The structure of this transformation product was confirmed by a reference standard.

Atomic Modification:

- C6 H5 N O2 S

Proposed Structure:

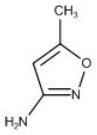

Confidence Level:

Level 1

SMX: Pterin-SMX + H_2O

Chromatogram

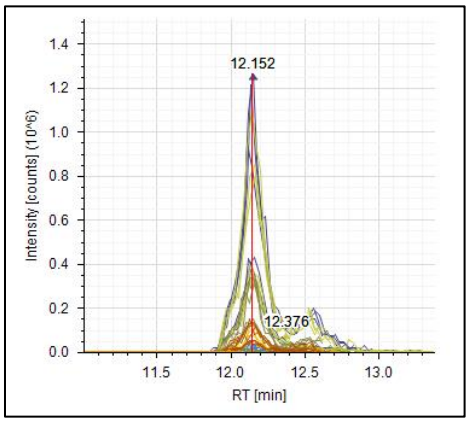

MS Spectrum

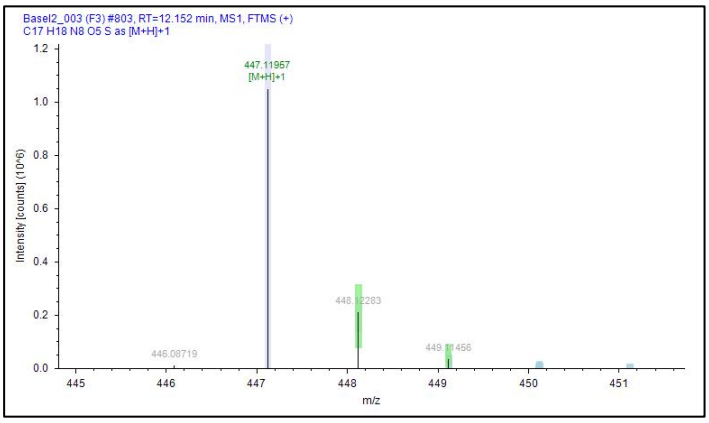

MS^2 Spectrum

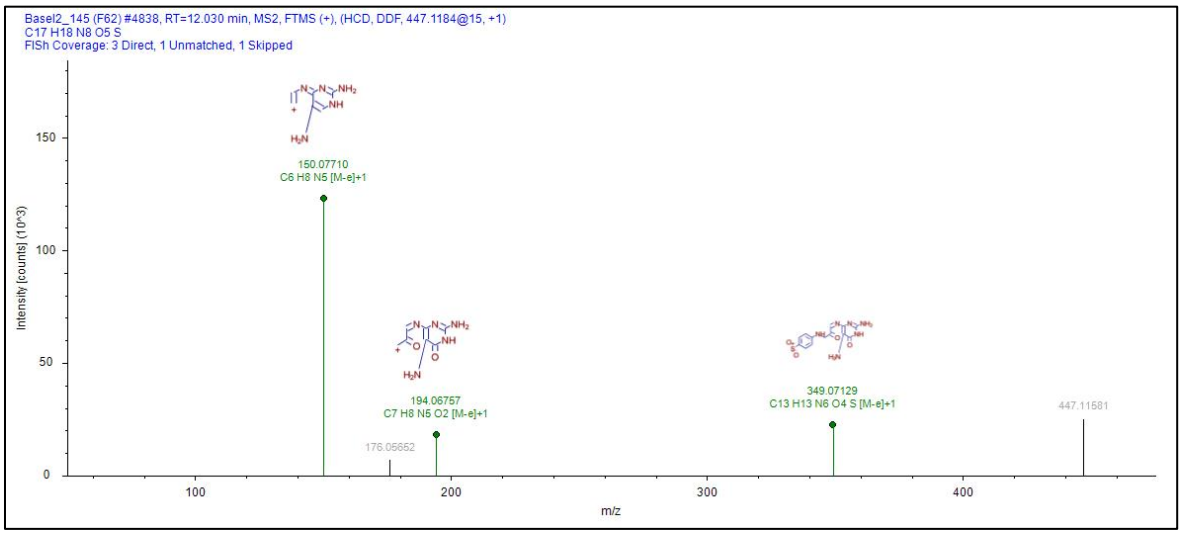

Formula:

C17 H18 N8 O5 S

Atomic Modification:

+ C7 H7 N5 O2

Comment:

Fragments matched with predictions for the two suggested structures. Unequivocal determination of the molecular structure was not further pursued.

Proposed Structures:

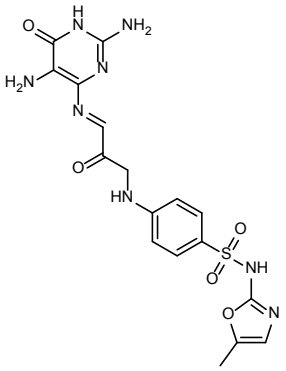

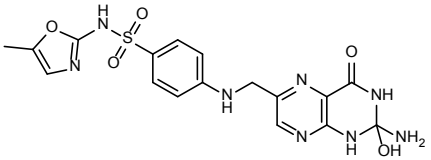

Confidence Level:

Level 3

SMX: Ac-OH-SMX

Chromatogram

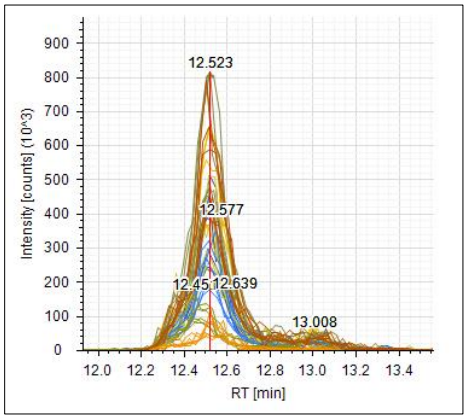

MS Spectrum

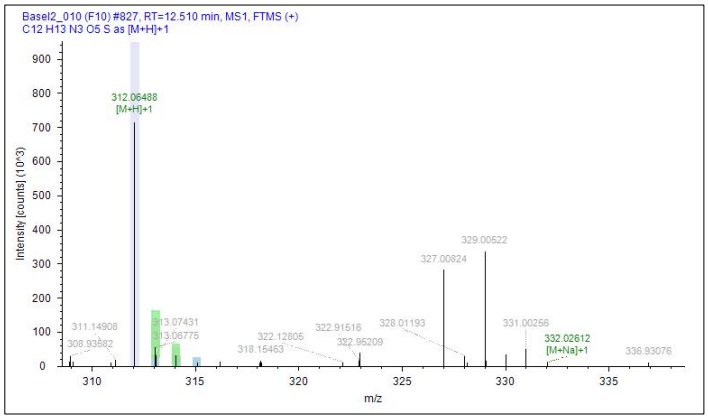

MS^2 Spectrum

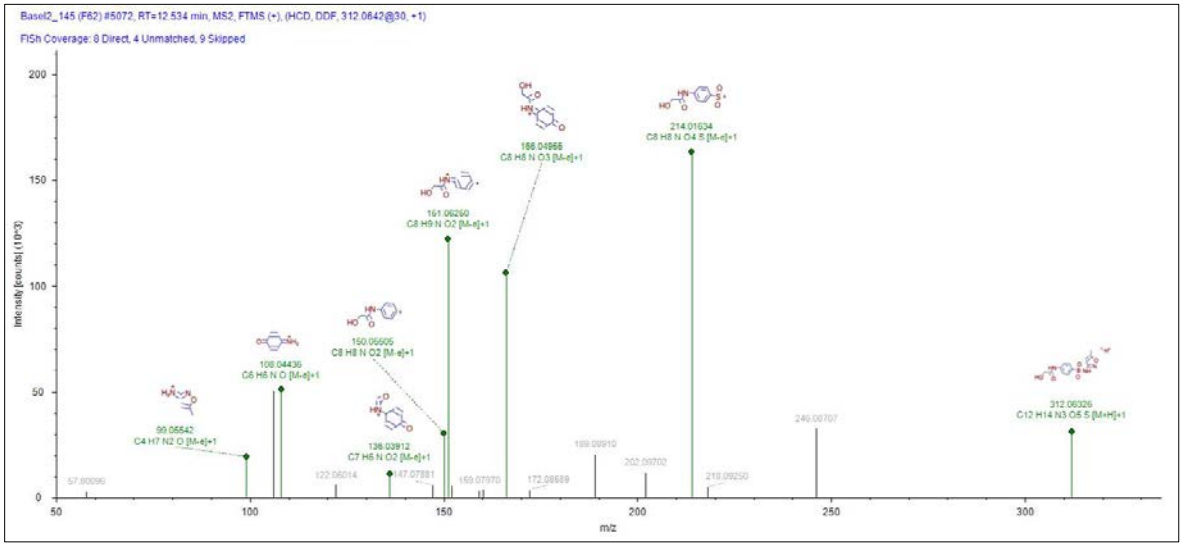

Formula:

C12 H13 N3 O5 S

Atomic Modification:

+ C2 H3 O2

Proposed Structure:

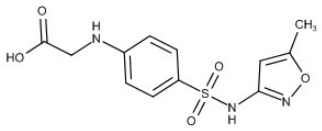

Confidence Level:

Level 3

SMX: N4-acetyl-SMX

Chromatogram

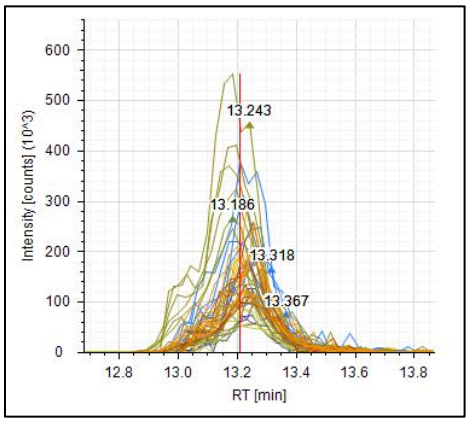

MS Spectrum

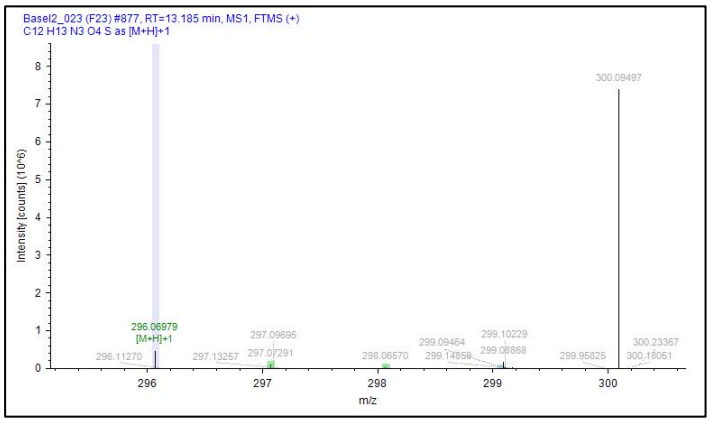

MS^2 Spectrum

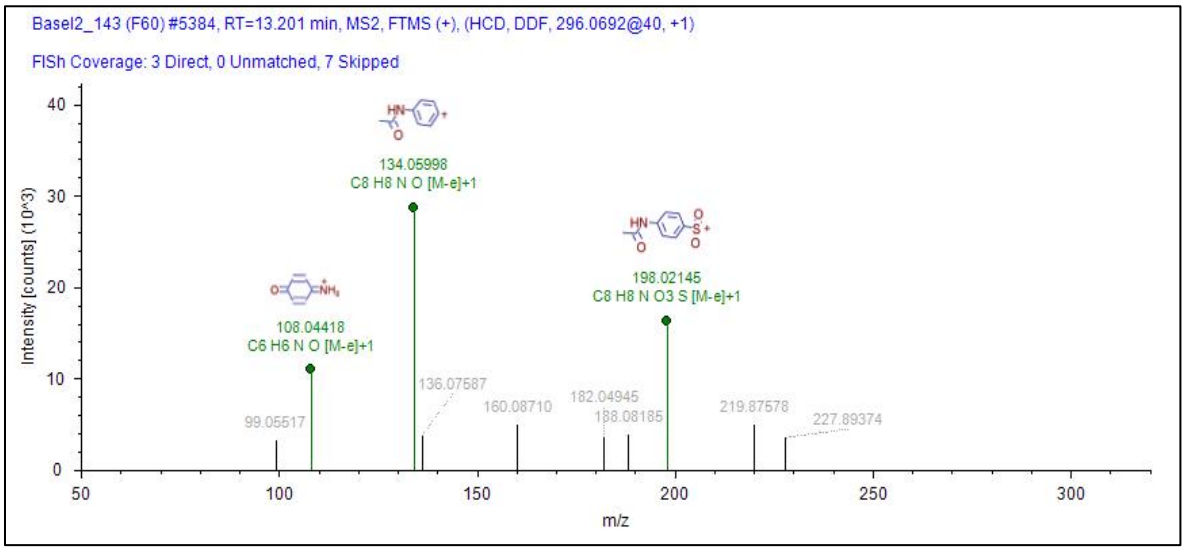

Formula:

C12 H13 N3 O5 S

Comment:

The structure of this transformation product was confirmed by a reference standard.

Atomic Modification:

+ C2 H2 O

Proposed Structure:

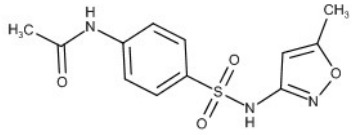

Confidence Level:

Level 1

SMX: 7,8-Dihydropterin-SMX

Chromatogram

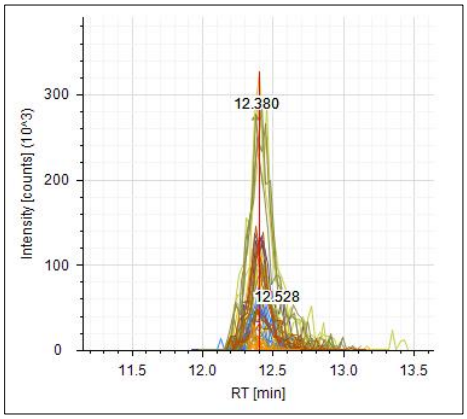

MS Spectrum

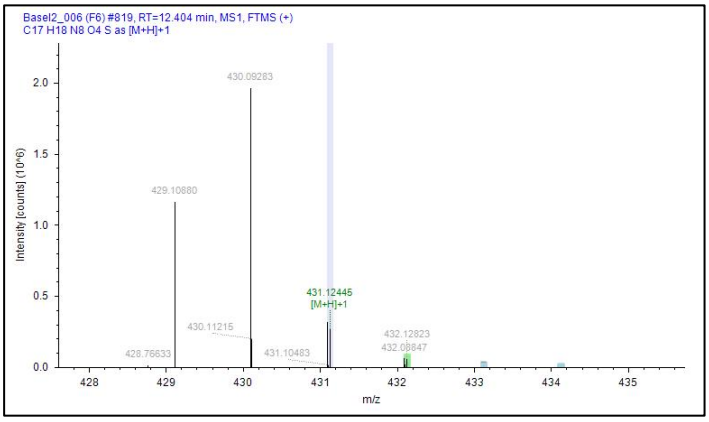

MS^2 Spectrum

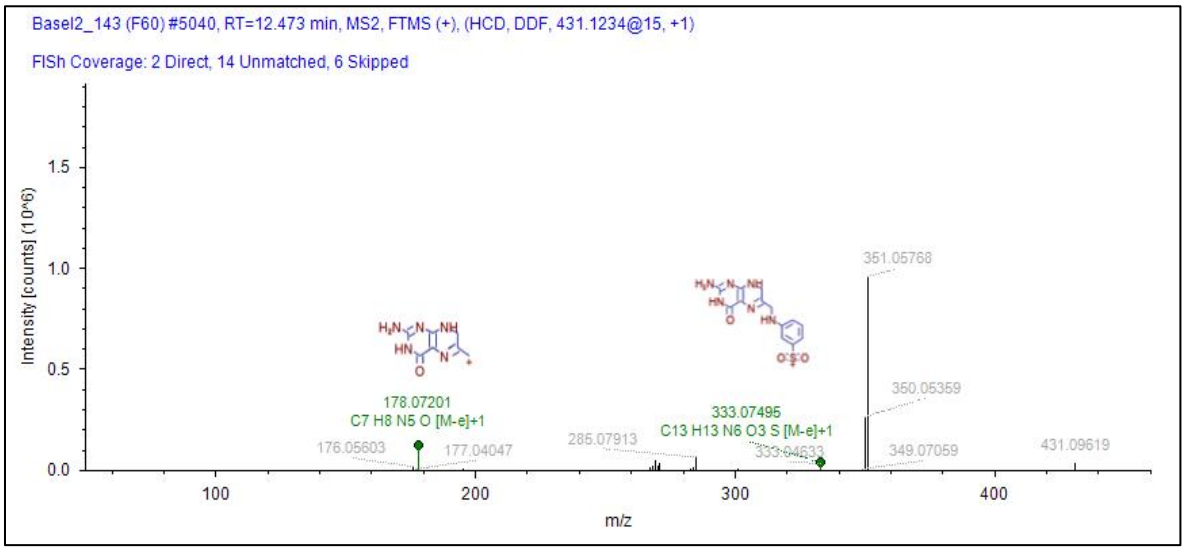

Formula:

C17 H18 N8 O4 S

Atomic Modification:

+ C7 H7 N5 O

Proposed Structure:

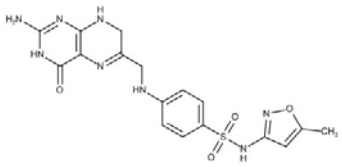

Confidence Level:

Level 3

SMX: Pterin-SMX + O

Chromatogram

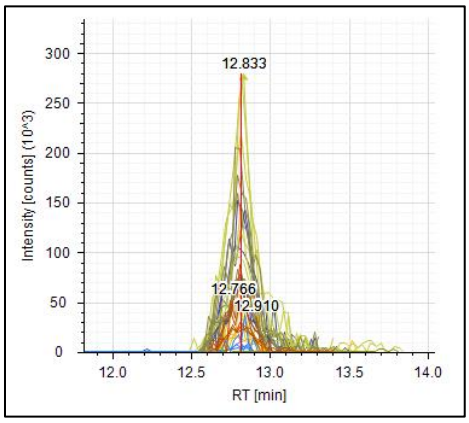

MS Spectrum

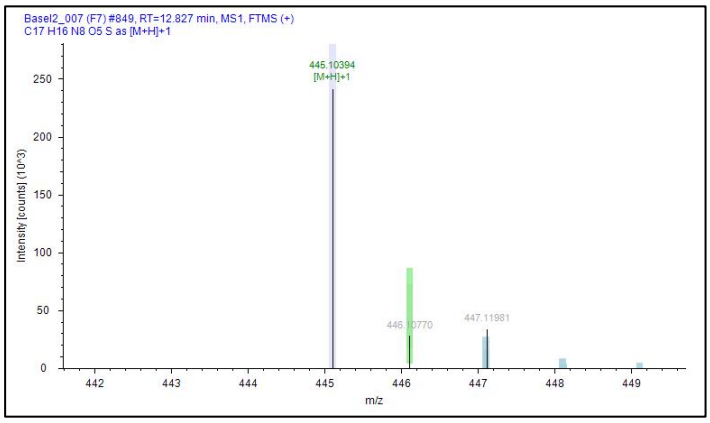

MS^2 Spectrum

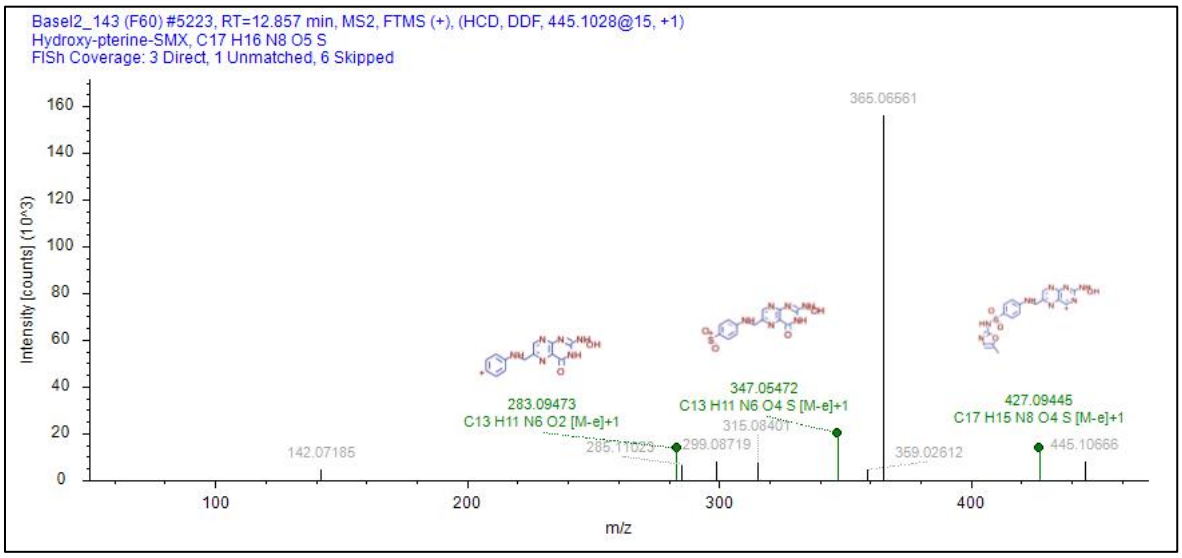

Formula:

C17 H16 N8 O5 S

Atomic Modification:

+ C7 H5 N5 O2

Comment:

Unequivocal determination of the molecular structure was not further pursued. Formation of the hydroxylamine-pterin-SMX represents one possible structure.

Confidence Level:

Level 4

SMX: SMX + $C_3H_2O_3$

Chromatogram

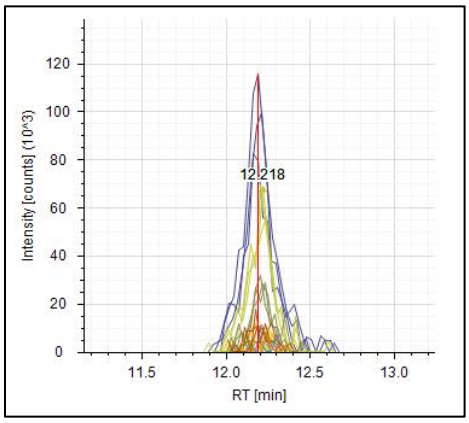

MS Spectrum

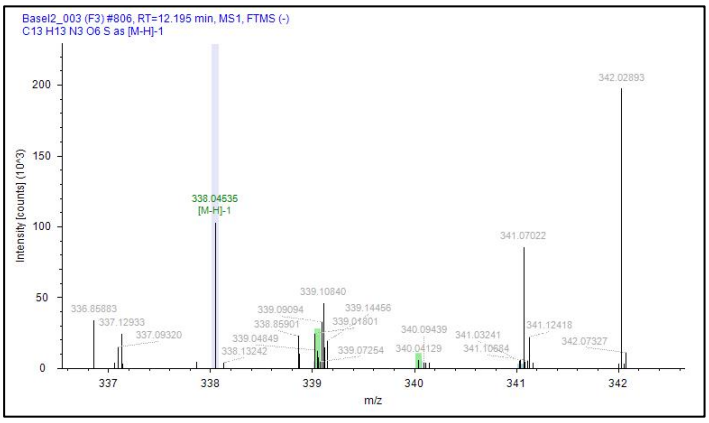

MS^2 Spectrum not available

Formula:

C13 H13 N8 O6 S

Atomic Modification:

+ C3 H2 O3

Confidence Level:

Level 4

SDZ: PtO-SDZ

Chromatogram

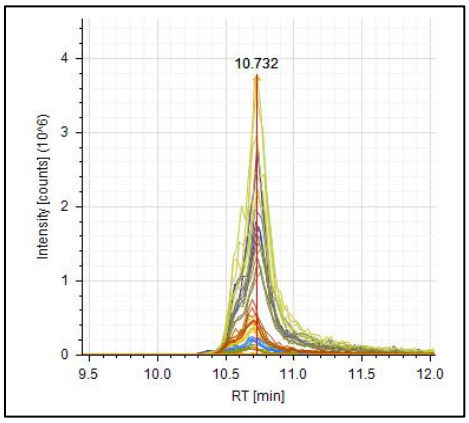

MS Spectrum

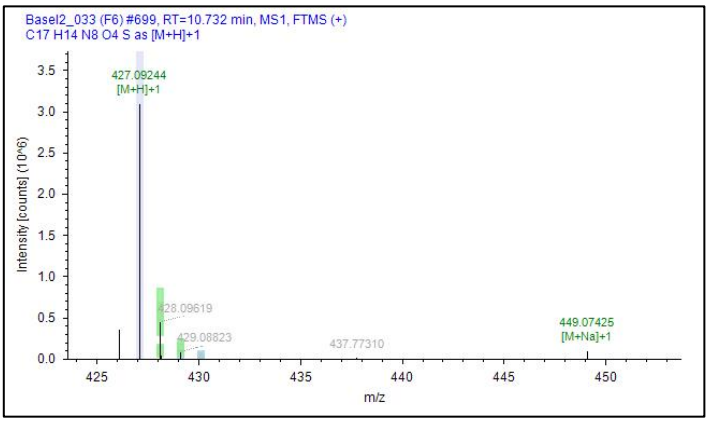

MS^2 Spectrum

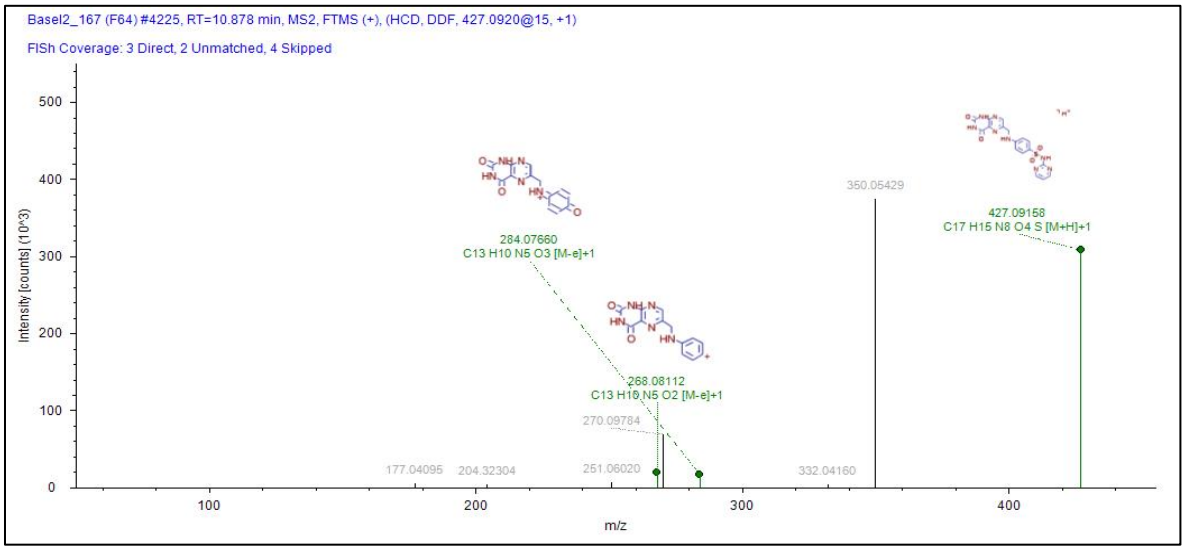

Formula:

C17 H14 N8 O4 S

Atomic Modification:

+ C7 H4 N4 O2

Proposed Structure:

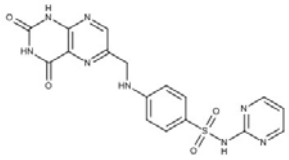

Confidence Level:

Level 2

SDZ: N4-formyl-SDZ

Chromatogram

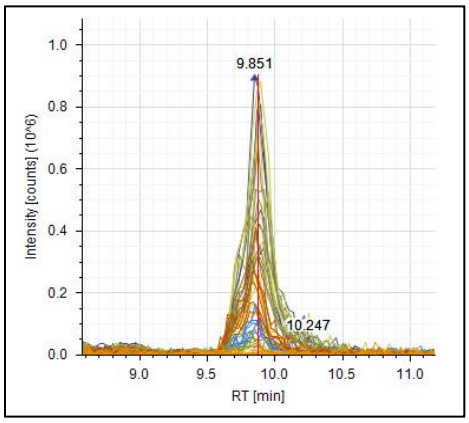

MS Spectrum

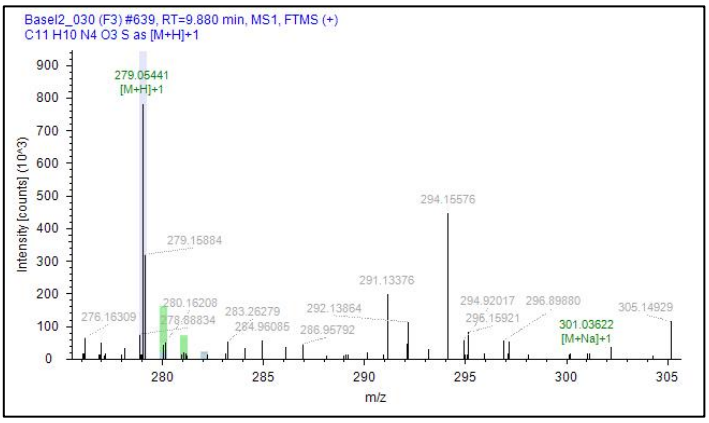

MS^2 Spectrum

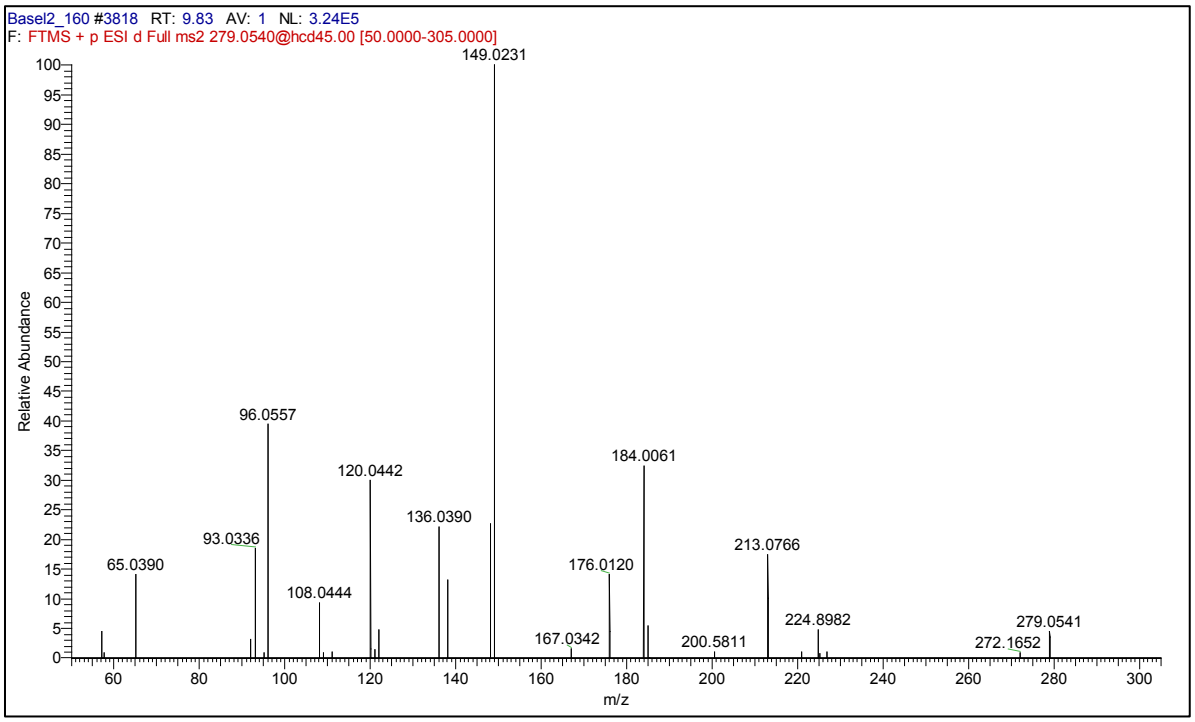

Formula:

C11 H10 N4 O3 S

Atomic Modification:

+ C O

Proposed Structure:

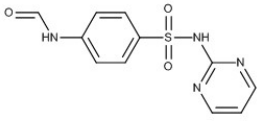

Confidence Level:

Level 2b

SDZ: SDZ + O

Chromatogram

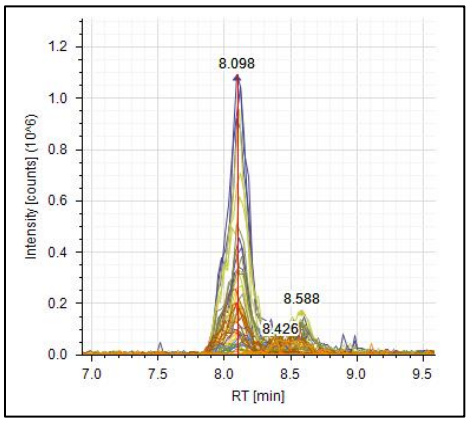

MS Spectrum

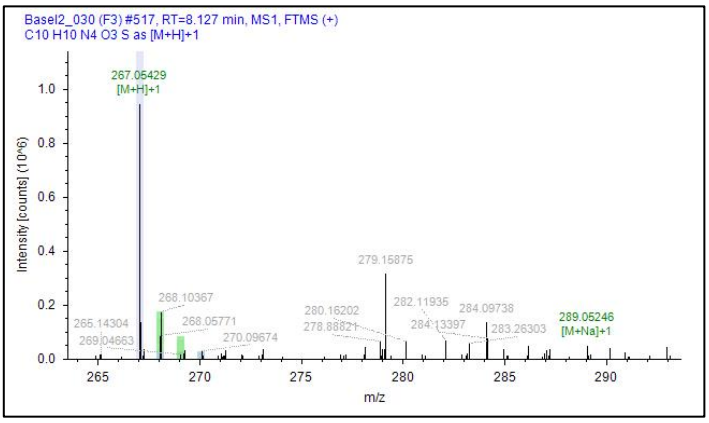

MS^2 Spectrum

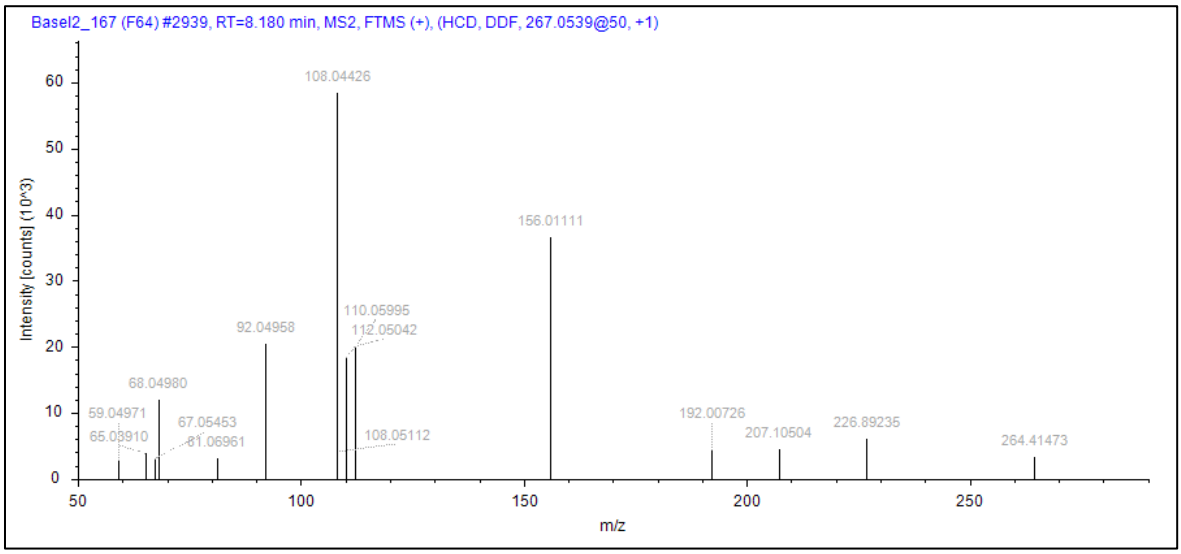

Formula:

C10 H10 N4 O3 S

Atomic Modification:

+ O

Confidence Level:

Level 4

SDZ: AcOH-SDZ

Chromatogram

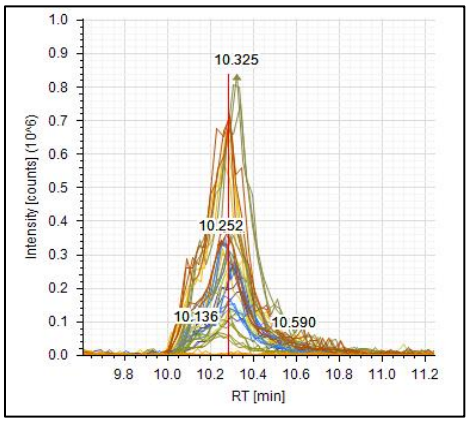

MS Spectrum

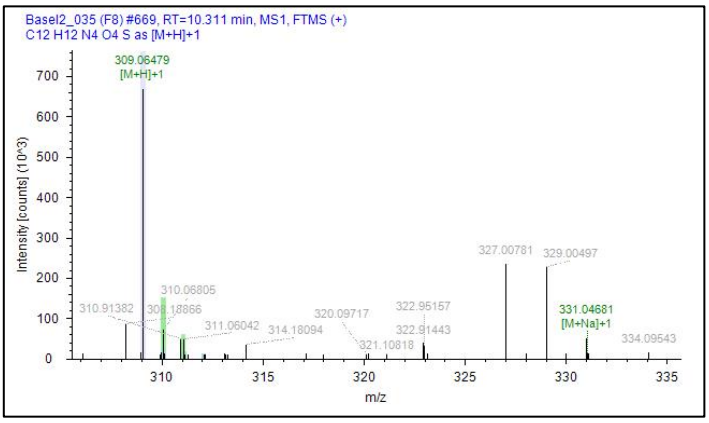

MS^2 Spectrum

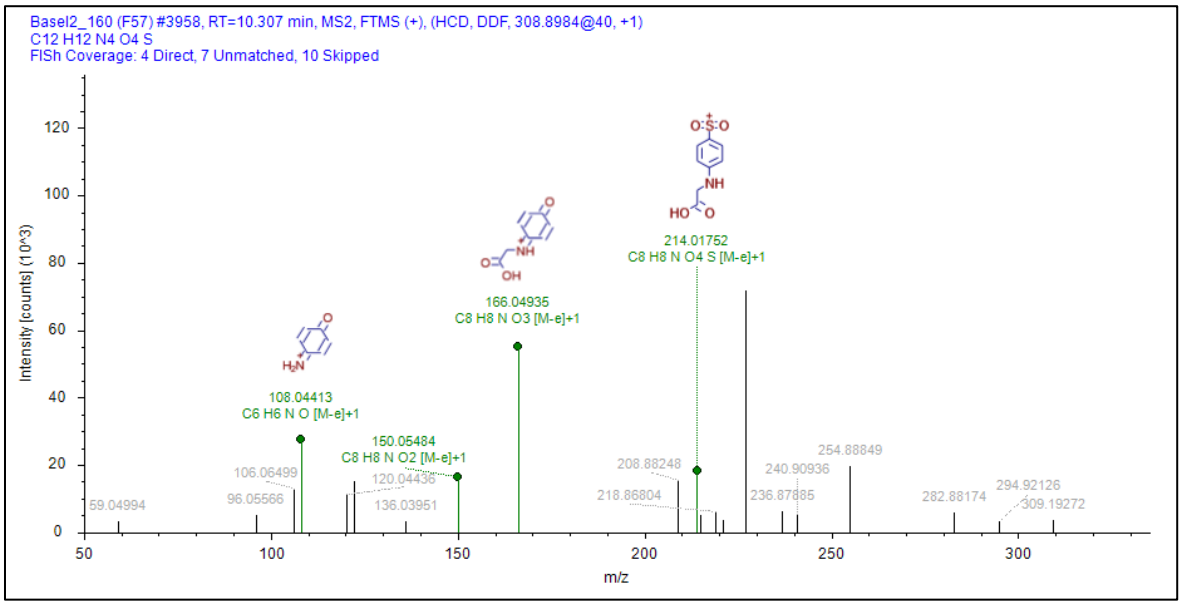

Formula:

C12 H12 N4 O4 S

Atomic Modification:

+ C2 H2 O2

Proposed Structures:

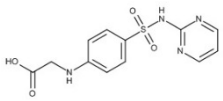

Confidence Level:

Level 3

SDZ: Pterin-SDZ

Chromatogram

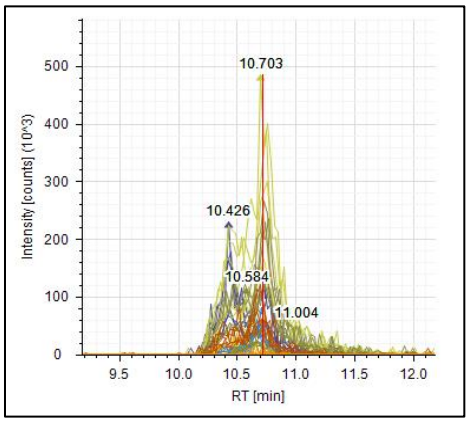

MS Spectrum

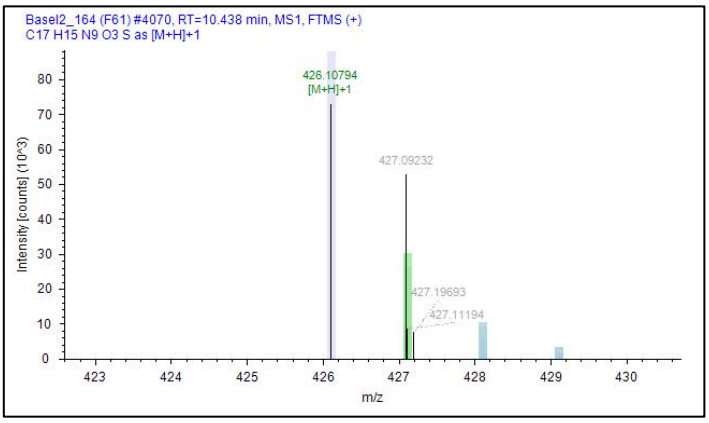

MS^2 Spectrum

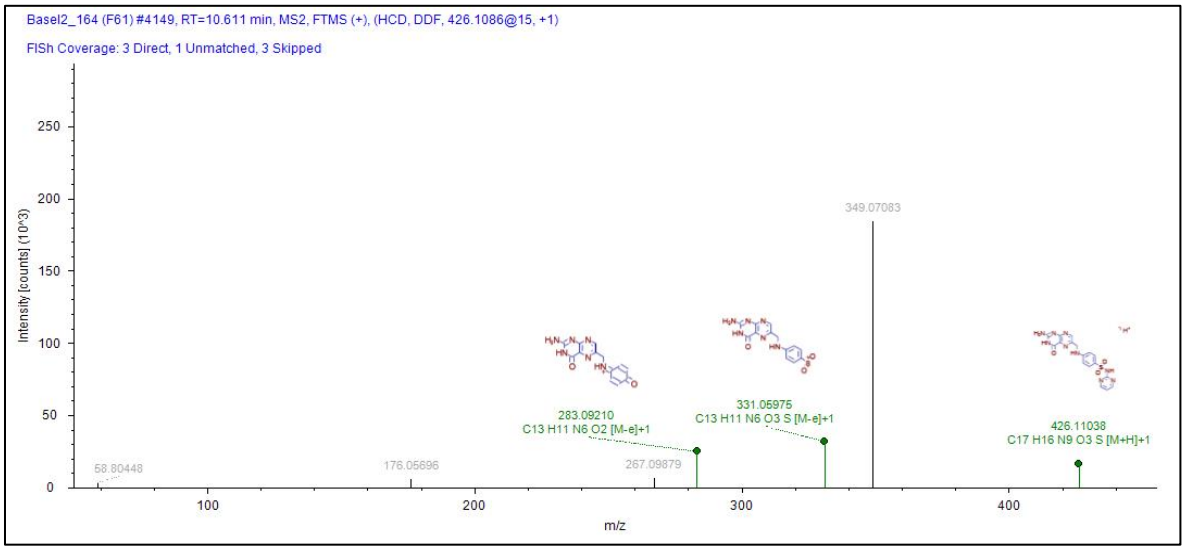

Formula:

C17 H15 N9 O3 S

Atomic Modification:

+ C7 H5 N5 O

Proposed Structure:

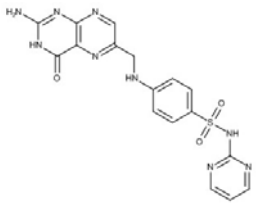

Confidence Level:

Level 2b

SDZ: Pterin-SDZ + O

Chromatogram

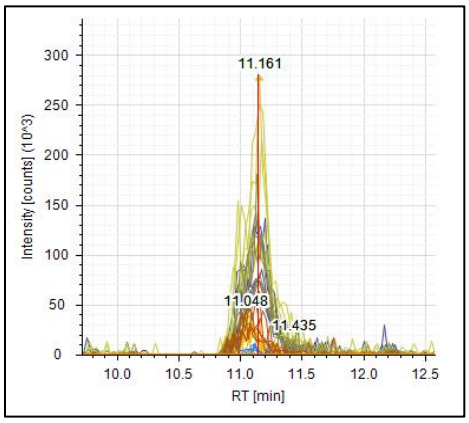

MS Spectrum

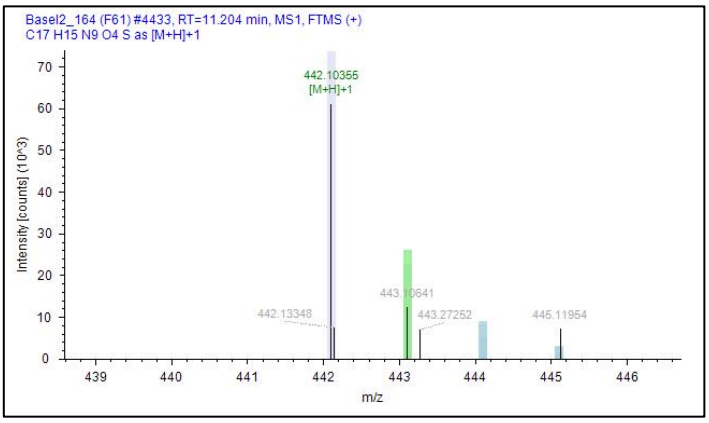

MS^2 Spectrum

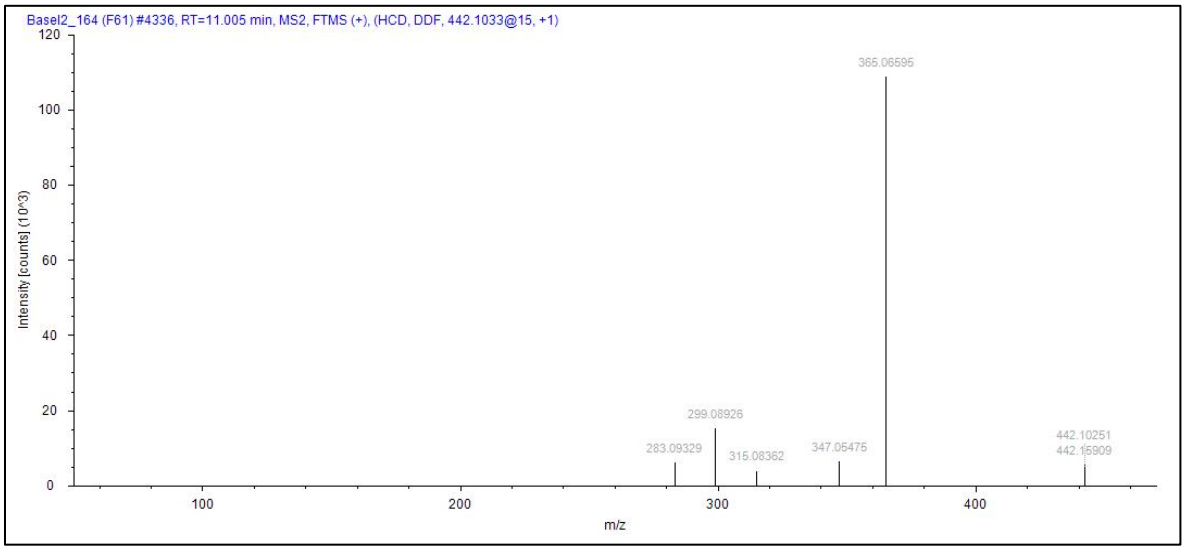

Formula:
C17 H17 N9 O4 S

Atomic Modification:
+ C7 H7 N5 O2

Confidence Level:
Level 4

SDZ: Pterin-SDZ + H_2O

Chromatogram

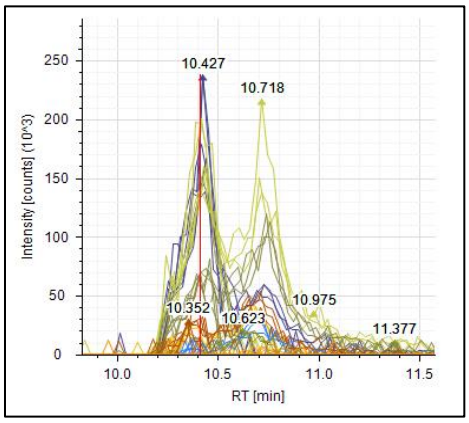

MS Spectrum

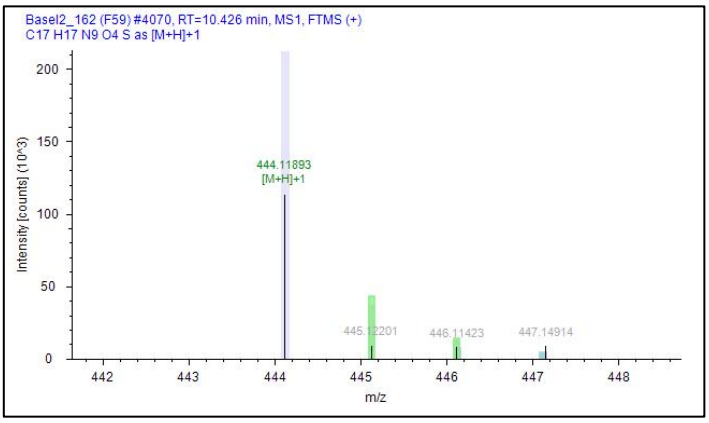

MS^2 Spectrum

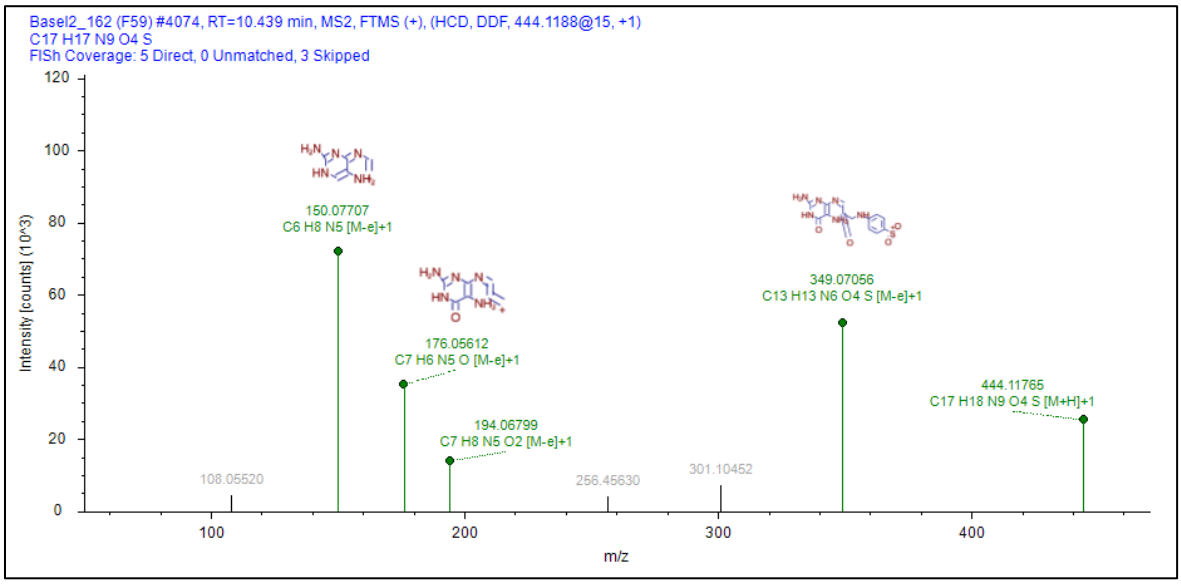

Formula:

C17 H17 N9 O4 S

Atomic Modification:

+ C7 H7 N5 O2

Comment:

Fragments match with predictions for the two suggested structures. Unequivocal determination of the molecular structure was not further pursued.

Proposed Structures:

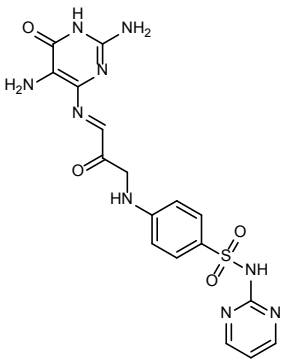

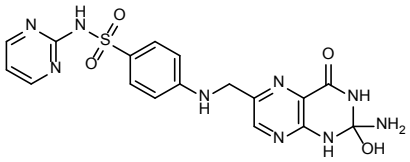

Confidence Level:

Level 3

SDZ: N4-acetyl-SDZ

Chromatogram

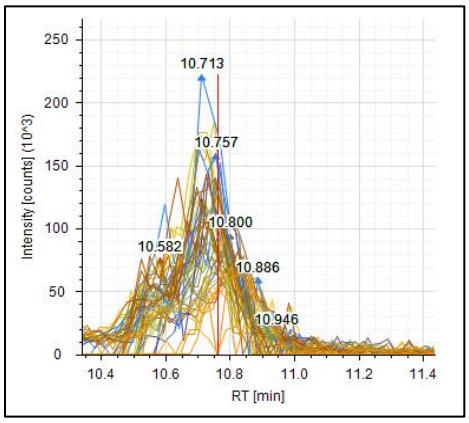

MS Spectrum

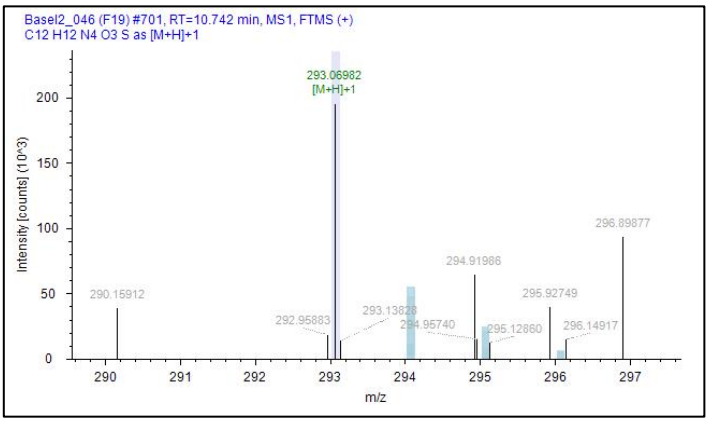

MS^2 Spectrum

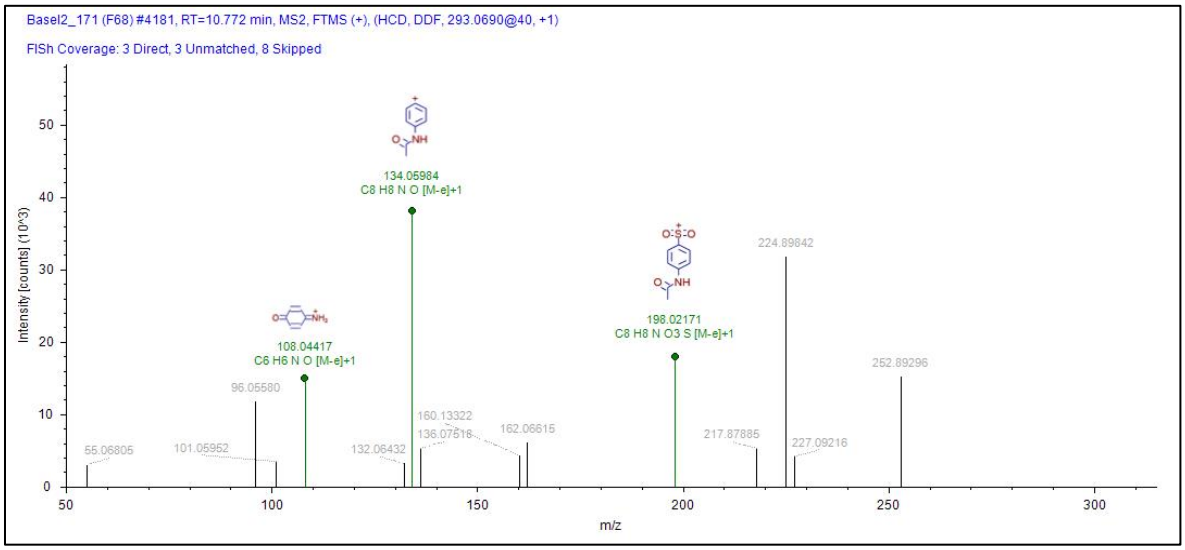

Formula:

C12 H12 N4 O3 S

Structure Interpretation:

The structure of this transformation product was confirmed by a reference standard.

Atomic Modification:

+ C2 H2 O

Proposed Structure:

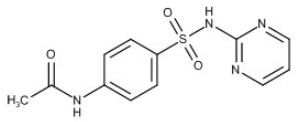

Confidence Level:

Level 1

SMZ: AcOH-SMZ

Chromatogram

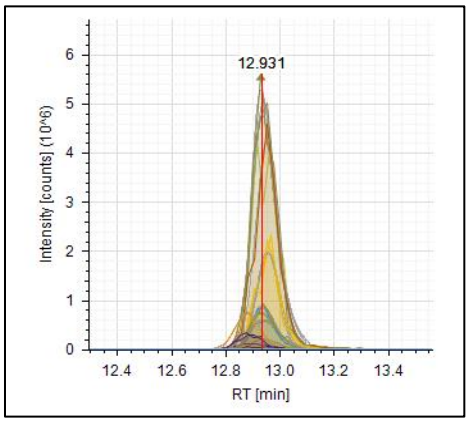

MS Spectrum

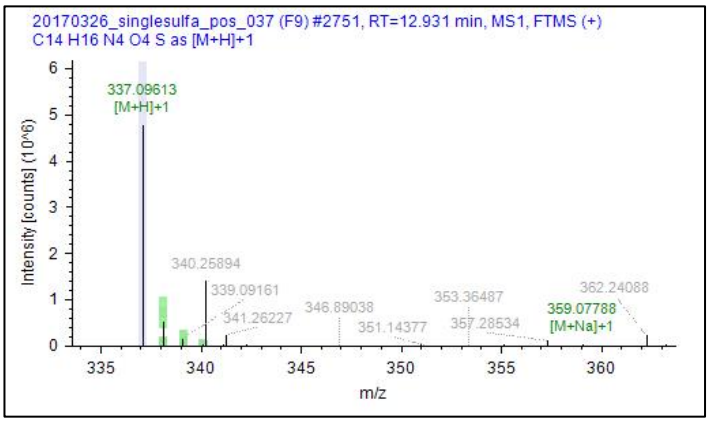

MS^2 Spectrum

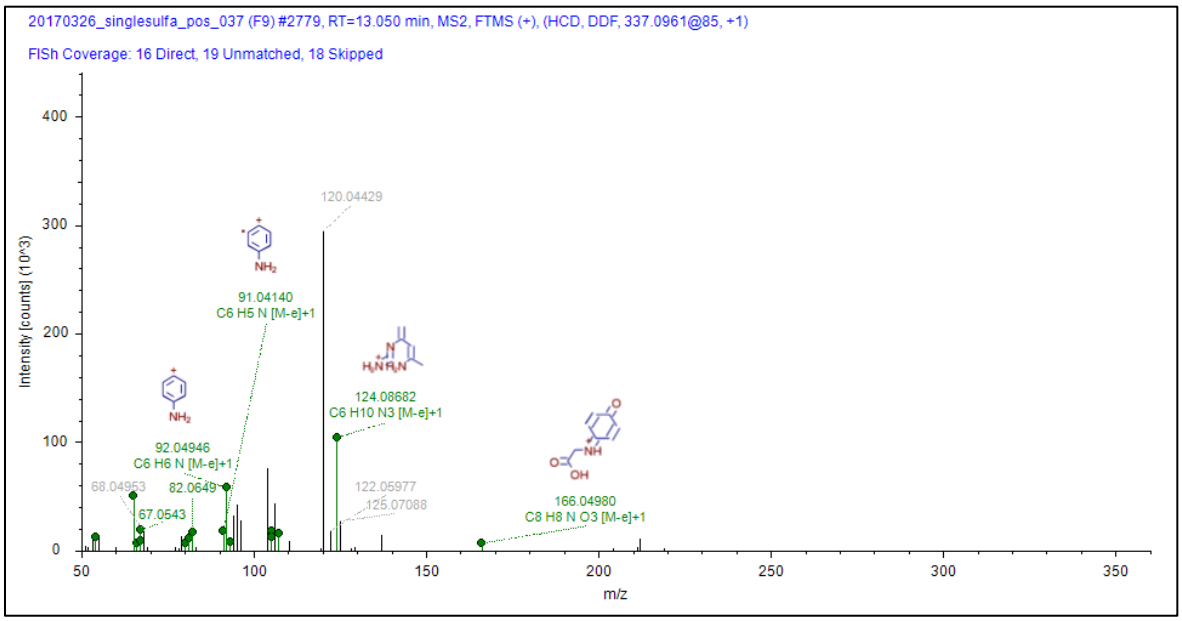

Formula:

C14 H16 N4 O4 S

Atomic Modification:

+ C2 H2 O2

Proposed Structure:

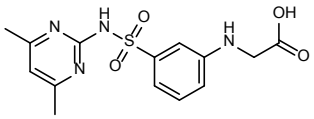

Confidence Level:

Level 3

SMZ: PtO-SMZ

Chromatogram

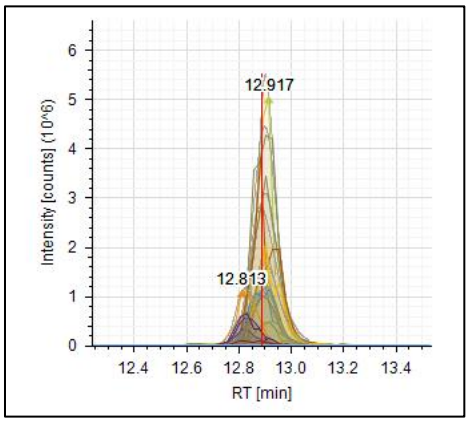

MS Spectrum

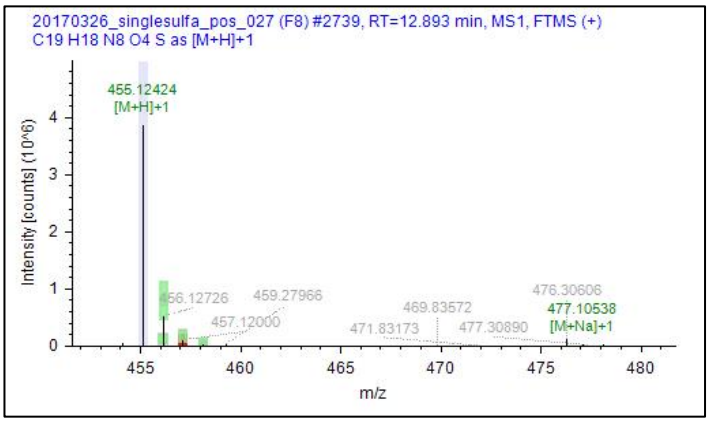

MS^2 Spectrum

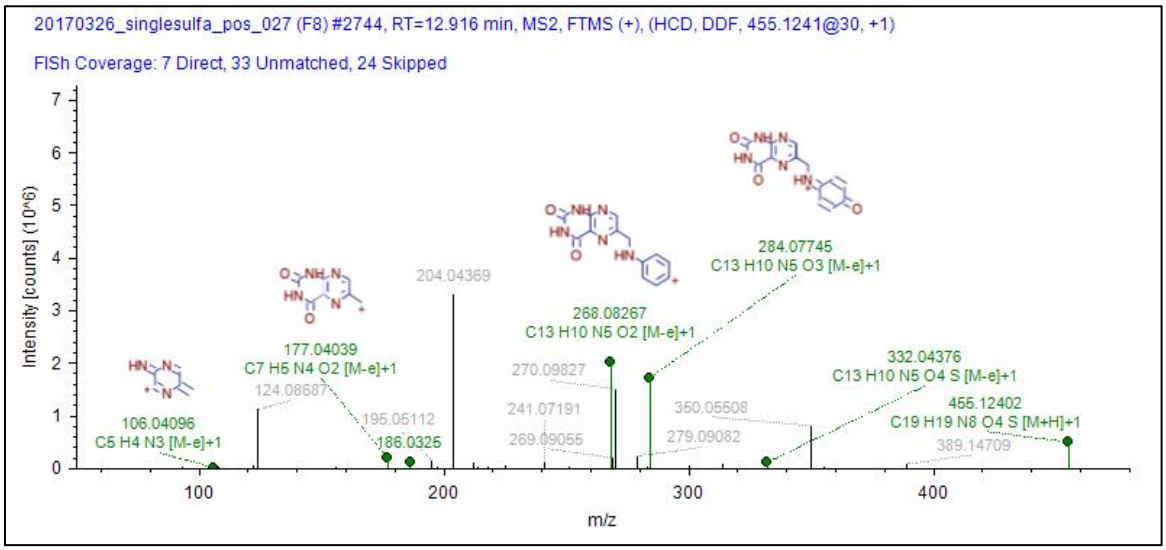

Formula:

C19 H18 N8 O4 S

Atomic Modification:

+ C7 H4 N4 O2

Proposed Structure:

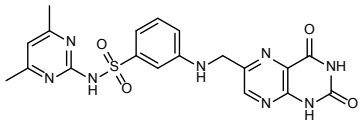

Confidence Level:

Level 2b

SMZ: N4-acetyl-SMZ

Chromatogram

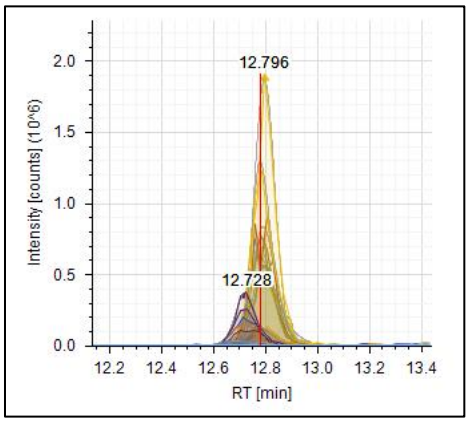

MS Spectrum

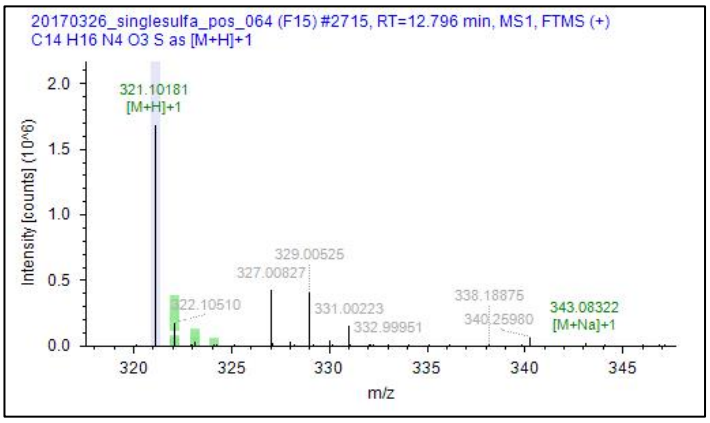

MS^2 Spectrum

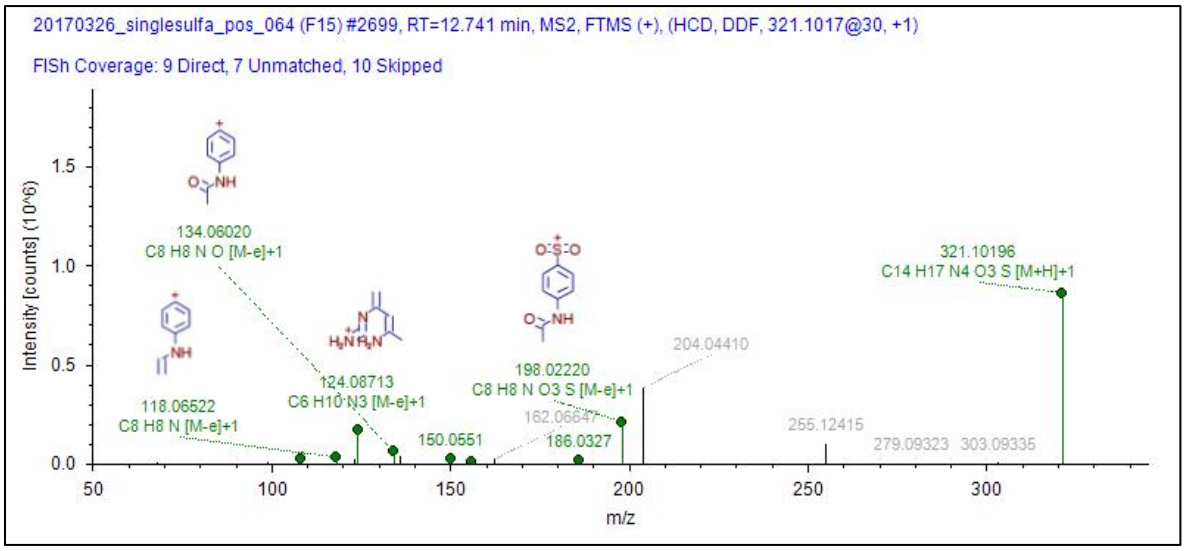

Formula:

C14 H16 N4 O3 S

Structure Interpretation:

The structure of this transformation product was confirmed by a reference standard.

Atomic Modification:

+ C2 H2 O

Proposed Structure:

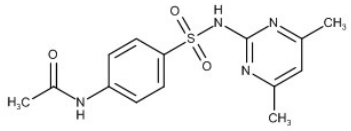

Confidence Level:

Level 1

SMZ: N4-formyl-SMZ

Chromatogram

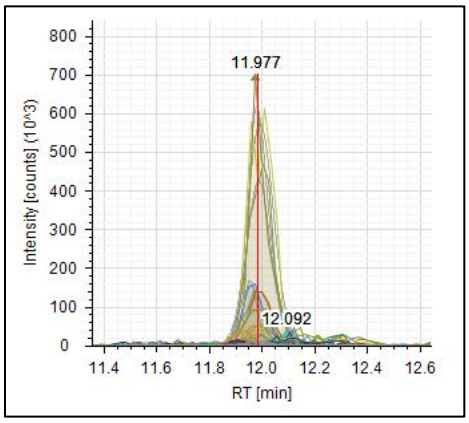

MS Spectrum

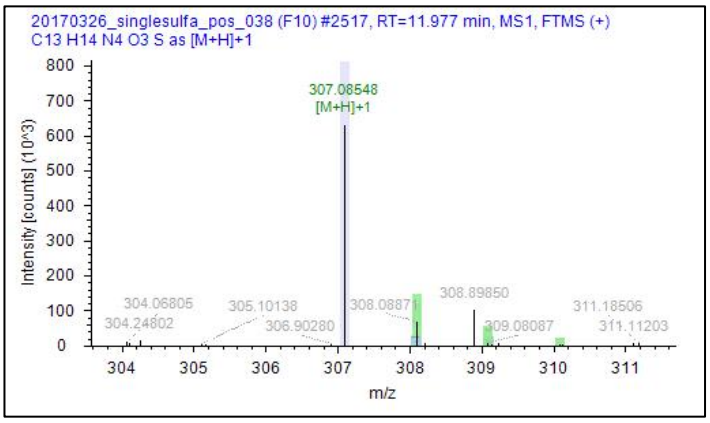

MS^2 Spectrum

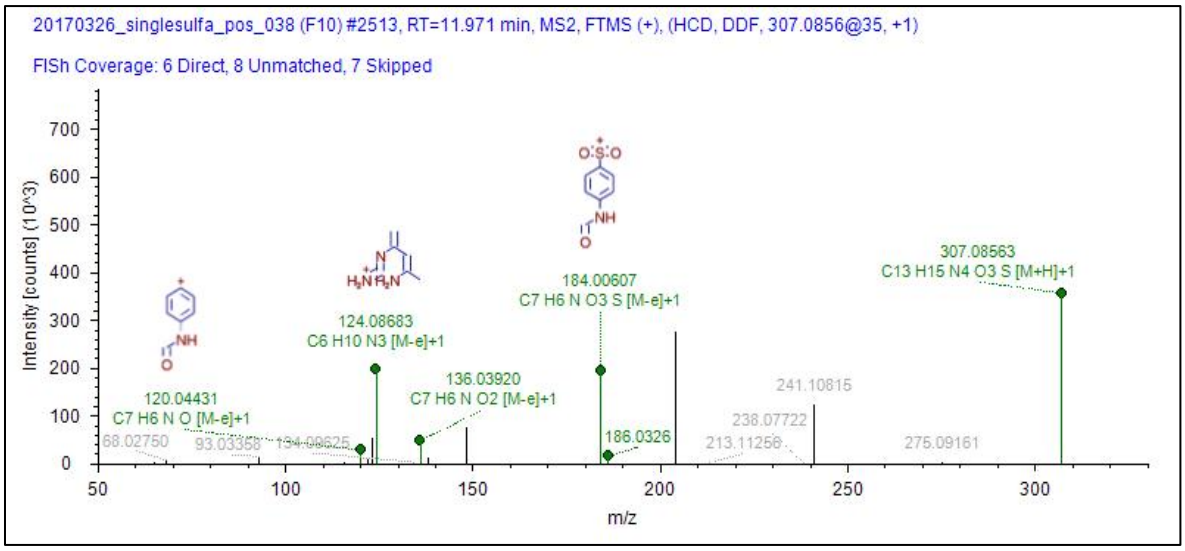

Formula:

C13 H14 N4 O3 S

Atomic Modification:

+ CO

Proposed Structure:

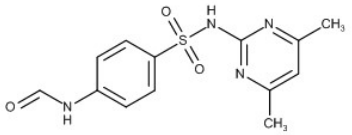

Confidence Level:

Level 2b

SMZ: SMZ + O

Chromatogram

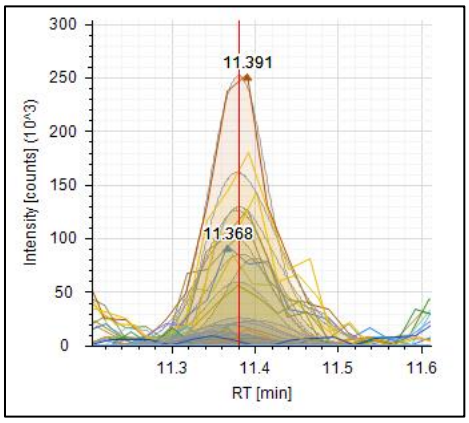

MS Spectrum

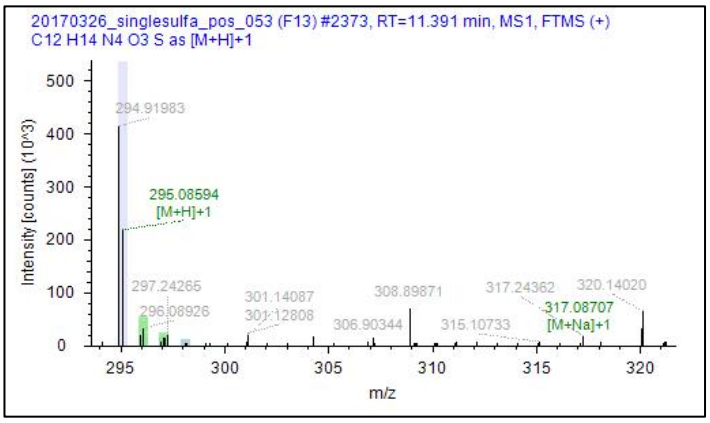

MS^2 Spectrum

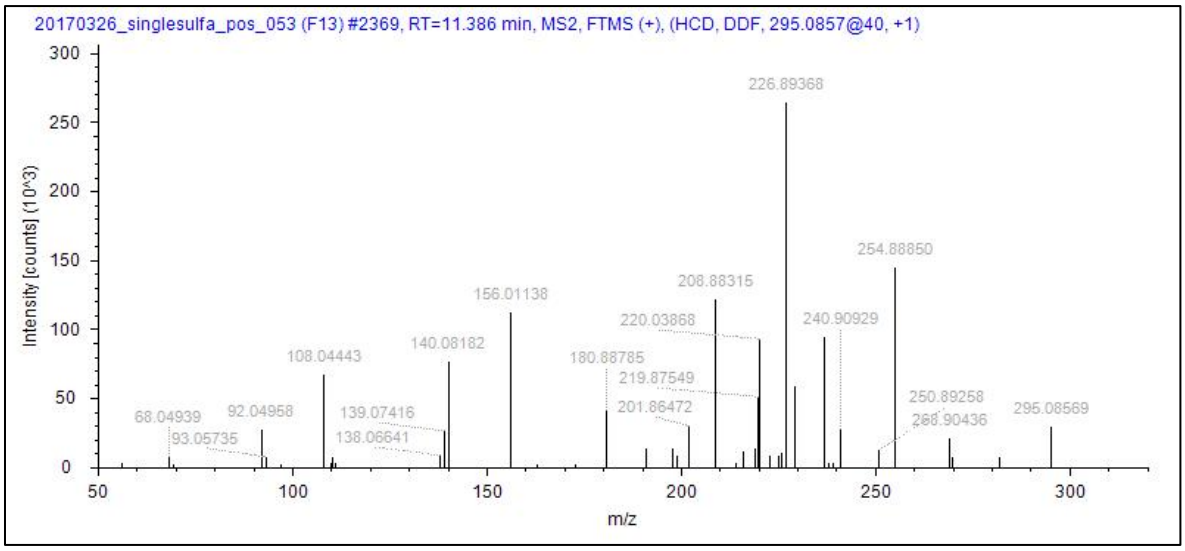

Formula:

C12 H14 N4 O3 S

Atomic Modification:

+ O

Confidence Level:

Level 4

SMZ: 2-amino-4,6-dimethylpyrimidine

Chromatogram

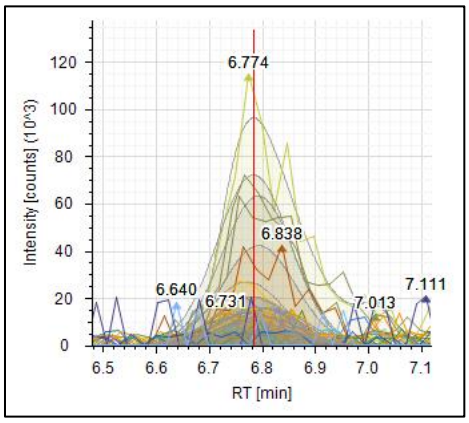

MS Spectrum

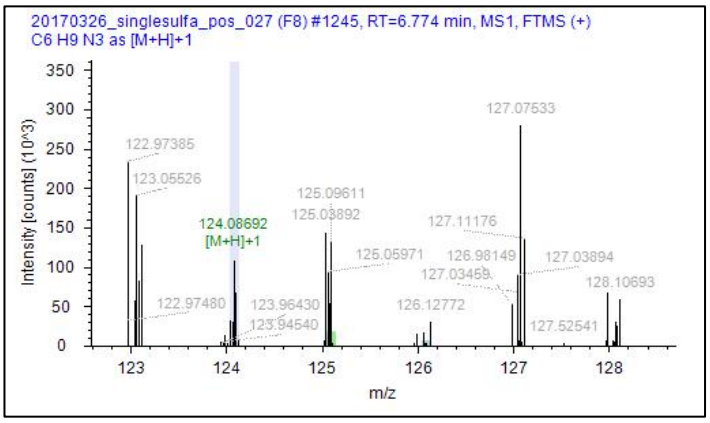

MS^2 Spectrum

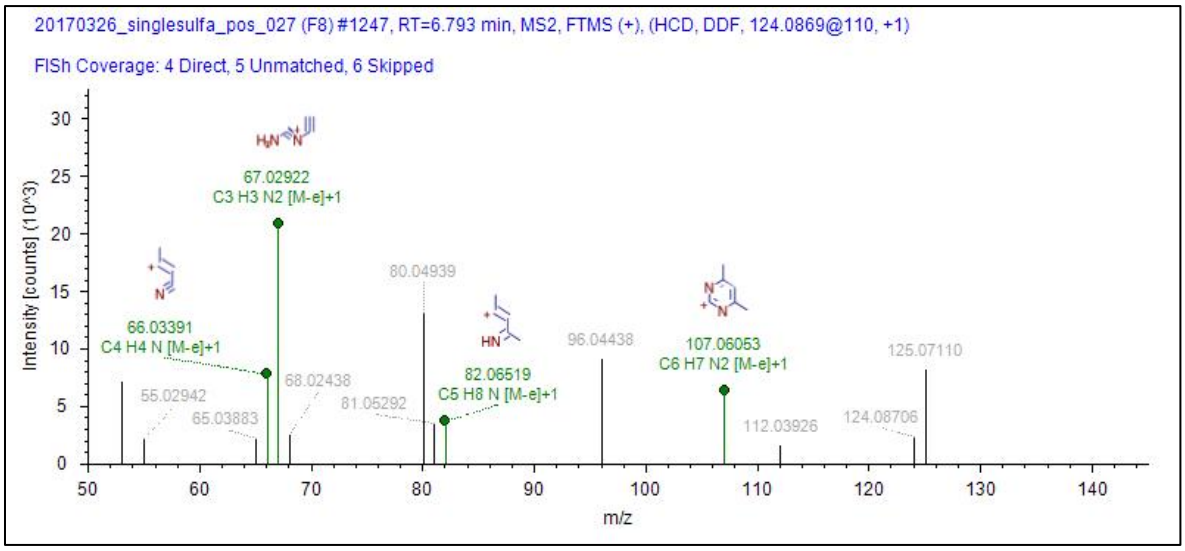

Formula:

C6 H9 N3

Atomic Modification:

- C6 H5 N O2 S

Proposed Structure:

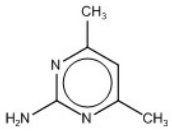

Confidence Level:

Level 2b

SMZ: Pterin-SMZ

Chromatogram

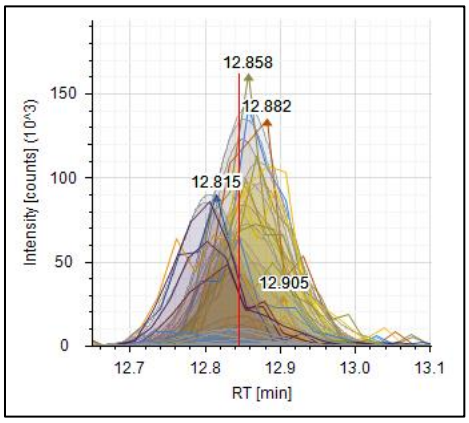

MS Spectrum

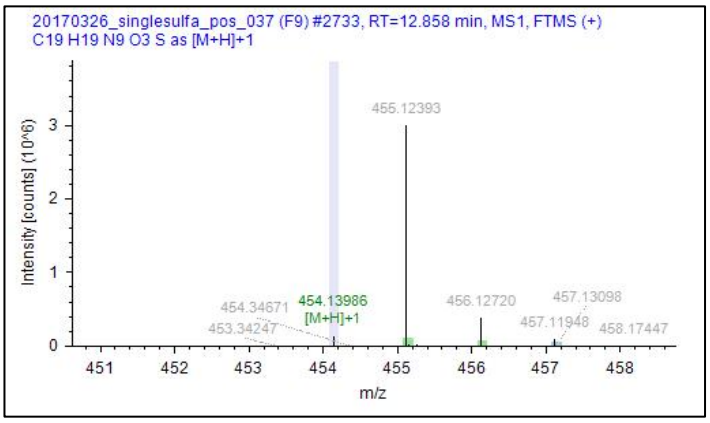

MS^2 Spectrum

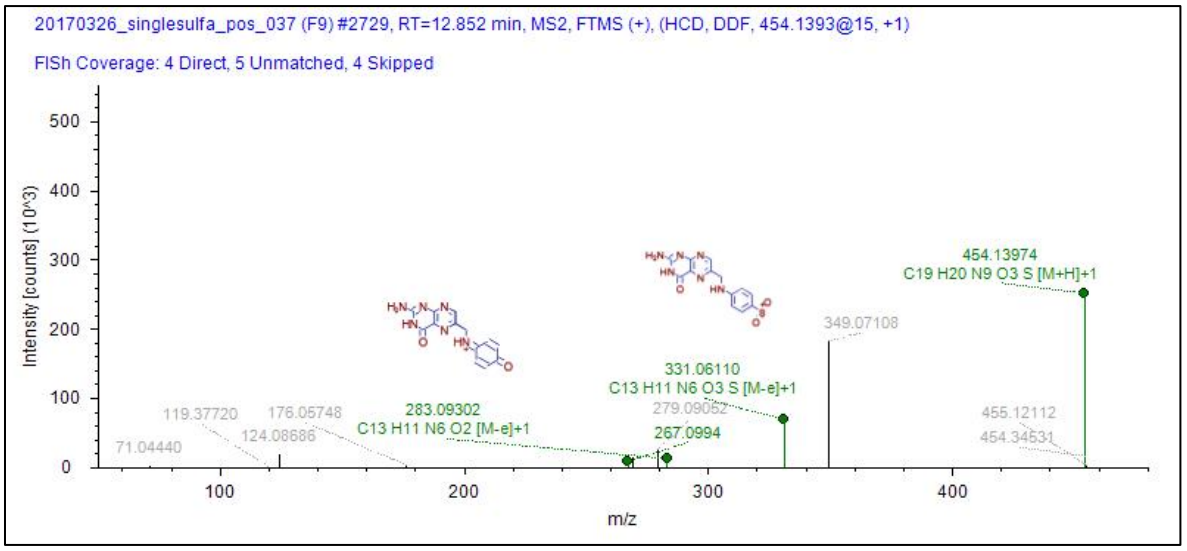

Formula:

C19 H19 N9 O3 S

Atomic Modification:

+ C7 H5 N5 O

Proposed Structure:

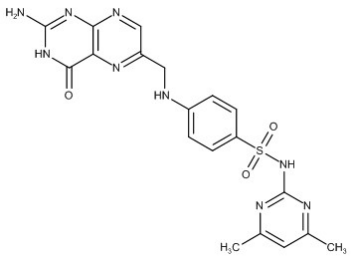

Confidence Level:

Level 2b

STZ: AcOH-STZ

Chromatogram

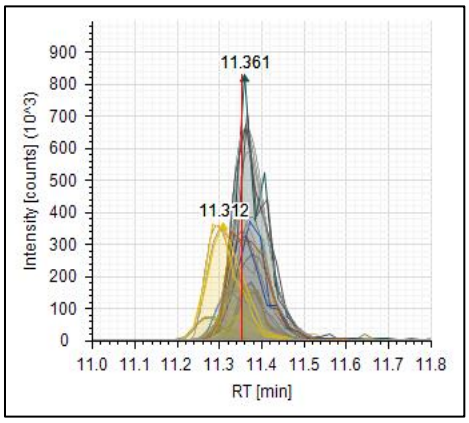

MS Spectrum

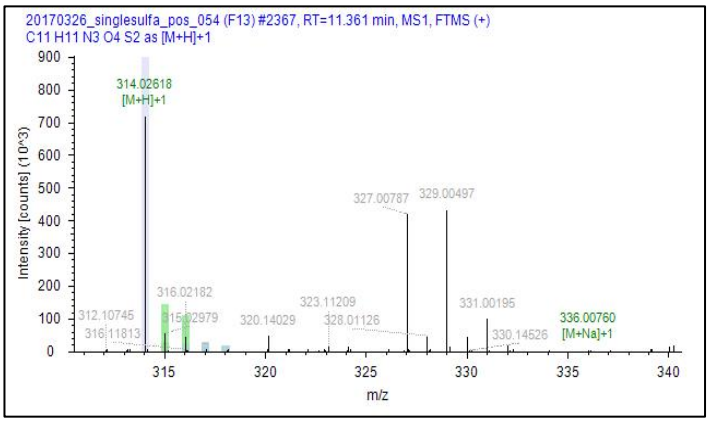

MS^2 spectrum not available

Formula:

C11 H11 N3 O4 S2

Atomic Modification:

+ C2 H2 O2

Proposed Structure:

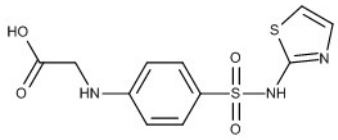

Confidence Level:

Level 3

STZ: PtO-STZ

Chromatogram

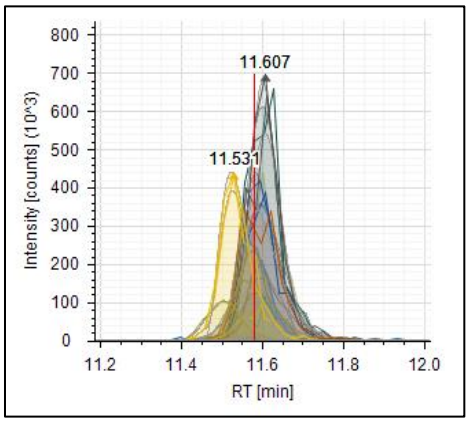

MS Spectrum

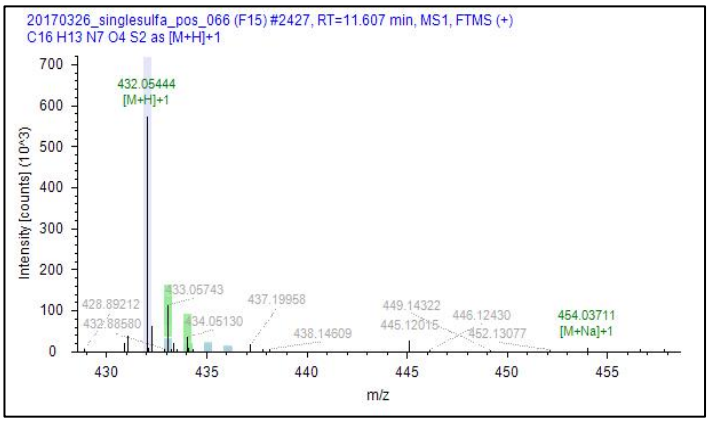

MS^2 spectrum not available

Formula:

C16 H13 N7 O4 S2

Atomic Modification:

+ C7 H6 N5 O2

Proposed Structure:

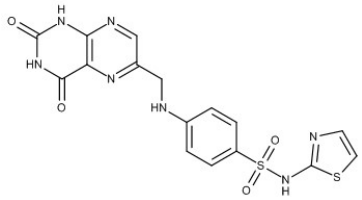

Confidence Level:

Level 2b

STZ: Pterin-STZ

Chromatogram

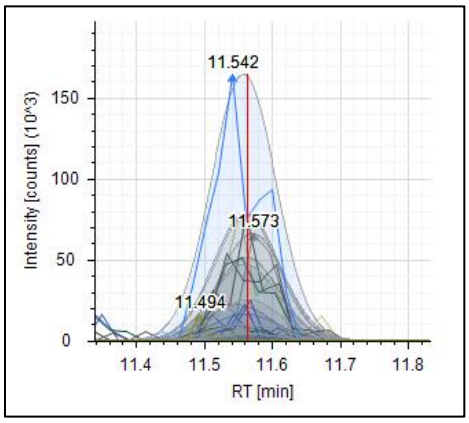

MS Spectrum

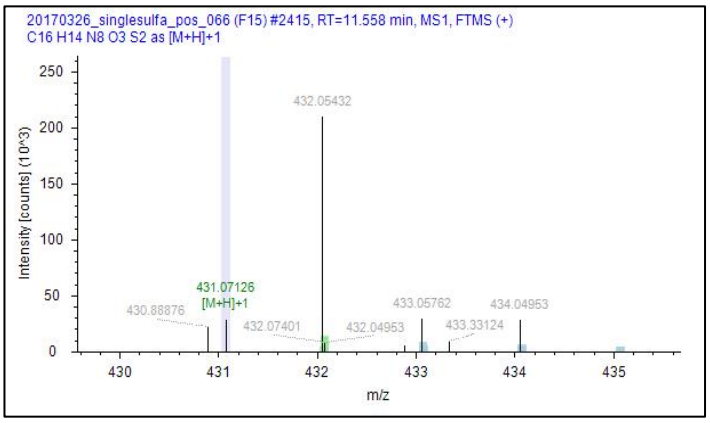

MS^2 Spectrum not available

Formula:

C16 H14 N8 O3 S2

Comment:

The structure of this transformation product was confirmed by a reference standard.

Atomic Modification:

+ C7 H5 N5 O

Proposed Structure:

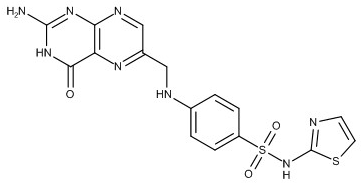

Confidence Level:

Level 1

STZ: N4-formyl-STZ

Chromatogram

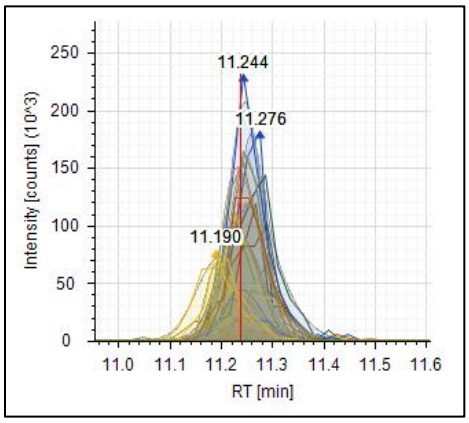

MS Spectrum

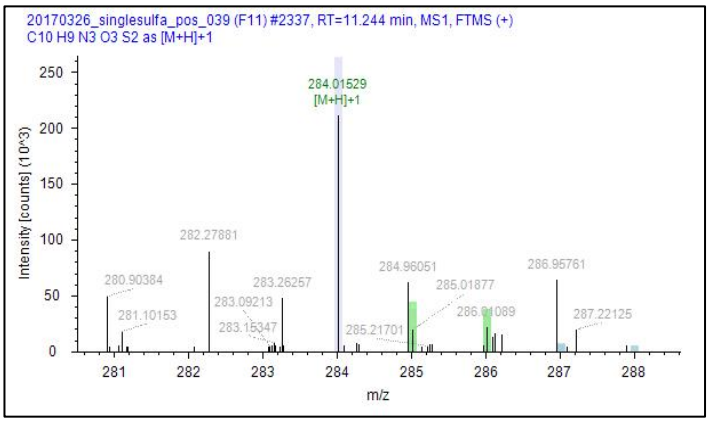

MS^2 Spectrum

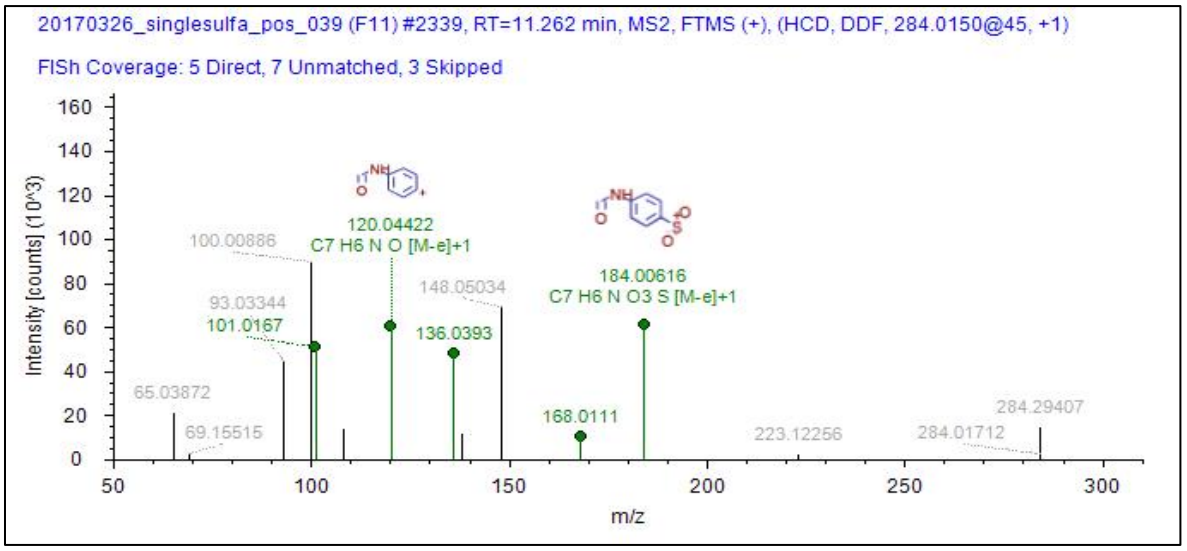

Formula:

C10 H9 N3 O3 S2

Atomic Modification:

+ C O

Proposed Structure:

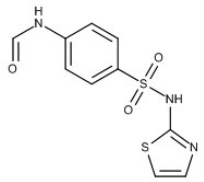

Confidence Level:

Level 2b

SPY: N4-formyl-SPY

Chromatogram

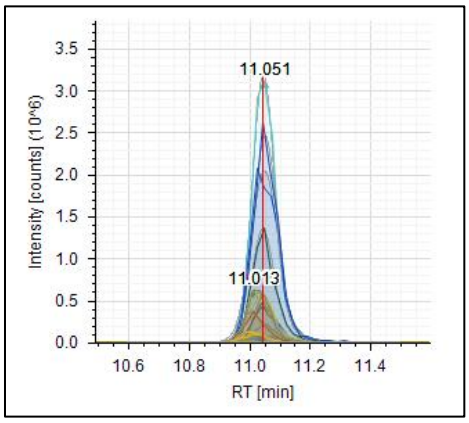

MS Spectrum

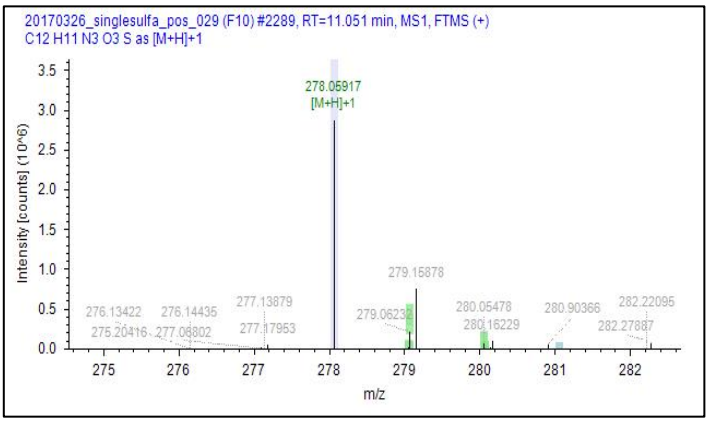

MS^2 Spectrum

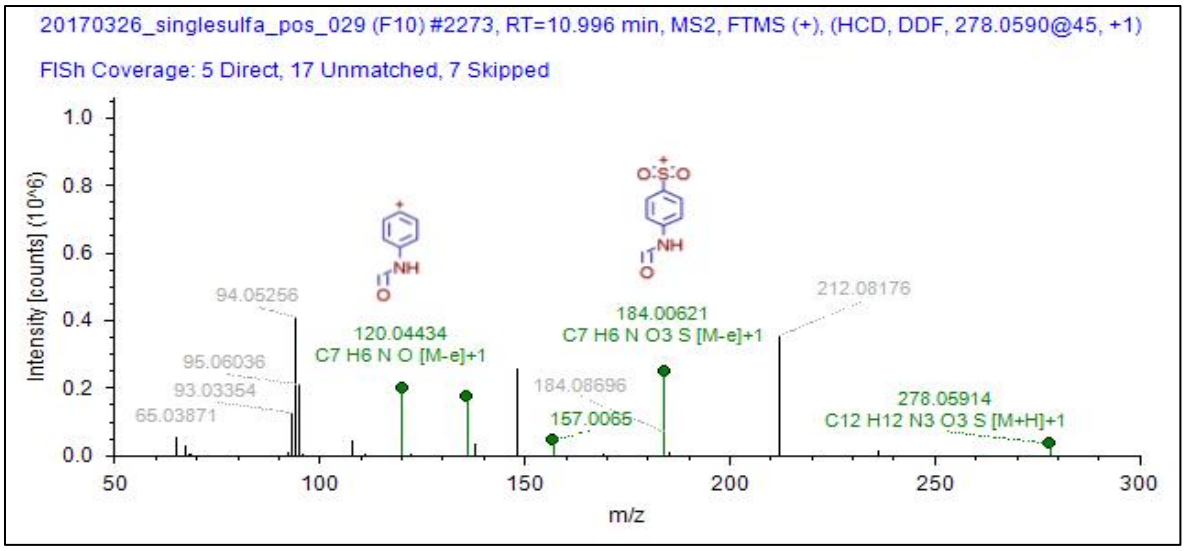

Formula:

C12 H11 N3 O3 S

Atomic Modification:

+ C O

Proposed Structure:

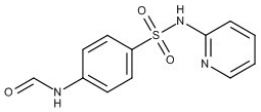

Confidence Level:

Level 2b

SPY: AcOH-SPY

Chromatogram

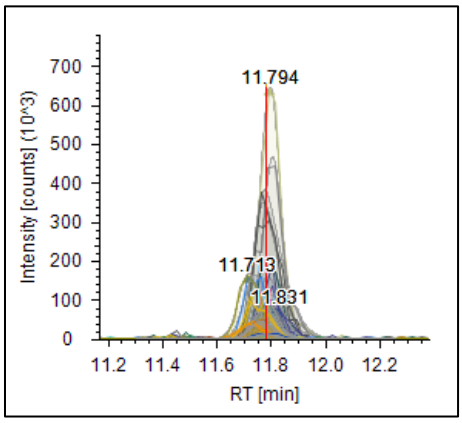

MS Spectrum

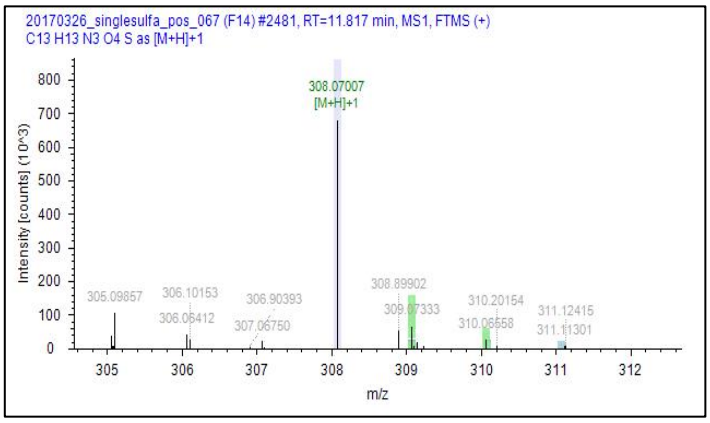

MS^2 Spectrum

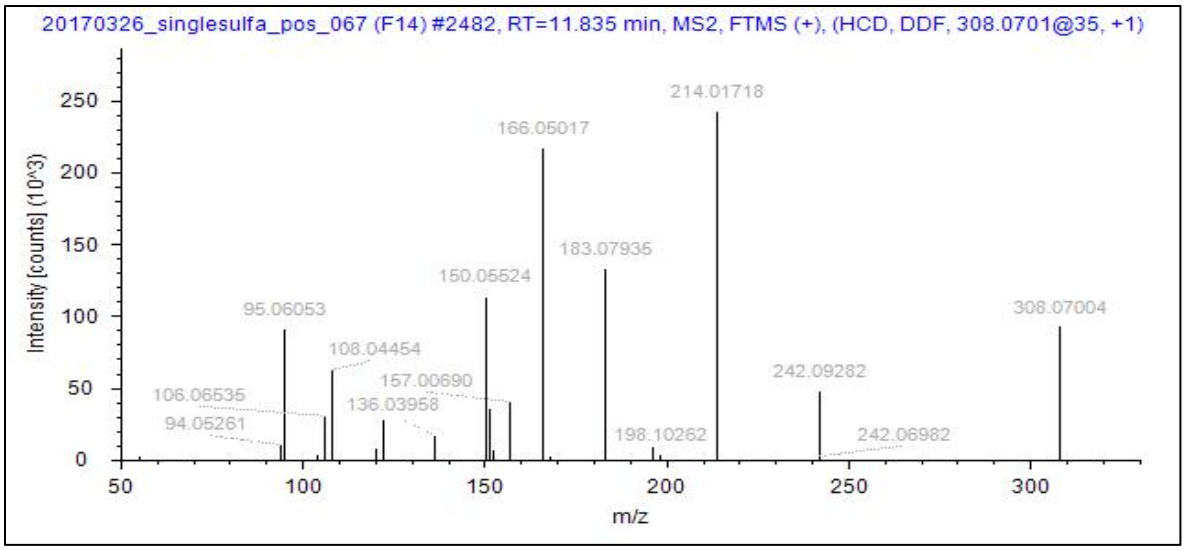

Formula:

C13 H13 N3 O4 S

Atomic Modification:

+ C2 H2 O2

Proposed Structure:

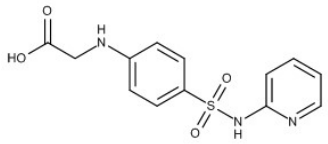

Confidence Level:

Level 3

SPY: SPY + O

Chromatogram

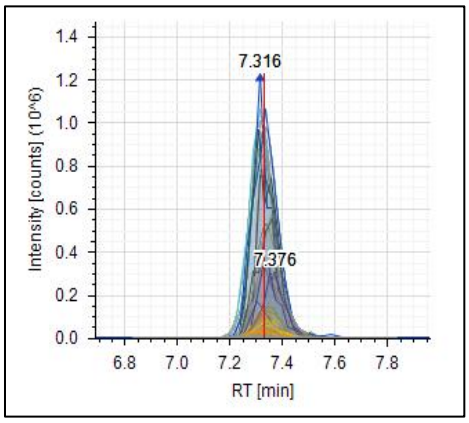

MS Spectrum

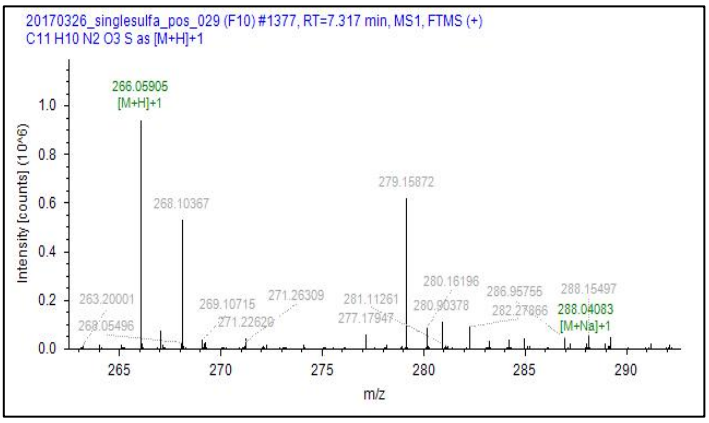

MS^2 Spectrum

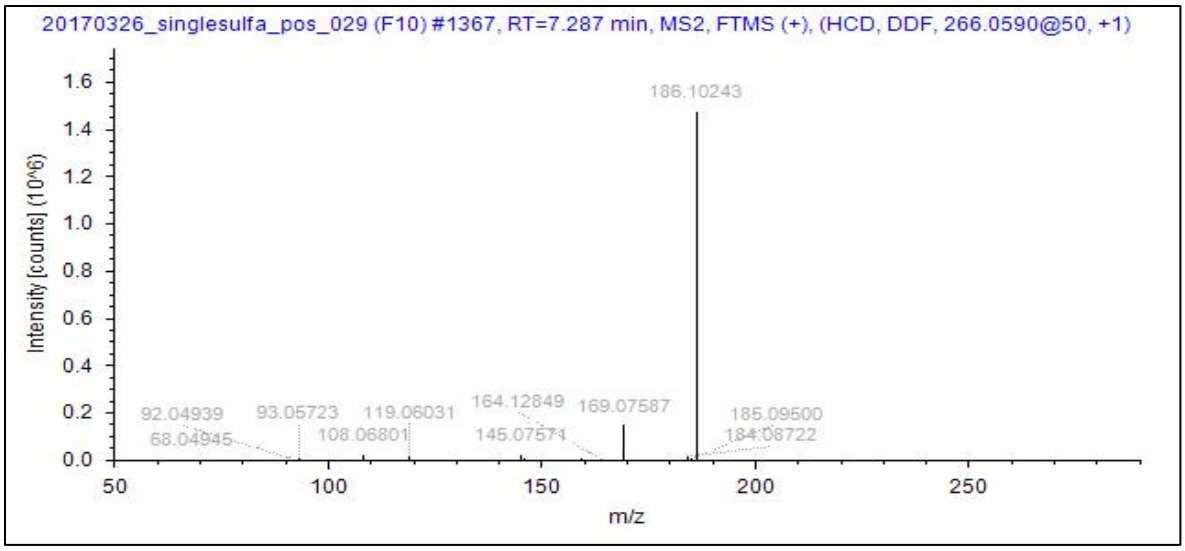

Formula:

C11 H11 N3 O3 S

Atomic Modification:

+ O

Confidence Level:

Level 4

SPY: PtO-SPY

Chromatogram

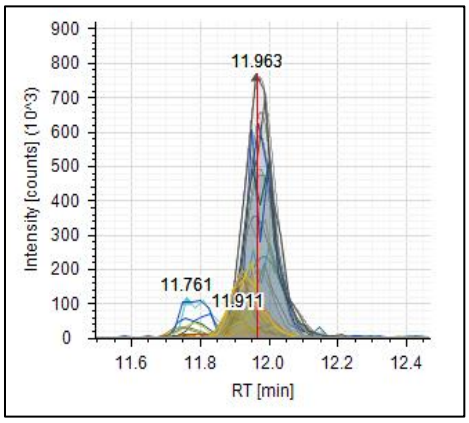

MS Spectrum

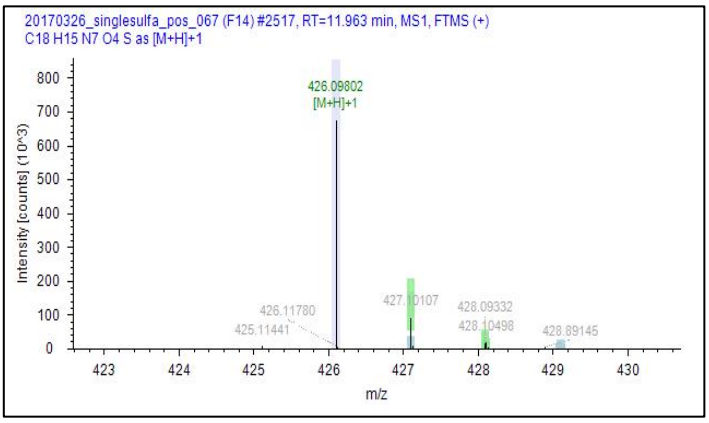

MS^2 Spectrum not available

Formula:

C18 H15 N7 O4 S

Atomic Modification:

+ C7 H4 N4 O2

Proposed Structure:

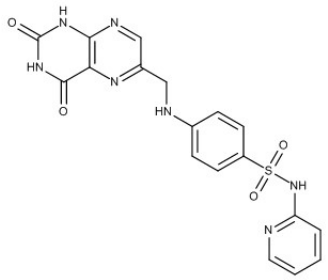

Confidence Level:

Level 2b

SPY: N4-acetyl-SPY

Chromatogram

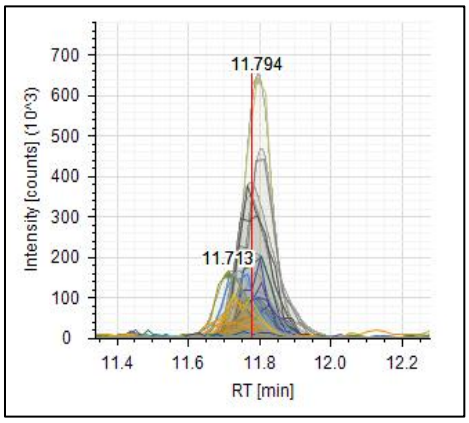

MS Spectrum

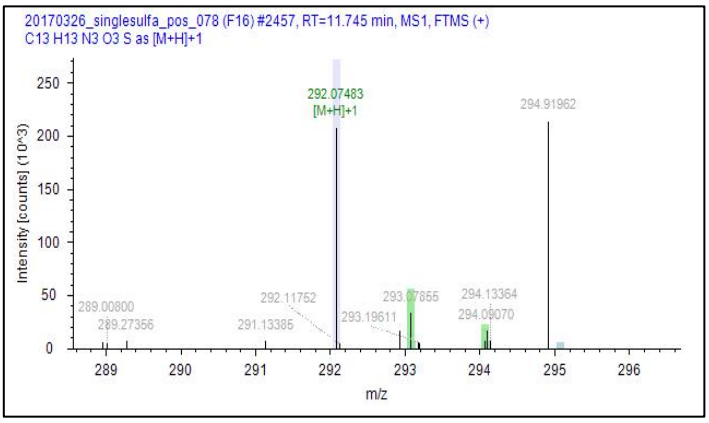

MS^2 Spectrum

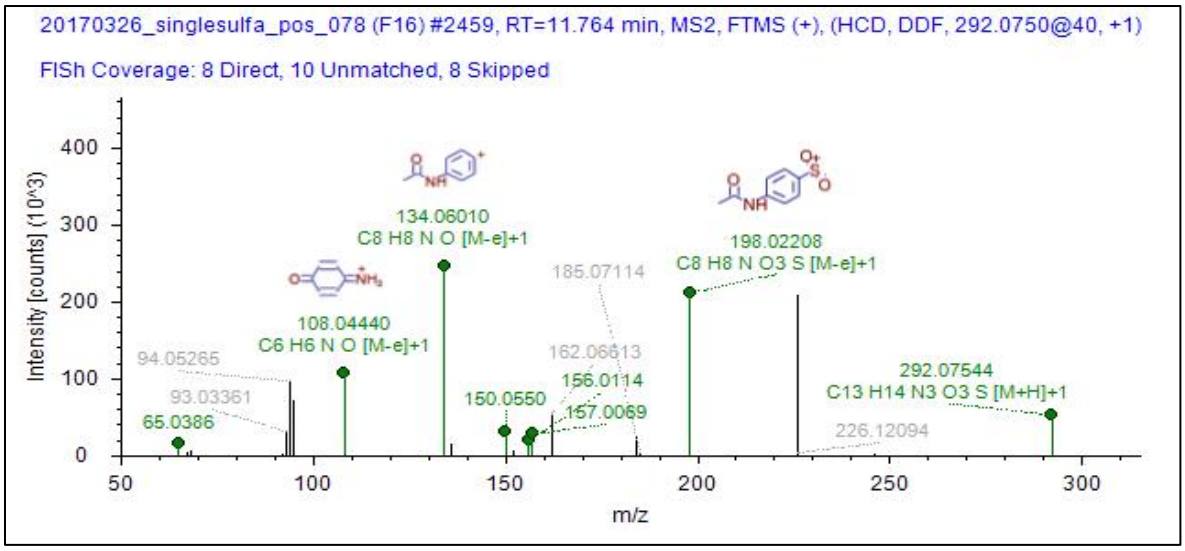

Formula:

C13 H13 N3 O3 S

Structure Interpretation:

The structure of this transformation product was confirmed by a reference standard.

Atomic Modification:

+ C2 H2 O

Proposed Structure:

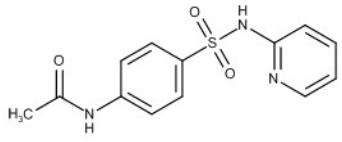

Confidence Level:

Level 1

SPY: SPY + $C_3H_2O_3$

Chromatogram

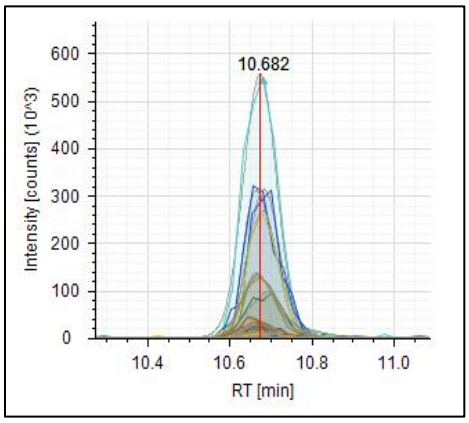

MS Spectrum

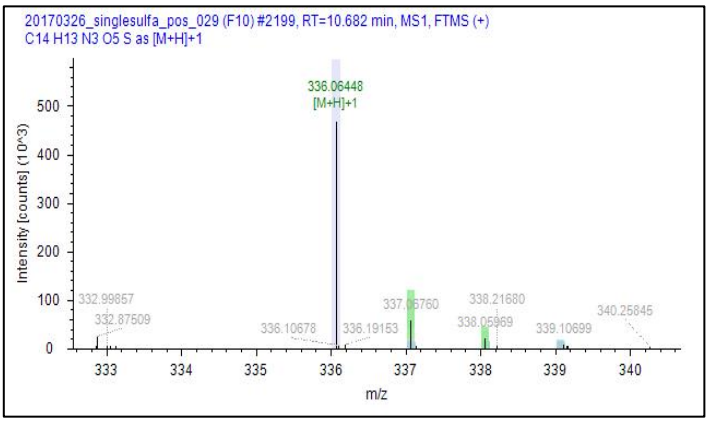

MS^2 Spectrum not available

Formula:
C14 H13 N3 O5 S

Atomic Modification:
+ C3 H2 O3

Confidence Level:
Level 4

SPY: Pterin-SPY

Chromatogram

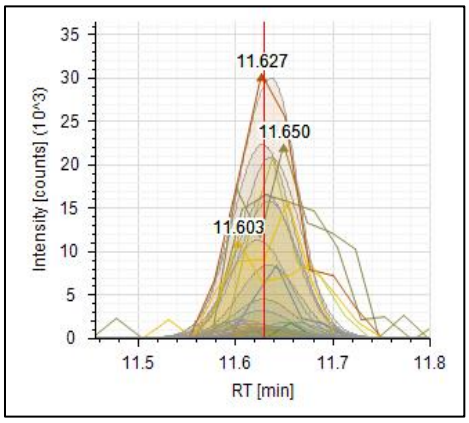

MS Spectrum

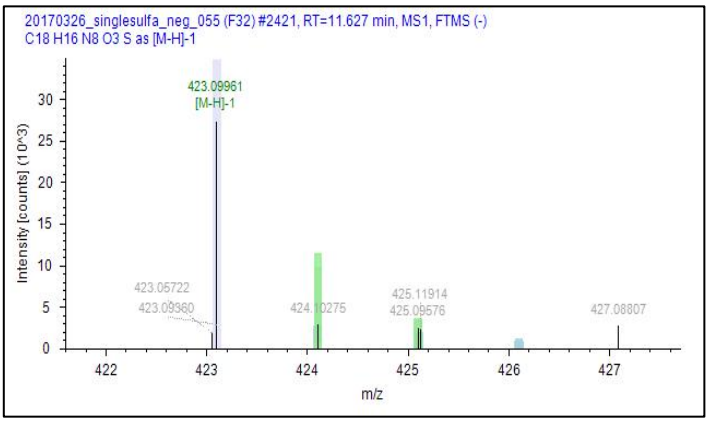

MS^2 Spectrum not available

Formula:

C13 H14 N4 O3 S

Atomic Modification:

+ C2 H3 N O

Proposed Structure:

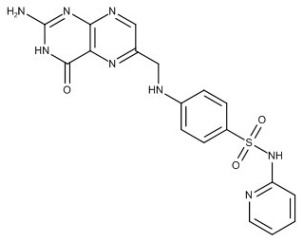

Confidence Level:

Level 3

S8 LC-HRMS/MS Measurements WWTP Samples

As stated in the main text, a modified method for enrichment and LC-HRMS/MS measurements was used based on a method described elsewhere.[30] In summary, after pretreatment (filtration and pH adjustment) 200 mL of sample were enriched on an in-house packed, three-layered SPE cartridge containing the sorbents Oasis HLB (layer 1), a mixture of Strata X-CW (Phenomenex), Strata X-AW (Phenomenex), and Isolute Env+ (Biotage) (layer 2), and EnviCarb (Sigma-Aldrich) (layer 3). After loading and drying, the cartridges were eluted sequentially with 6 mL basic and 3 mL acidic methanol/ethyl acetate mixture (v:v 50:50) and 2 mL methanol in backflush. The extracts were dried under a gentle nitrogen stream and reconstituted to a final volume of 1 mL resulting in a concentration factor of 200. Internal standards (isotope-labeled sulfonamides) were spiked at a concentration of 200 ng/L to the initial sample to account for compound losses and interferences in the LC-HRMS/MS measurement.

In total, 20 µL of the extract were separated with a reversed phase column (XBridge C-18, 2.1x50mm, 3.5 µm; with a 2.1x10 mm guard column containing the same material). The eluents were nanopure water (Barnstead Nanopure, Thermo Scientific) and methanol (HPLC grade, Fisher Scientific), both acidified with 0.1% formic acid. The gradient for the separation was as follows with a flow rate of 0.2 mL/min and a column temperature of 30 °C: 0−4 min linear gradient from 10% to 50% methanol, 4−17 min linear gradient to 95% methanol, 17−23 min constant at 95% methanol followed by equilibration (10% methanol) prior to the next injection for 4 min.

Mass detection was performed on a QExactive (Thermo Fisher Scientific). Each sample was run separately in positive (spray voltage 4 kV) and negative (spray voltage 3 kV) electrospray ionization mode. Full scan spectra were recorded from *m/z* 100−1000 with a resolution of 140000 at *m/z* 200. Data independent fragmentation scans were additionally run with the following mass ranges: *m/z* 100–175, *m/z* 175–250, *m/z* 250–325, *m/z* 325–400 and *m/z* 400–1000 (Resolution: 17'500; stepped higher-energy collisional dissociation (HCD) fragmentation with energies: 52.5–70–87.5; 45–60–75; 37.5–50–62.5; 30–40–50; 15–20–25 NCE (Normalized Collision Energy) respective to the mass ranges). Mass calibration and mass accuracy were checked (deviation <5 ppm) with an in-house amino acid solution prior to the measurements.

S9 Biotransformation of ^{14}C-SDZ

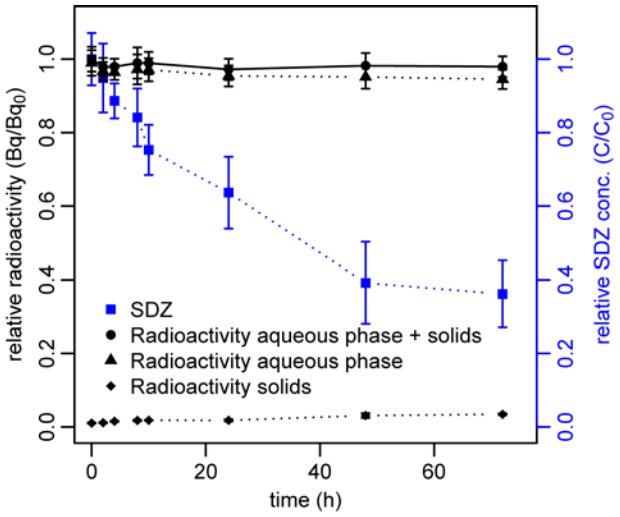

Figure S9.1: Biotransformation of ^{14}C-SDZ. Radioactivity measured in solids, aqueous phase and the sum thereof as fractions of the total radioactivity measured after spiking. Relative concentration of SDZ over time is shown in blue. Error bars represent the standard deviation from triplicate reactors.

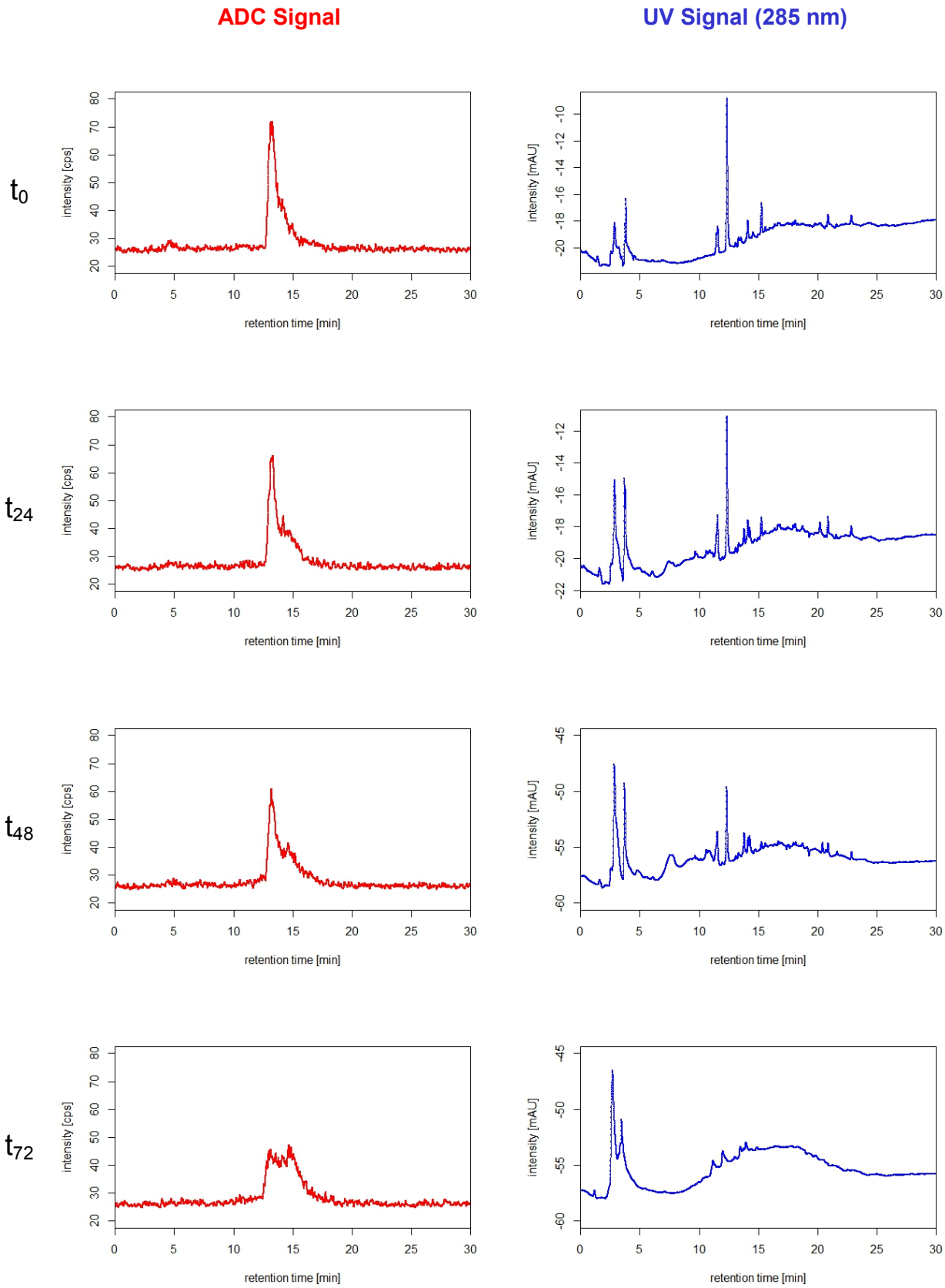

Figure S9.2: HPLC-DAD-LSC chromatograms of ^{14}C-SDZ samples.

S10 Mineralization

In preliminary ^{14}C-SMX biotransformation experiments using sealed reactors and CO_2 traps as described previously,[1] only minor fractions of radioactivity were recovered (below 2% in all measurements, data not shown), indicating a low degree of mineralization. Similarly, previously published results showed that, under a set of different conditions, the recovered radioactivity from $^{14}CO_2$ traps always remained below 5%.[1]

Since the pH was consistently slightly basic during the experiments, radioactive fractions dissolved as bicarbonate or carbonate were assessed at two time points (24 h and 72 h). To this end, in addition to the samples described in the main text, 1.5 mL of sludge were sampled from the radioactive biotransformation reactors (^{14}C-SMX and ^{14}C-SDZ) and from a control batch reactor and transferred into 1.5-mL Eppendorf tubes. Samples were then centrifuged for 10 minutes at 21500 rpm at 20 °C. Two aliquots of 500 µL of the resulting supernatant were pipetted into two 6-mL polypropylene LSC vials each. In one vial, 50 µL of HCl was added to obtain a pH < 1 (verified using pH indicator paper). Samples from sampling point 24 h were then sonicated for 15 minutes as described by Shrestha *et al.*,[31] and the 72 h samples were degassed with nitrogen for 2 minutes. Thereafter, 5 mL of LSC cocktail (Hionic Fluor, Perkin Elmer) were added, and the radioactivity was measured. The differences between untreated and acidified samples were minor, indicating that no or only very minor amounts of $^{14}CO_2$ were present in the dissolved form: SMX: 24 h: 0.53 ± 0.97%, 72 h: -1.3 ± 0.9%, SDZ: 24 h: 1.4 ± 0.3%, 72 h: 3.4 ± 2.1% (shown as percentage of total radioactivity in the aqueous fraction).

S11 Sorption and Abiotic Controls

^{14}C-SMX and ^{14}C-SDZ autoclaved controls:

In abiotic controls, radioactivity recovered from the washed solids contributed less than 2% of the total added radioactivity at all measured time points (Figure S11.1). The average total recovered radioactivity (medium + solids) for later time points (2, 24, 48 and 72 h) was 99.1 ± 0.7% (SMX) and 100.7 ± 1.6% (SDZ).

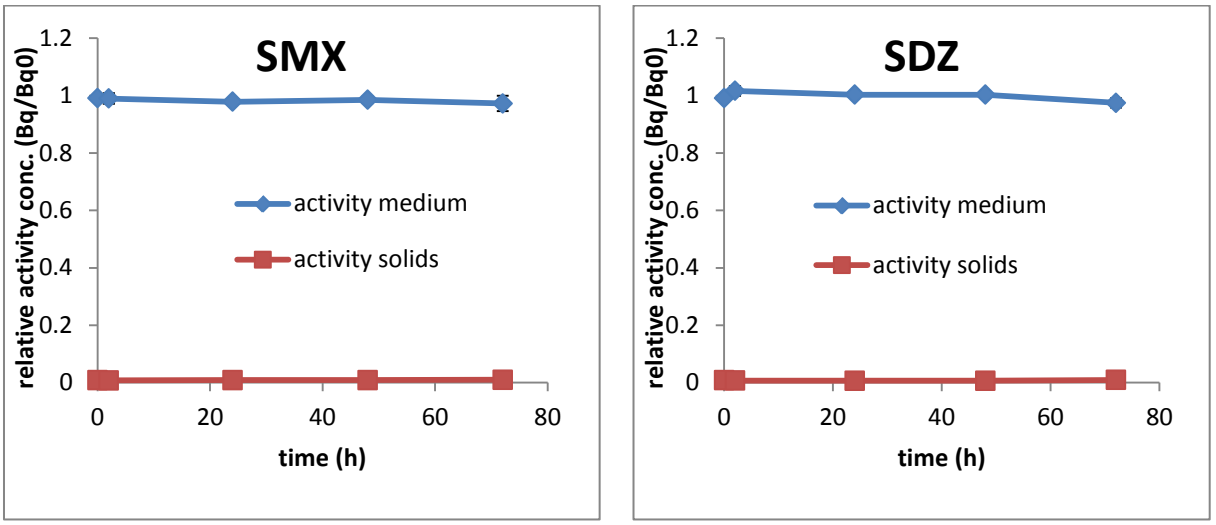

Figure S11.1: Radioactivity in aqueous phase (medium) and solids measured in the autoclaved samples (left: SMX, right: SDZ)

SPY, STZ and SMZ autoclaved controls:

Controls with autoclaved activated sludge and autoclaved activated sludge filtrate did not reveal substantial sorption or abiotic transformation for SPY, STZ or SMZ (Table S11.1, see methods section for details on quantification).

Table S11.1: Sulfonamide concentrations recovered after 72 h as fraction of the spiked concentration in control reactors.

SA	c/c0 abiotic 72h		c/c0 sorption 72h	
	replicate 1	replicate 2	replicate 1	replicate 2
SPY	0.95	1.00	0.97	0.91
STZ	1.01	0.89	1.02	0.81
SMZ	0.99	1.04	0.95	0.96

S12 Biotransformation of ^{14}C-SMX

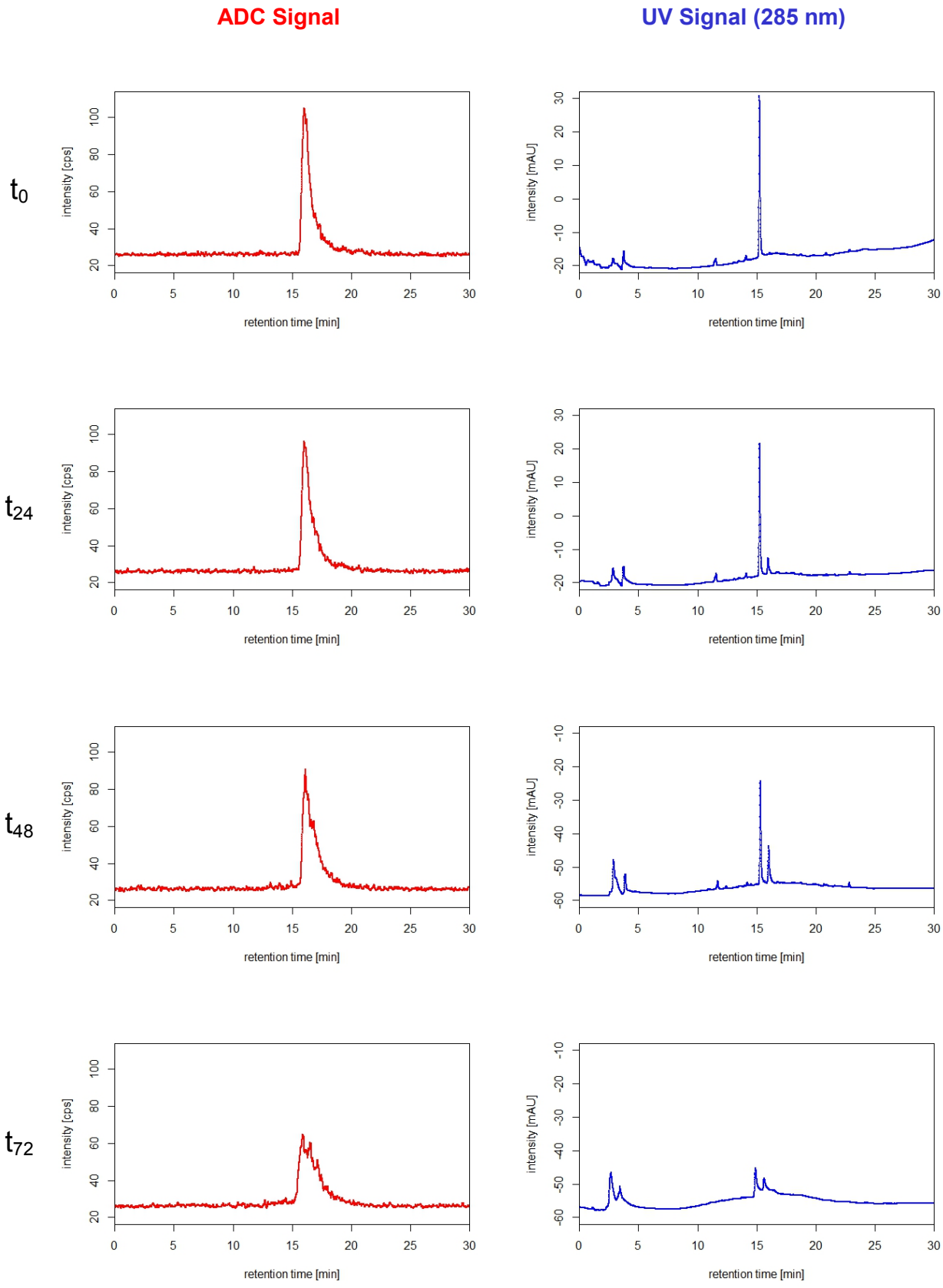

Figure S12.1: HPLC-DAD-LSC chromatograms of ^{14}C-SMX samples.

S13 TP formation for SDZ, SMZ, SPY and STZ

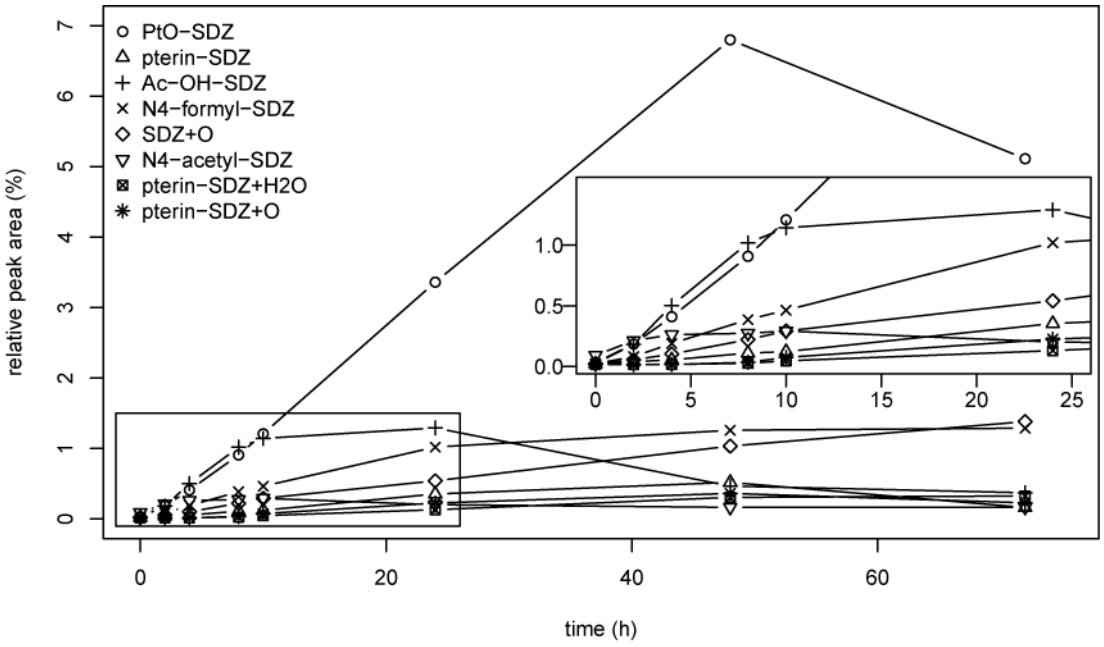

Figure S13.1: Time trends of transformation products of SDZ over time. Peak areas of TPs are shown as percentage of the SDZ peak area in the first sample after spiking.

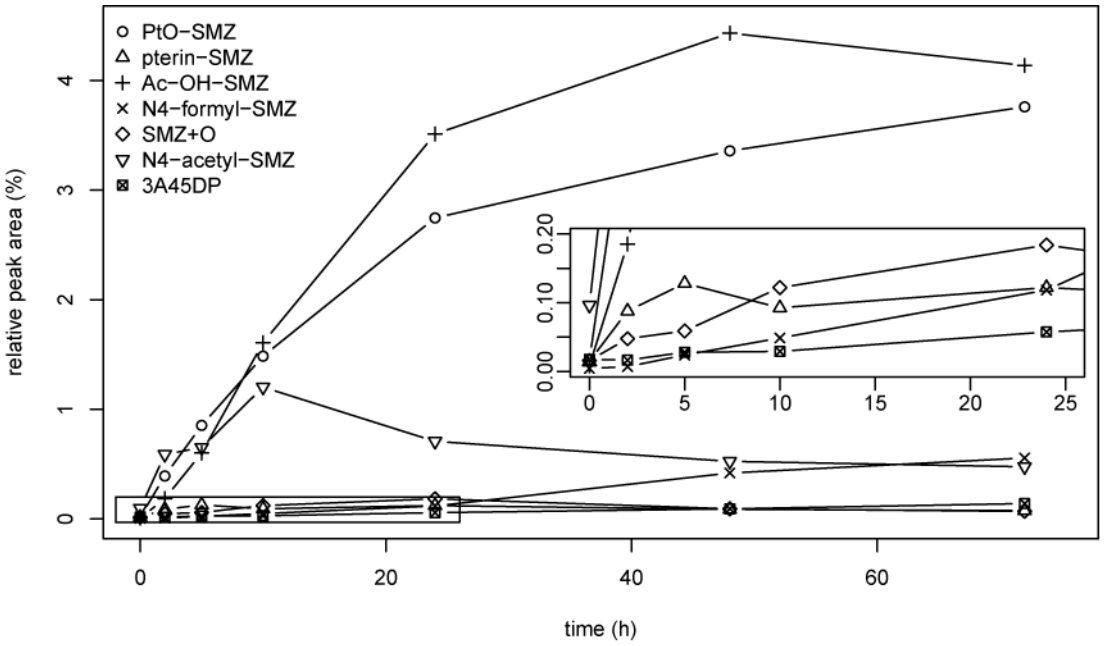

Figure S13.2: Time trends of transformation products of SMZ over time. Peak areas of TPs are shown as percentage of the SMZ peak area in the first sample after spiking.

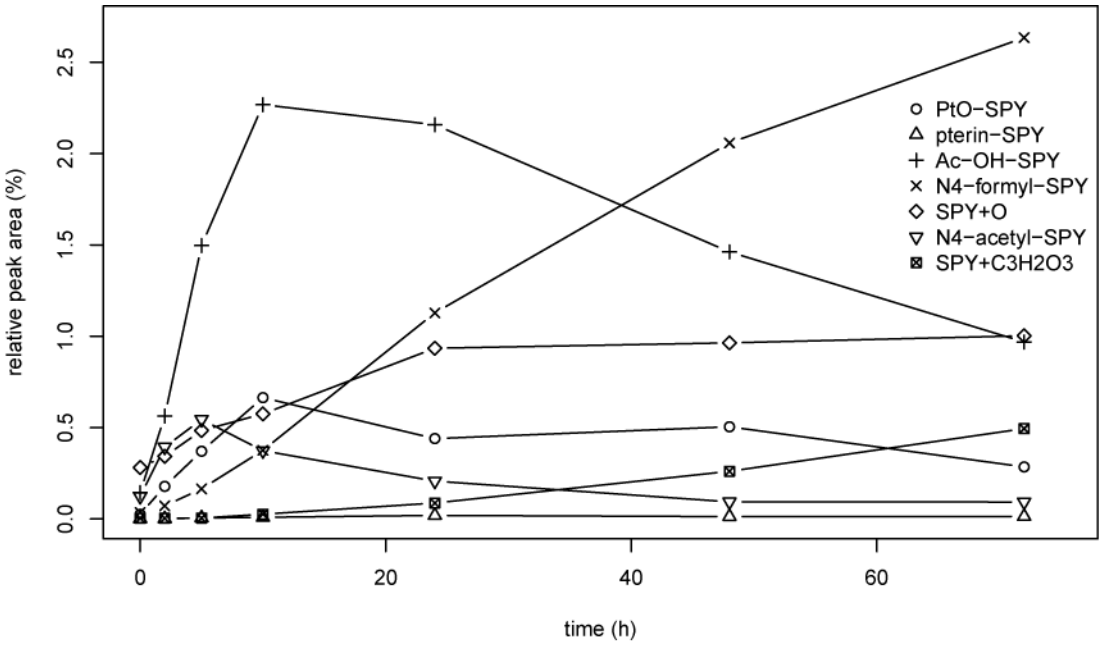

716

717 **Figure S13.3: Time trends of transformation products of SPY over time.** Peak areas of TPs are
718 shown as percentage of the SPY peak area in the first sample after spiking.

719

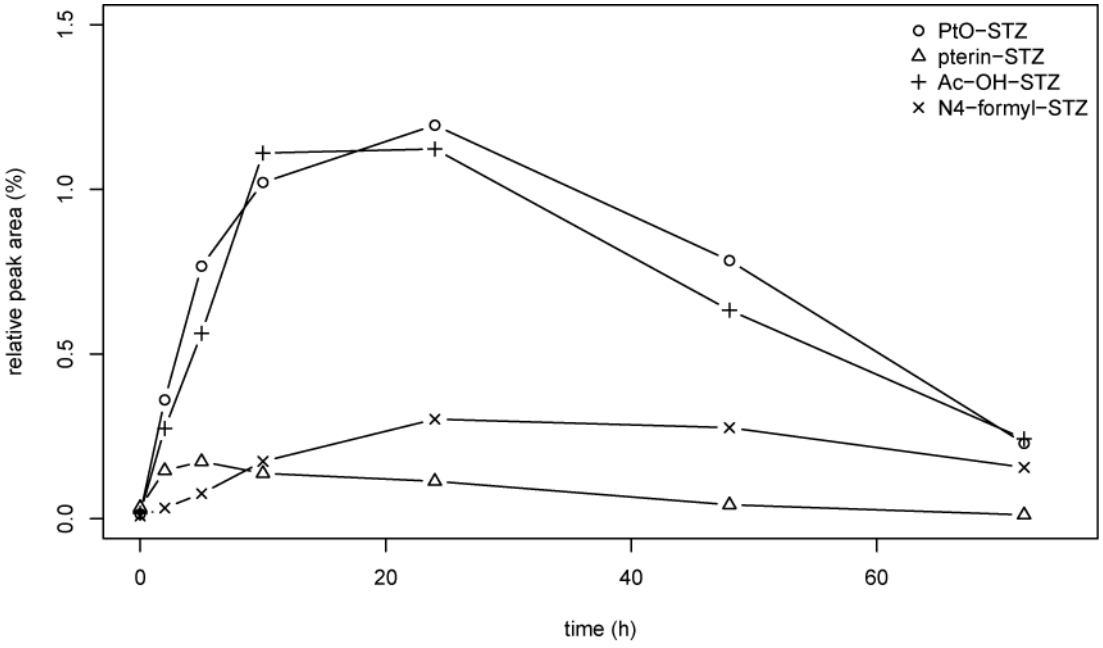

720

721 **Figure S13.4: Time trends of transformation products of STZ over time.** Peak areas of TPs are
722 shown as percentage of the STZ peak area in the first sample after spiking.

723

724

725

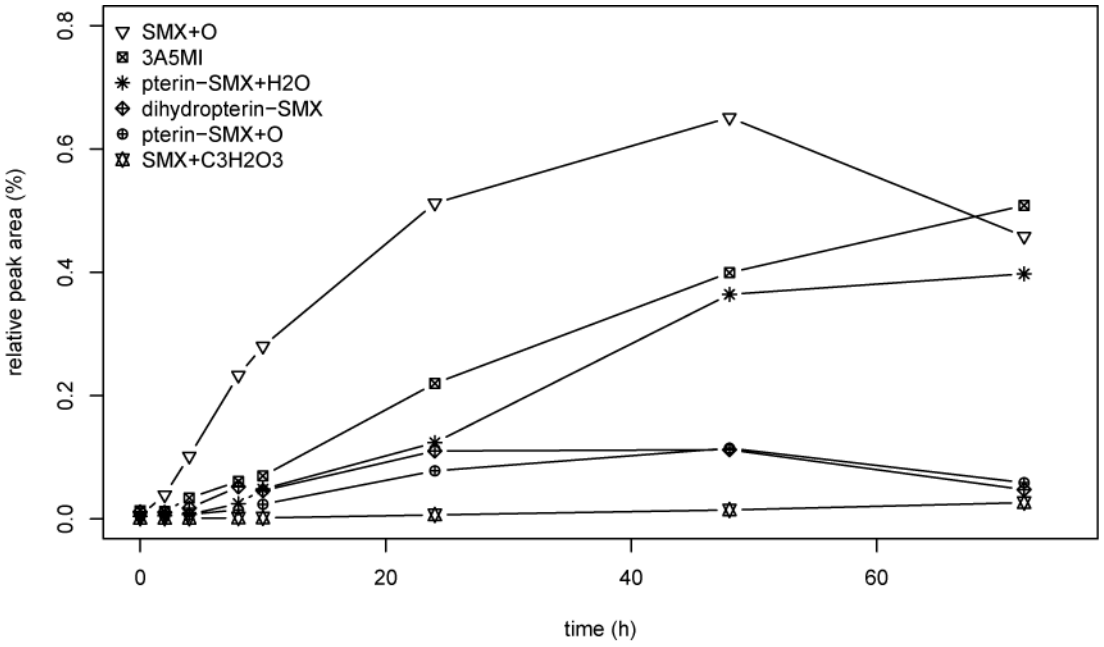

726

727 **Figure S13.5: Time trends of transformation products of SMX over time that are not shown in**
728 **Figure 3 in the main text.** Peak areas of TPs are shown as percentage of the SMX peak area in the
729 first sample after spiking.

730

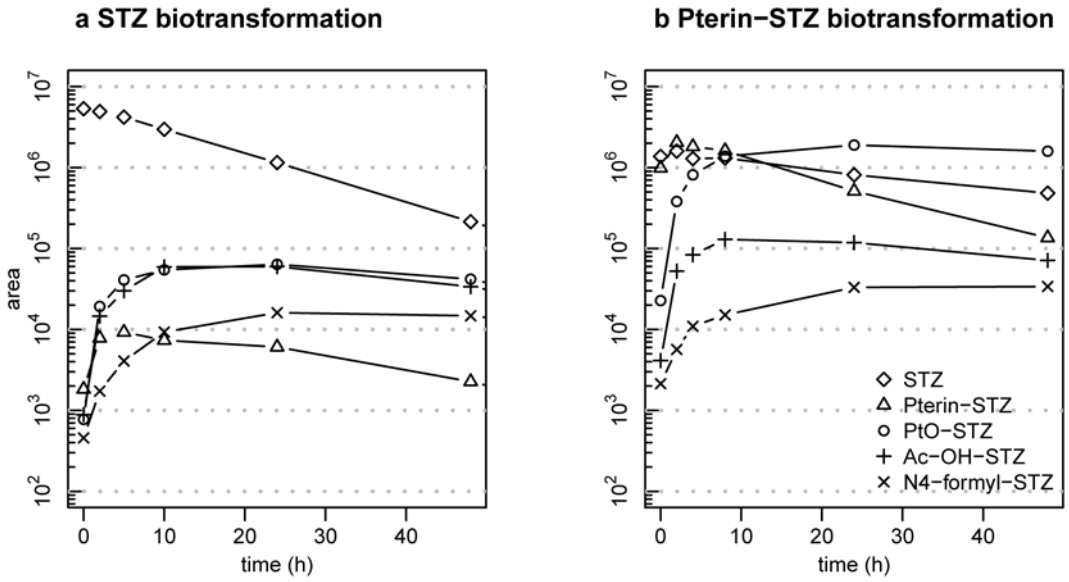

731

732 **Figure S13.6: Biotransformation of STZ (a) and pterin-STZ (b). Time courses of TP peak areas**
733 **for TPs of STZ.**

734

735

736

737

738

739

S14 Biotransformation of N4-Acetyl-SAs

For N4-acetyl SMX, rapid transformation to SMX was observed (Figure S14.1). The logarithmic representation reveals that N4-acetyl-SMX does not completely disappear but stagnates at a low level. Since we have also observed formation of N4-acetyl SMX in biotransformation experiments with SMX, the data presented here confirms the reversibility of the N4-acetylation reaction.

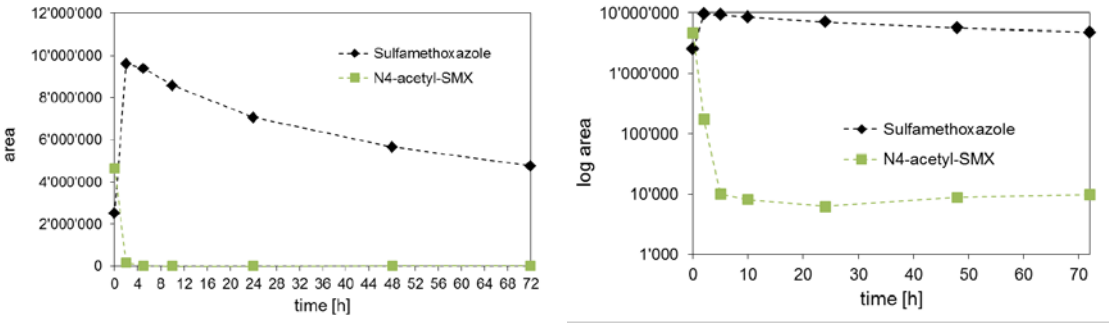

Figure S14.1: Biotransformation of N4-acetyl-SMX shown with (a) non-logarithmic peak areas and (b) logarithmic peak areas.

S15 Transformation Product Mass Balance Estimation

For SMX, the only available TP standards were 3A5MI and N4-acetyl-SMX. For these two TPs, response factors (concentration/peak area) were determined and compared to the response factor of SMX. Relative ionization efficiencies (response factor (TP) / response factor (SMX)) of 1.4 (3A5MI) and 0.7 (N4-acetyl-SMX) were obtained. Consequently, for mass balance estimation purposes, the same relative ionization efficiency of 0.7 observed for N4-acetyl-SMX was applied to the structurally similar TPs N4-formyl-SMX and Ac-OH-SMX for which no standards were available. For STZ, a standard for pterin-STZ was available, and a relative ionization efficiency of 0.1 was obtained compared to STZ. Because of a lack of standards for pterin-SMX and PtO-SMX, we again applied the same relative ionization efficiency of 0.1 to pterin-SMX and PtO-SMX relative to SMX for mass balance estimation purposes (Table S15.1). The relative difference between SMX and STZ is comparably small (STZ/SMX: 0.63). Using the estimated ionization efficiencies and considering differences in molecular weight, molar concentrations of TPs were estimated at the different sampling time points to obtain approximate estimates of molar mass balances (Figure S15.1). Similarly, mass balances were estimated for SDZ, SMZ, SPY and STZ (Table S15.1, Figures S15.2−S15.5). The ionization efficiencies for all five parent SAs were found to be in a similar range (SDZ/SMX: 0.74, SMZ/SMX: 1.30 SPY/SMX: 1.38).

Table S15.1: Applied ionization efficiency factors for TPs.

Name	molecular formula	molecular weight	response relative to parent SA	measured/estimated from
SMX	C10H11N3O3S	253.05	1	measured
PtO-SMX	C17H15N7O5S	429.09	0.1	pterin-STZ/STZ
pterin-SMX	C17H16N8O4S	428.10	0.1	pterin-STZ/STZ
N4-formyl-SMX	C11H11N3O4S	281.05	0.7	N4-acetyl-SMX/SMX
SMX+O	C10H11N3O4S	269.05	1	SMX
3-amino-5-methylisoxazole	C4H6N2O	98.05	1.4	measured
pterin-SMX+H2O	C17H18N8O5S	446.11	0.1	pterin-STZ/STZ
Ac-OH-SMX	C6H14N7O4PS	311.06	0.7	N4-acetyl-SMX/SMX
N4-acetyl-SMX	C12H13N3O4S	295.06	0.7	measured
dihydropterin-SMX	C17H18N8O4S	430.12	0.1	pterin-STZ/STZ
pterin-SMX+O	C17H16N8O5S	444.10	0.1	pterin-STZ/STZ
SMX+C3H2O3	C13H13N3O6S	339.05	0.7	N4-acetyl-SMX/SMX
SDZ	C10H10N4O2S	250.05	1	measured
PtO-SDZ	C17H14N8O4S	426.09	0.1	pterin-STZ/STZ
N4-formyl-SDZ	C11H10N4O3S	278.05	0.5	N4-acetyl-SDZ/SDZ
SDZ+O	C10H10N4O3S	266.05	1	SDZ
Ac-OH-SDZ	C12H12N4O4S	308.06	0.5	N4-acetyl-SDZ/SDZ
pterin-sulfadiazine	C17H15N9O3S	425.10	0.1	pterin-STZ/STZ
pterin-SDZ+H2O	C17H17N9O4S	443.11	0.1	pterin-STZ/STZ
N4-acetyl-SDZ	C12H12N4O3S	292.06	0.5	measured
pterin-SDZ+O	C17H15N9O4S	441.42	0.1	pterin-STZ/STZ
SMZ	C12H14N4O2S	278.08	1	measured
Ac-OH-SMZ	C14H16N4O4S	336.09	0.2	N4-acetyl-SMZ/SMZ
PtO-SMZ	C19H18N8O4S	454.12	0.1	pterin-STZ/STZ
N4-acetyl-SMZ	C14H16N4O3S	320.09	0.2	measured
N4-formyl SMZ	C13H14N4O3S	306.08	0.2	N4-acetyl-SMZ/SMZ
SMZ+O	C12H14N4O3S	294.08	1	SMZ
2A46DP[a]	C6H9N3	123.08	1.6	2-aminopyridine/SPY
Pterin-SMZ	C19H19N9O3S	453.13	0.1	pterin-STZ/STZ
SPY	C11H11N3O2S	249.06	1	measured
N4-formyl-SPY	C12H11N3O3S	277.05	0.4	N4-acetyl-SPY/SPY
Ac-OH-SPY	C13H13N3O4S	307.06	0.4	N4-acetyl-SPY/SPY
SPY + O	C11H11N3O3S	265.05	1	SPY
PtO-SPY	C18H15N7O4S	425.09	0.1	pterin-STZ/STZ
N4-acetyl-SPY	C13H13N3O3S	291.07	0.4	measured
SPY+C3H2O3	C14H13N3O5S	335.06	0.4	N4-acetyl-SPY/SPY
Pterin-SPY	C18H16N8O3S	424.11	0.1	pterin-STZ/STZ
STZ	C9H9N3O2S2	255.01	1	measured
Ac-OH-STZ	C11H11N3O4S2	313.02	0.5	N4-acetyl-STZ/STZ
PtO-STZ	C16H13N7O4S2	431.05	0.1	pterin-STZ/STZ
Pterin-STZ	C16H14N8O3S2	430.06	0.1	measured
N4-formyl-STZ	C10H9N3O3S2	283.01	0.5	N4-acetyl-STZ/STZ

[a]2-Amino-4,6-dimethylpyrimidine

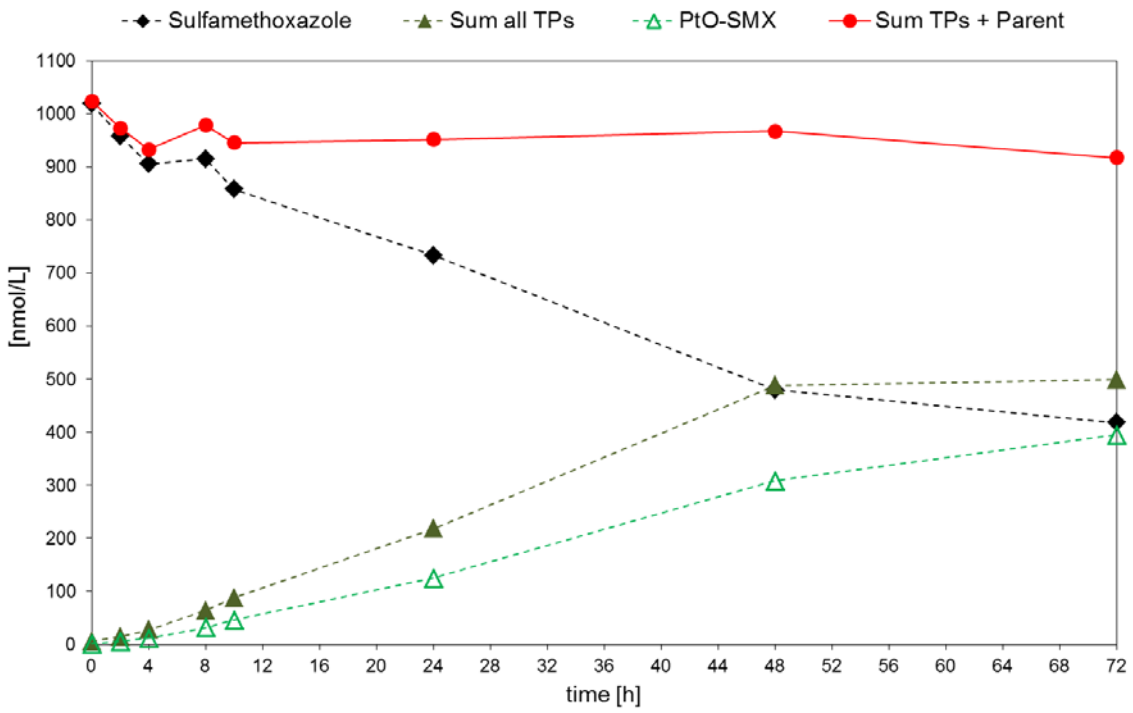

Figure S15.1: Estimated molar concentrations of SMX, detected TPs of SMX and the sum thereof over the time course of the experiment.

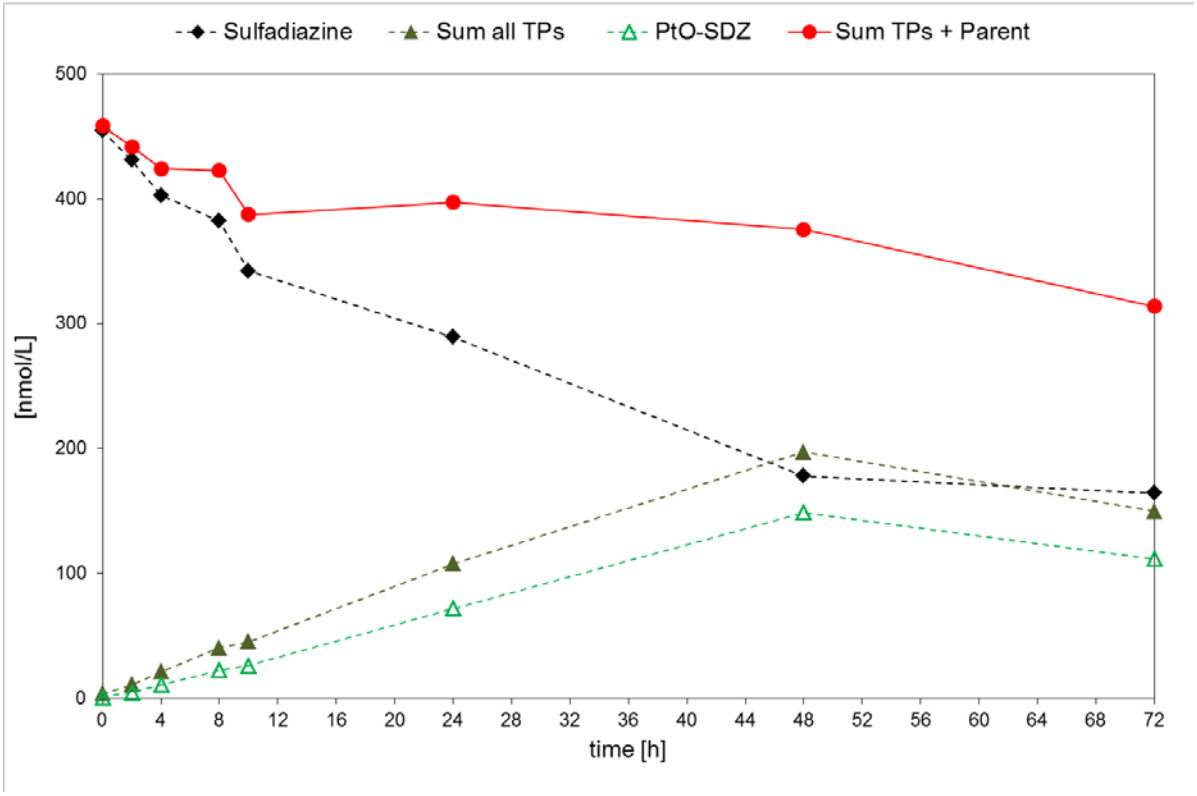

Figure S15.2: Estimated molar concentrations of SDZ, detected TPs of SDZ and the sum thereof over the time course of the experiment.

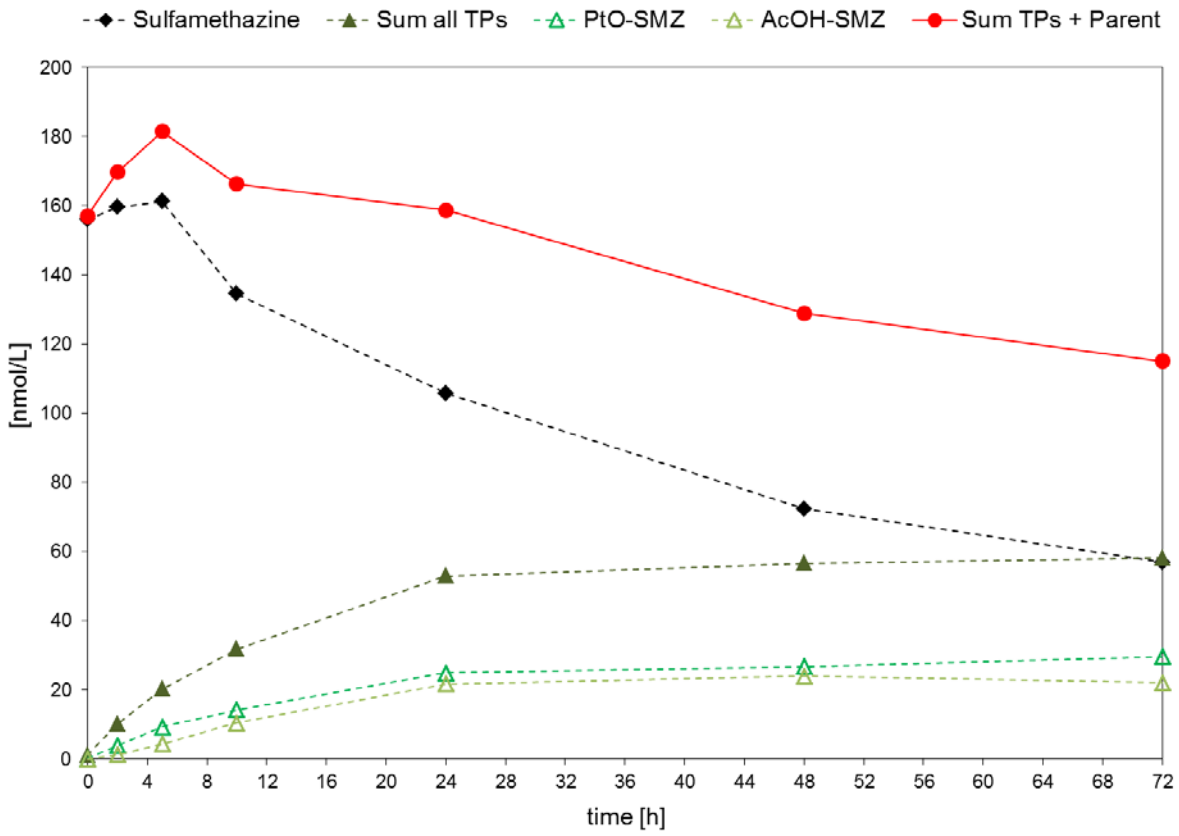

Figure S15.3: Estimated molar concentrations of SMZ, detected TPs of SMZ and the sum thereof over the time course of the experiment.

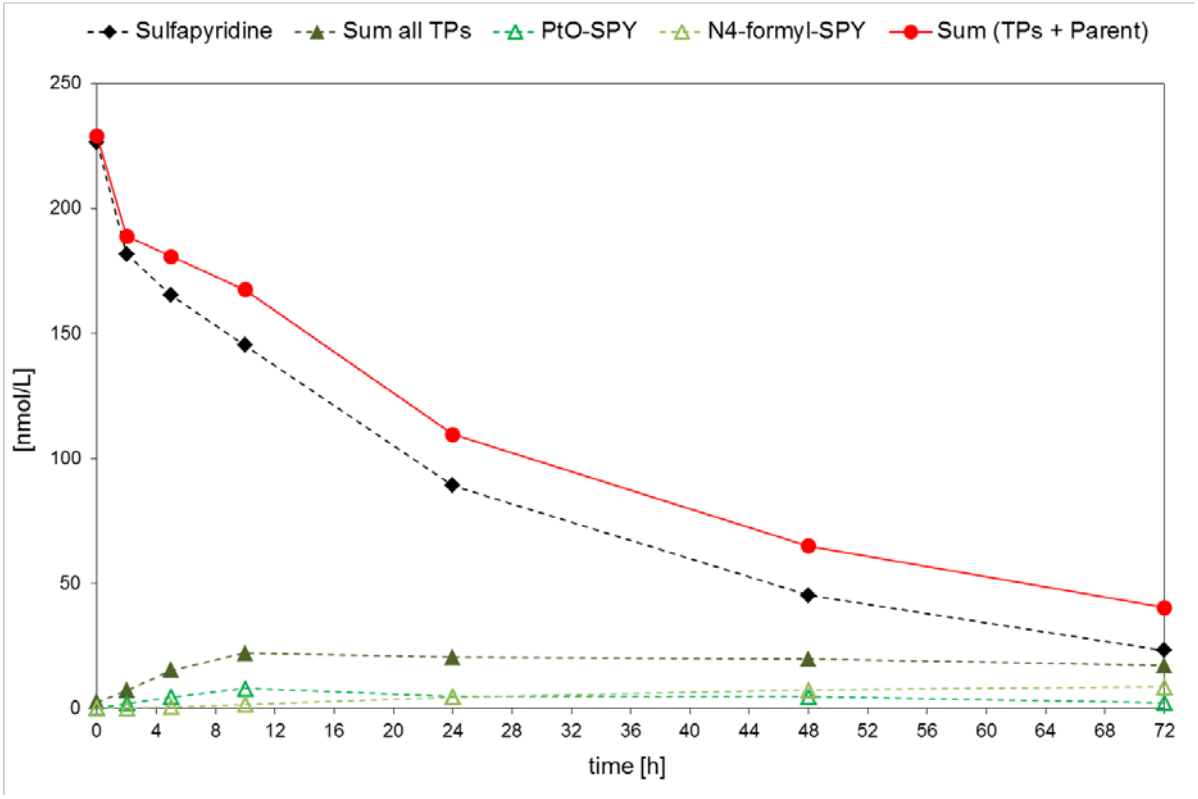

Figure S15.4: Estimated molar concentrations of SPY, detected TPs of SPY and the sum thereof over the time course of the experiment.

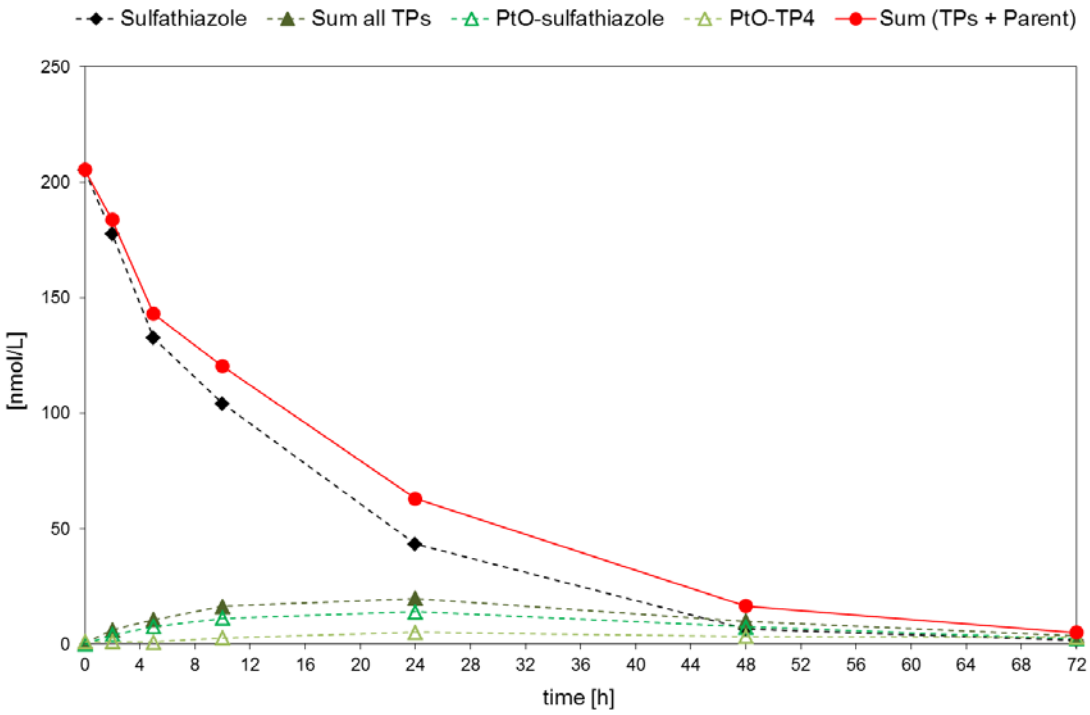

795

796 **Figure S15.5: Estimated molar concentrations of STZ, detected TPs of STZ and the sum thereof**
797 **over the time course of the experiment.**

798

799

S16 Pterin-Conjugate Pathway Related TPs in WWTPs

Table S16.1: Dimensions and operational parameters of WWTPs considered in this study.

WWTP	population equivalent	annual discharge	solids retention time	hydraulic retention time (biological treatment)
		[m^3/year]	[d]	[h]
WWTP1	470000	32672600	1.7	3.9
WWTP2	130000	1448442	10.4	24
WWTP3	1300	304546	n/a	5
WWTP4	12500	550000	10	n/a
WWTP5	25000	6200000	10	6
WWTP6	105000	7500000	11-14	17
WWTP7	3000	335000	1	n/a
WWTP8	5250	597611	9	n/a
WWTP9	40000	n/a	6	4

References

1. Alvarino, T.; Nastold, P.; Suarez, S.; Omil, F.; Corvini, P. F.; Bouju, H., Role of biotransformation, sorption and mineralization of ^{14}C-labelled sulfamethoxazole under different redox conditions. *Sci. Total Environ.* **2016**, *542*, 706-715.
2. Schmidt, B.; Ebert, J.; Lamshoft, M.; Thiede, B.; Schumacher-Buffel, R.; Ji, R.; Corvini, P. F.; Schaffer, A., Fate in soil of 14C-sulfadiazine residues contained in the manure of young pigs treated with a veterinary antibiotic. *J. Environ. Sci. Health., Part B* **2008**, *43*, 8-20.
3. Richter, M. K.; Focks, A.; Siegfried, B.; Rentsch, D.; Krauss, M.; Schwarzenbach, R. P.; Hollender, J., Identification and dynamic modeling of biomarkers for bacterial uptake and effect of sulfonamide antimicrobials. *Environ. Pollut.* **2013**, *172*, 208-215.
4. Bourgin, M.; Beck, B.; Boehler, M.; Borowska, E.; Fleiner, J.; Salhi, E.; Teichler, R.; von Gunten, U.; Siegrist, H.; McArdell, C. S., Evaluation of a full-scale wastewater treatment plant upgraded with ozonation and biological post-treatments: Abatement of micropollutants, formation of transformation products and oxidation by-products. *Water Res.* **2018**, *129*, 486-498.
5. *Standard methods for the examination of water and wastewater*. 21th Edition ed.; American Public Health Association: 2005.
6. Gulde, R.; Meier, U.; Schymanski, E. L.; Kohler, H. P.; Helbling, D. E.; Derrer, S.; Rentsch, D.; Fenner, K., Systematic Exploration of Biotransformation Reactions of Amine-Containing Micropollutants in Activated Sludge. *Environ. Sci. Technol.* **2016**, *50*, 2908-2920.
7. Helbling, D. E.; Hollender, J.; Kohler, H. P.; Singer, H.; Fenner, K., High-throughput identification of microbial transformation products of organic micropollutants. *Environ. Sci. Technol.* **2010**, *44*, 6621-6627.
8. Ternes, T.; Joss, A., *Human pharmaceuticals, hormones and fragrances*. IWA publishing: 2007.
9. Joss, A.; Zabczynski, S.; Göbel, A.; Hoffmann, B.; Löffler, D.; McArdell, C. S.; Ternes, T. A.; Thomsen, A.; Siegrist, H., Biological degradation of pharmaceuticals in municipal wastewater treatment: proposing a classification scheme. *Water Res.* **2006**, *40*, 1686-1696.
10. Helbling, D. E.; Hollender, J.; Kohler, H.-P. E.; Fenner, K., Structure-Based Interpretation of Biotransformation Pathways of Amide-Containing Compounds in Sludge-Seeded Bioreactors. *Environ. Sci. Technol.* **2010**, *44*, 6628-6635.
11. Schwarzenbach, R. P.; Gschwend, P. M.; Imboden, D. M., *Environmental organic chemistry*. John Wiley & Sons: 2005.
12. Gulde, R.; Helbling, D. E.; Scheidegger, A.; Fenner, K., pH-dependent biotransformation of ionizable organic micropollutants in activated sludge. *Environ. Sci. Technol.* **2014**, *48*, 13760-13768.
13. Fernandez-Fontaina, E.; Gomes, I. B.; Aga, D. S.; Omil, F.; Lema, J. M.; Carballa, M., Biotransformation of pharmaceuticals under nitrification, nitratation and heterotrophic conditions. *Sci. Total Environ.* **2016**, *541*, 1439-1447.
14. Bratbak, G.; Dundas, I., Bacterial dry matter content and biomass estimations. *Applied and Environment Microbiology* **1984**, *48*, 755-757.
15. Poirier-Larabie, S.; Segura, P. A.; Gagnon, C., Degradation of the pharmaceuticals diclofenac and sulfamethoxazole and their transformation products under controlled environmental conditions. *Sci. Total Environ.* **2016**, *557-558*, 257-267.
16. Nödler, K.; Licha, T.; Barbieri, M.; Perez, S., Evidence for the microbially mediated abiotic formation of reversible and non-reversible sulfamethoxazole transformation products during denitrification. *Water Res.* **2012**, *46*, 2131-2139.
17. Kassotaki, E.; Buttiglieri, G.; Ferrando-Climent, L.; Rodriguez-Roda, I.; Pijuan, M., Enhanced sulfamethoxazole degradation through ammonia oxidizing bacteria co-metabolism and fate of transformation products. *Water Res.* **2016**, *94*, 111-119.

18. Stravs, M. A.; Pomati, F.; Hollender, J., Exploring micropollutant biotransformation in three freshwater phytoplankton species. *Environ. Sci. Proc. Imp.* **2017**, *19*, 822-832.
19. Reis, P. J.; Reis, A. C.; Ricken, B.; Kolvenbach, B. A.; Manaia, C. M.; Corvini, P. F.; Nunes, O. C., Biodegradation of sulfamethoxazole and other sulfonamides by Achromobacter denitrificans PR1. *J. Hazard. Mater.* **2014**, *280*, 741-749.
20. Majewsky, M.; Glauner, T.; Horn, H., Systematic suspect screening and identification of sulfonamide antibiotic transformation products in the aquatic environment. *Anal. Bioanal. Chem.* **2015**, *407*, 5707-5717.
21. Deng, Y.; Mao, Y.; Li, B.; Yang, C.; Zhang, T., Aerobic Degradation of Sulfadiazine by Arthrobacter spp.: Kinetics, Pathways, and Genomic Characterization. *Environ. Sci. Technol.* **2016**, *50*, 9566-9575.
22. Schymanski, E. L.; Jeon, J.; Gulde, R.; Fenner, K.; Ruff, M.; Singer, H. P.; Hollender, J., Identifying small molecules via high resolution mass spectrometry: communicating confidence. *Environ. Sci. Technol.* **2014**, *48*, 2097-2098.
23. Jayaraman, A.; Thandeeswaran, M.; Priyadarsini, U.; Sabarathinam, S.; Nawaz, K. A.; Palaniswamy, M., Characterization of unexplored amidohydrolase enzyme-pterin deaminase. *Appl. Microbiol. Biotechnol.* **2016**, *100*, 4779-4789.
24. Levenberg, B.; Hayaishi, O., A bacterial pterin deaminase. *J. Biol. Chem.* **1959**, *234*, 955-961.
25. McNutt, W. S., The enzymic deamination and amide cleavage of folic acid. *Arch. Biochem. Biophys.* **1963**, *101*, 1-6.
26. Rappold, H.; Bacher, A., Bacterial degradation of folic acid. *J. Gen. Microbiol.* **1974**, *85*, 283-290.
27. Fan, H.; Hitchcock, D. S.; Seidel, R. D.; Hillerich, B.; Lin, H.; Almo, S. C.; Sali, A.; Shoichet, B. K.; Raushel, F. M., Assignment of pterin deaminase activity to an enzyme of unknown function guided by homology modeling and docking. *J. Am. Chem. Soc.* **2013**, *135*, 795-803.
28. Lamshöft, M.; Sukul, P.; Zuhlke, S.; Spiteller, M., Metabolism of 14C-labelled and non-labelled sulfadiazine after administration to pigs. *Anal. Bioanal. Chem.* **2007**, *388*, 1733-1745.
29. Garcia-Galan, M. J.; Rodriguez-Rodriguez, C. E.; Vicent, T.; Caminal, G.; Diaz-Cruz, M. S.; Barcelo, D., Biodegradation of sulfamethazine by Trametes versicolor: Removal from sewage sludge and identification of intermediate products by UPLC-QqTOF-MS. *Sci. Total Environ.* **2011**, *409*, 5505-5512.
30. Moschet, C.; Piazzoli, A.; Singer, H.; Hollender, J., Alleviating the Reference Standard Dilemma Using a Systematic Exact Mass Suspect Screening Approach with Liquid Chromatography-High Resolution Mass Spectrometry. *Anal. Chem.* **2013**, *85*, 10312-10320.
31. Shrestha, P.; Junker, T.; Fenner, K.; Hahn, S.; Honti, M.; Bakkour, R.; Diaz, C.; Hennecke, D., Simulation Studies to Explore Biodegradation in Water-Sediment Systems: From OECD 308 to OECD 309. *Environ. Sci. Technol.* **2016**, *50*, 6856-6864.